



Norwegian University
of Life Sciences

Master's Thesis 2024 60 ECTS

Faculty of Environmental Sciences and Natural Resource Management

Acid leaching of gneisses in southern Norway: An evaluation of H_2O_2 oxidation testing for the determination of the acid-producing potential of sulphide-rich rocks

Ada Marie Orthe Karlsen

Miljøvitenskap (Environment and Natural Resources)

Abstract

The amphibolite- to granulite- facies gneisses exposed in southern Norway are causing environmental problems as they produce an acidic solution with high metal content when exposed to the atmosphere. As such, these rocks are commonly referred to as “*acid-producing gneisses*”. This has, for example, led to problems with fish dying in nearby streams and rivers. Therefore, a guide was created for how the acid-producing gneiss should be managed and characterised. The guide “*Retningslinjer for tiltak i områder med syredannende gneis*” by the Project Group for Control of Sulphurous Runoff in Agder, known as the Agder Method, which is currently used. The Agder method involves a three-step assessment: degree of weathering, sulphur (S) content, and temperature change after 25 minutes when hydrogen peroxide (H_2O_2) has been added (H_2O_2 test). Experiments using the H_2O_2 test indicate that the Agder method leads to false classification of acid-producing gneiss. Consequently, acid-producing rocks have been placed in non-approved landfills, and non-acid-producing rocks have been placed in approved landfills with obviously environmental and financial consequences.

The rationale behind the H_2O_2 test is that the exothermic oxidation of sulphide minerals, such as pyrite, releases heat. In the Agder method, the threshold values are set at $0.7\text{ }^\circ\text{C}$, i.e. a rock is not acid-producing if $\Delta T_{25\text{min}} < 0.7\text{ }^\circ\text{C}$, whereas if $\Delta T > 0.7\text{ }^\circ\text{C}$ the rock is potentially acid-producing. However, acid leaching from a rock is not only caused by sulphide minerals, but also by jarosite, which does not react exothermically with H_2O_2 . In addition, H_2O_2 may also react exothermally with other minerals that do not produce any acid whatsoever. In this study, I investigate how secondary minerals, with a particular focus on iron oxides, could contribute to the false classification of the acid-producing potential. The “*single NAG test*” method was also tested to compare the relevance of measuring NAG pH vs. temperature upon H_2O_2 oxidation.

Three gneiss samples and various mixtures of pure mineral phases, including pyrite (sulphide), ferrihydrite (Fe hydroxide), and quartz (inert), were selected for laboratory tests. The tests performed included the single NAG test with temperature logging, the Agder H_2O_2 method, paste pH and oxalate extraction of Fe oxides.

The main findings are that ferrihydrite and pyrite alone react exothermically, but when ferrihydrite and pyrite are mixed, the exothermic reaction is inhibited. This shows that in natural rock, where Fe oxides and sulphide minerals can be expected to coexist, the temperature response to H_2O_2 does not provide a reliable indication of sulphide oxidation potential. Experiments were carried out to remove Fe oxides prior to the H_2O_2 test. For all gneiss samples tested, oxalate extracted samples changed the

temperature reaction pattern to smaller temperature increases. The single NAG test was also tested and gave results that were in agreement with the reliable column leaching tests performed by Lindum AS.

Based on the findings in this study, it can be concluded that there is an urgent need for a change in the current guideline for the characterisation of gneiss in southern Norway in order to avoid further environmental and related financial damage. I recommended that the Agder H₂O₂ test is replaced by the AMIRA single NAG method.

Sammendrag

Amfibolitt- til granulitt gneisene i Sør-Norge skaper miljøproblemer når de eksponeres til atmosfæren. Dette gjør at de produserer sur avrenning med et høyt metallinnhold. Disse gneisene blir ofte omtalt som «syredannende gneiser». Den sure avrenningen har blant annet ført til problemer med fiskedød i nærliggende bekker og elver. Derfor ble det laget en veileder for hvordan syredannende gneis skal håndteres og karakteriseres. Veilederen «Retningslinjer for tiltak i områder med syredannende gneis» av Prosjektgruppen for kontroll av svovelholdig avrenning i Agder, kalt Agder metoden, er den som brukes i dag. Agder metoden innebærer en tretrinnsvurdering: forvitningsgrad, innhold av svovel (S), og temperaturendring ved 25 minutter etter tilførsel av hydrogenperoksid (H_2O_2). Forsøk med H_2O_2 testen tyder på at Agder metoden fører til feilklassifisering av syredannende gneiser. Dette har ført til at syredannende gneis ikke blir deponert og rene gneiser blir deponert, som fører til miljømessige og økonomiske konsekvenser.

Teorien bak H_2O_2 testen er at den eksoterme oksidasjonen av sulfidmineraler frigjør varme, som for eksempel pyritt. I Agder metoden er terskelverdiene satt til $0,7\text{ }^\circ\text{C}$, det vil si at en gneis ikke er syredannende dersom $\Delta T_{25\text{min}} < 0,7\text{ }^\circ\text{C}$, men hvis $\Delta T_{25\text{min}} > 0,7\text{ }^\circ\text{C}$ er potensielt syredannende. Syredannelse skjer i midlertidig ikke bare av sulfidmineraler, men også av jarositt som ikke reagerer eksotermt med H_2O_2 . I tillegg kan H_2O_2 også reagere eksotermt med andre mineraler som ikke er syredannende. Denne masteroppgaven undersøker hvordan sekundær mineraler, med særlig søkelys på jernoksider, kan bidra til feil klassifisering av gneis. Metoden «single NAG test» ble også utført for å sammenligne relevansen av å måle NAG pH vs. temperatur ved H_2O_2 oksidasjon.

Det ble valgt ut tre gneisprøver og ulike blandinger av rene mineralfaser, som inkluderer pyritt (sulfid), ferrihydritt (Fe-hydroksid), og kvarts (inert) for laboratorietester. Testene som ble utført var AMIRA single NAG test med temperaturlogging, Agder metodens H_2O_2 -test, abrasjons pH og oksalatekstraksjon av Fe-oksider på gneis prøver.

Hovedfunnene viser at ferrihydritt og pyritt alene reagerer eksotermt, men når ferrihydritt og pyritt blandes så hemmes den eksoterme reaksjonen. Dette indikerer at i en naturlig bergart, der man kan forvente at Fe-oksider og sulfidmineraler eksisterer side om side, gir ikke temperatur respons på H_2O_2 testen en pålitelig indikasjon på sulfidoksidasjonspotensialet. Det ble utført eksperimenter for å fjerne Fe-oksider i gneis prøvene før H_2O_2 test ble utført. Oksalatekstraherte prøver endret reaksjonsmønsteret til lavere temperatur økninger. Single NAG metoden ga resultater i samsvar med de pålitelige kolonne utlekingstestene som ble utført av Lindum AS.

Basert på funnene i denne masteroppgaven kan det konkluderes med at det er ett behov for endring av dagens måte å karakterisere gneis på for å unngå ytterligere miljømessige og økonomiske skader. Derfor anbefaler jeg at Agder metodens H₂O₂ test erstattes av AMIRA single NAG metoden.

Acknowledgements

This master's thesis marks the end of my 5-year study program at NMBU. The thesis is written at NMBU in collaboration with NMBU, the Norwegian Geotechnical Institute (NGI), and Lindum AS through earthresQue.

I would like to thank my supervisors Jan Marten Huizenga at NMBU, Gabrielle Dublet-Adli at NGI, and Sandra Heldal at Lindum. Jan Marten, thank you for your support and guidance throughout the process, especially in the writing process. Gabrielle, thank you for your good follow-up throughout the laboratory work and, valuable discussion and feedback, and not at least the loan of the laboratory at NGI. Sandra, thank you for the discussions and the opportunity to collaborate with Lindum.

There have been many good helpers and discussions throughout the year. Ruth Vingerhagen (Norconsult), thank you for sharing your expertise, valuable discussion, and input on the experiments and results. Kathinka Khran (Lindum), thank you for the discussions, input, and cooperation at Lindum in Drammen. Anne Line Hexeberg, thank you for your encouraging words, discussion, and input during the lab work and the good coffee breaks.

I would also like to thank my family and friends for providing good breaks and support during the year, and to my roommate and friend, Pauline Bolte, thank you for your company and motivation during the last year – suddenly, we both had delivered a master thesis.

Ada Marie O. Karlseth

14.05.2024

Table of content

Abstract	ii
Sammendrag	iv
Acknowledgements	vi
List of tables.....	x
List of figures	xiii
1 Introduction.....	1
1.1 Why this study	1
1.2 Guidelines for characterisation of ARD	2
1.2.1 The Agder guideline.....	2
1.2.2 AMIRA guidelines	4
1.2.3 Summary of AMIRA method and Agder method	5
1.3 Previous work done on acid-producing on gneiss in Norway	5
1.4 Aims of this study	6
1.5 Organisation of this thesis.....	7
2 Geological environmental conditions.....	9
3 Background.....	13
3.1 What is acid drainage?	13
3.2 Environmental impact	13
3.3 Oxidation of sulphide minerals.....	13
3.4 The role of secondary minerals in acid drainage.....	14
3.5 Summary of produced H ⁺ upon the oxidation of sulphides	15
4 Material and method.....	17
4.1 Samples	17
4.1.1 Selection of the gneiss samples for petrographic description, mineralogy, and whole-rock geochemical analysis	17
4.1.2 Selection of gneiss samples for single NAG test.....	17
4.1.3 Selection of pure mineral phases for single NAG test	18
4.2 Sample collection, crushing and milling	19
4.2.1 Sample collection	19
4.2.2 Sample crushing	19
4.2.3 Agat milling and sieving.....	20
4.3 Mineralogy and geochemistry of gneiss samples.....	21
4.3.1 X-ray diffraction	21

4.3.2 Whole-rock geochemical analysis	21
4.4 Paste pH and electric conductivity test	21
4.5 AMIRA single NAG tests.....	22
4.5.1 Single NAG test	22
4.6 Oxalate extraction for removal of Fe(III).....	23
4.6.1 Oxalate extraction of Fe and Al oxide procedure	23
4.6.2 Preparing material for single NAG test.....	23
4.7 NAG calculation in AMIRA single NAG test.....	24
4.8 Water analyses of extracted solution and supernatants	24
4.9 Agder method.....	25
5 Results	27
5.1 Petrographic description of gneiss samples	27
5.2 Mineralogical and geochemical characteristics of the gneisses of diverse response to H ₂ O ₂ test	34
5.2.1 Major and trace element geochemistry	34
5.2.2 Mineralogy of gneiss samples	36
5.3 Classification according to the Agder method.....	37
5.3.1 Classification of the gneisses by the Agder method.....	37
5.3.2 Manual temperature logging during the Agder method H ₂ O ₂ test	39
5.3.3 Column experiment at Lindum	40
5.4 Single NAG test on gneiss samples	41
5.4.1 Net acid generation characterisation of the gneisses	41
5.4.2 Temperature logging during the single NAG test of the gneisses	42
5.4.3 Summary of gneiss characteristics by AMIRA method	43
5.5 Single NAG test of mixtures of known proportions of pyrite and ferrihydrite	44
5.5.1 Classification of pyrite-ferrihydrite-quartz mixtures	44
5.5.2 Temperature logging during the single NAG test for pyrite-quartz and ferrihydrite-pyrite-quartz mixtures	46
5.6 Comparison of pyrite-quartz and ferrihydrite-pyrite-quartz mixtures.....	48
5.6.1 Maximum temperature change compared with the S content in the samples.....	48
5.6.2 Net acid generation pH and S content.....	49
5.6.3 Net acid generation and S content	51
5.7 Reaction with H ₂ O ₂	53
5.8 Water chemistry	55
5.9 Crystalline and amorphous Fe and S in the gneisses.....	56

6 Interpretation and discussion of results.....	59
6.1 Oxide/hydroxide bias to temperature change.....	59
6.1.1 Oxides/oxyhydroxide and the effect of H ₂ O ₂	59
6.1.2 The effect of removal of amorphous Fe oxides in the gneiss samples on temperature	63
6.1.3 Other oxide minerals affecting H ₂ O ₂ and temperature changes	65
6.2 Mineralogy bias on temperature in the gneisses	66
6.2.1 Mineralogy description of the gneisses in the southern Norway	66
6.2.2 Minerals in the gneisses affecting the H ₂ O ₂ test	69
6.3 Limitations by the Agder method	71
6.3.1 Criterion used for quantifying the temperature response	71
6.3.2 Environmental conditions bias to temperature change	73
6.4 Evaluation of the AMIRA method	74
6.4.1 Evaluation of H ₂ O ₂ used in the single NAG test	74
6.4.2 Considerations during the AMIRA single NAG procedure	76
6.4.3 Advantages and disadvantages of the AMIRA	76
6.5 Representative sampling	77
6.5.1 Sampling	77
6.5.2 Biological matter and reaction with H ₂ O ₂	77
7 Conclusion	79
8 Future work for improvement in assessment of acid-producing rocks.....	81
9 References list.....	82
Appendix.....	86
Appendix A: Paste pH and EC of gneiss samples, quartz and ferrihydrite.....	86
Appendix B: Geochemical raw data.....	87
Appendix C: Raw data from single NAG test by AMIRA	91
Appendix D: Raw data from oxalate extraction.....	94
Appendix E: Overview of existing data on gneiss samples	95
Appendix F: Blank samples for water chemistry analysis.....	97
Appendix G: Raw data from XRD analysis	98

List of tables

Table 1: Overview of the Adger method and AMIRA method, including similarities and differences. ...	5
Table 2: The main differences between the Agder and AMIRA guidelines for using the H ₂ O ₂ test. Note that in the AMIRA method, it is possible to measure the temperature increase, but this is not used in the prediction of the acid-producing potential.	5
Table 3: Overview of previous work done on acid-producing gneiss in Norway.	6
Table 4: Overview of released H ⁺ ions by oxidation with oxygen. Sphalerite and galena are not producing any H ⁺ during this reaction but are producing SO ₄ ²⁻ . Reaction equations are idealised reactions when the sulphide mineral is oxidised by oxygen. The table is modified from Dold (2017).	15
Table 5: An overview of minerals oxidised by Fe ³⁺ and the corresponding release of H ⁺ . For using Fe ³⁺ as an oxidant it needs to be produced in advance, and this reaction normally consumes H ⁺ , see eq. 3. The release of H ⁺ indicated here is not corrected for the initial step of aqueous Fe ³⁺ production. The table is modified from Dold (2017).	15
Table 6: Dissolution of secondary minerals and their release of H ⁺ . The table is modified from Dold (2017).	15
Table 7: Chosen samples based on Sluttrapport from Lindum and the following sample sites (Lindum AS, 2023). The highlighted samples are further investigated with H ₂ O ₂ tests using both the AMIRA single NAG test and the Agder method in this study.	17
Table 8: Overview of selected gneiss sample for further testing with H ₂ O ₂ . Sample information is from Lindum Skattefunnsluttrapport, and the samples were tested by the Agder method. Table modified from Lindum AS (2023).	18
Table 9: Selection of samples from other sources than gneiss. Purity results by XRD are provided by NGI.	18
Table 10: Pyrite-quartz mixtures.	18
Table 11: Pyrite, ferrihydrite, quartz mixtures. Ferrihydrite amount is fixed at 0.5 g.	18
Table 12: Pyrite-ferrihydrite-quartz mixtures. Pyrite amount is fixed at 0.25 g.	19
Table 13: Pyrite – LS-tailings – quartz mixtures.	19
Table 14: Overview of selected extraction solutions for water analysis for samples Birkeland 5, Tingsaker skole #3, Arendal legevakt 4, and the pure mineral phases mixtures between ferrihydrite-pyrite-quartz and pyrite-quartz. The mark “X” marks the treatment before water analysis.	24
Table 15: Major element geochemistry of gneiss samples in wt.%. Elemental concentrations are calculated from the oxides. bdl stands for below detection limit.	35
Table 16: Trace element contents in ppm. bdl stands for below detection limit.	36
Table 17: XRD mineralogy presented in wt.%. The abbreviation TR stands for trace. Bold black are minerals that contain Fe(II), red are minerals with Fe(III), and purple are minerals with Fe(II/III).	37
Table 18: XRD mineralogy of gneiss samples Tingsaker skole #1, Tingsaker skole #3 and Birkeland 5 in wt. %. Results are obtained from NGI. The amorphous content was not measured. Bold black are minerals that contain Fe(II), red are minerals with Fe(III).	37
Table 19: Overview of gneiss samples and their properties, modified from Lindum AS (2023). pH from the column test is presented as pH (weeks). pH was measured in the column leachate, and “weeks” stands for the number of weeks since the experiment started. The criteria for the degree of weathering were based on the colour of the samples (Adam Pearce, e-mail correspondence, March 2024). ARD stands for acid rock drainage. The colours are organised as follows: red colour means high value (S content: > 0.8 wt.%, ΔT _{25min} : > 1.2 °C), orange is medium (S content: 0.15-0.8 wt.%, ΔT _{25min} :	

0.7-1.2 °C), and green is low (S content: < 0.15 wt.%, ΔT_{25min} : < 0.7 °C). Threshold values are from the Agder guideline (Prosjektgruppen for kontroll på svovelholdig avrenning i Agder, 2021)..... 38

Table 20: Categorising selected gneiss samples using the Agder method by the results from this thesis. The degree of weathering is provided by Lindum AS (2023). S content is the result from whole-rock geochemistry, and ΔT_{25min} is the results from the Agder H₂O₂ test performed by the author. Red colour means high value (S content: > 0.8 wt.%, ΔT_{25min} : > 1.2 °C), orange is medium (S content: 0.15-0.8 wt.%, ΔT_{25min} : 0.7-1.2 °C), and green is low (S content: < 0.15 wt.%, ΔT_{25min} : <0.7 °C). Threshold values are from the Agder guideline (Prosjektgruppen for kontroll på svovelholdig avrenning i Agder, 2021). The criteria for the degree of weathering were based on the colour of the samples (Adam Pearce, e-mail correspondence, March 2024). ARD stands for acid rock drainage. The column exposure to light describes the light conditions in the room during the experiment..... 38

Table 21: Acid potential of selected gneiss sample. Paste pH is calculated from triplicates, presented in Appendix A. NAG pH and NAG are used to determine the acid potential of the samples. Red colour means that the values are below the acid potential limits, where NAG pH < 4.5 and NAG > 5 are coloured red (Smart et al., 2002). NAF: Non-acid-forming, PAF: potentially acid-forming. 41

Table 22: Pre-treated gneiss samples with oxalate extraction and the acid potential. NAG pH and NAG are used to determine the acid potential of the samples. Red colour means that the values are below the acid potential limits, where NAG pH < 4.5 and NAG > 5 are coloured red (Smart et al., 2002). NAF: Non-acid-forming, PAF: potentially acid-forming. 41

Table 23: A summary of the standard AMIRA single NAG test and the modified single NAG test with pre-treated oxalate extracted samples material. Paste pH is presented as an average from triplicates, and NAG pH, NAG, ΔT_{max} , and ΔT_{25min} are presented as an average from duplicates. Red colour means that the values are below the acid potential limits, where NAG pH < 4.5 and NAG > 5 are coloured red (Smart et al., 2002). NAF: Non-acid-forming, PAF: potentially acid-forming..... 44

Table 24: Acid potential of the mixed samples from pyrite and ferrihydrite (duplicate tests). Paste pH is done on pure quartz and pure ferrihydrite. NAG pH and NAG are used to determine the acid potential of the mixtures. Red colour indicates values below the acid potential limits, where NAG pH < 4.5 is coloured red, and NAG > 5 is coloured red (Smart et al., 2002). NAF: non-acid-forming, PAF: potentially acid-forming, PAF-LC: potential acid-forming – lower capacity. PAF-LC is described as material that may be able to treat with lime or other NAF material (Smart et al., 2002). ΔT_{max} is the average from the duplicates of samples..... 45

Table 25: Quantitative test of different salts and minerals mixed with H₂O₂. Iron(III) reacts strongly with H₂O₂. A strong reaction is visible as the sample boiled over. A small reaction is only detected by the temperature logger. 53

Table 26: Water chemistry of gneiss, ferrihydrite-pyrite-quartz (ferrihydrite fixed at 0.5 g), and pyrite-quartz mixtures. The gneiss samples are presented as H₂O₂ tested solution, oxalate extraction solution, and solution from H₂O₂ test solution from pre-treated sample material with oxalate extraction. Analysis of the mixtures ferrihydrite-pyrite-quartz (pyrite fixed at 0.025g) and pyrite-quartz is presented from the oxalate extraction. The unit for the elements is mg/L. Note that bdl indicates below detection limit. 56

Table 27: Total, amorphous, and crystalline Fe presented in ppm. Percentage of amorphous and crystalline is calculated as a percentage of total Fe. 57

Table 28: Total, amorphous, and crystalline S presented in ppm. Percentage of amorphous and crystalline is calculated as a percentage of total S. 57

Table 29: Summary table of reaction related to Fe related to H₂O₂. Oxidation of pyrite through H₂O₂ produces SO₄²⁻ which is used as a ligand to the products from the Fenton reaction. Fenton reaction and reactions with SO₄²⁻ as a ligand are modified from De Laat et al. (2004)..... 62

Table 30: Major elements compared with the upper continental crust (UCC). Values are calculated as my values/UCC, where ratio > 1 means enrichment compared with UCC (red numbers), and ratio < 1 is depleted compared to UCC (black numbers). Upper continental crust values are from Table 5 in McLennan (2001). Unit is wt.%. 68

Table 31: Trace elements contents normalised against the upper continental crust (UCC) values. Values are calculated as my results/UCC, where ratio > 1 means enrichment compared with UCC (red numbers), and ratio < 1 is depleted compared to UCC (black numbers). Upper continental crust values are from Table 5 in McLennan (2001). Unit is ppm. 68

Table 32: Summary of results connected to S content (wt.%) (from Table 16), S minerals, detected S minerals during petrographic description, and the pH from column experiments from Lindum (2023). Note that Fe oxides minerals could also not contain S, and are therefore just an implication that it can contain S. Red colour means high value (S content: > 0.8 wt.%, ΔT_{25min}: > 1.2 °C), orange is medium (S content: 0.15-0.8 wt.%, ΔT_{25min}: 0.7-1.2 °C), and green is low (S content: < 0.15 wt.%, ΔT_{25min}: < 0.7 °C). Threshold values are from the Agder guideline (Prosjektgruppen for kontroll på svovelholdig avrenning i Agder, 2021). Concentrations below the detection limit are indicated as bdl. 69

Table 33: The gneiss samples presented as ΔT_{25min} and ΔT_{max} with associated reaction time by the Agder method. Table is modified from Lindum (2023). For temperature columns: red colour means high value (ΔT_{25min}: > 1.2 °C), orange is medium (ΔT_{25min}: 0.7-1.2 °C), and green is low (ΔT_{25min}: < 0.7 °C). Threshold values are from the Agder guideline (Prosjektgruppen for kontroll på svovelholdig avrenning i Agder, 2021). In characterisation: green is not acid-producing, red is acid-producing. 73

List of figures

Figure 1: Flowchart of the three-step assessment of classification of gneiss. The figure is modified from Prosjektgruppen for kontroll på svovelholdig avrenning i Agder (2021). The degree of weathering decides whether the rock is further tested with S content and H ₂ O ₂ test. If the rock has a high degree of weathering, the rocks are automatically acid-producing. If the rocks have a high S content, they are acid-producing, while the low and medium categories result in H ₂ O ₂ testing. If the rock has a high temperature change, it is classified as acid-producing without taking S content into account. The medium is dependent on the S content, where low results are not acid-producing, and medium results are acid-producing. The low is also dependent on the S content, whereas the low and medium results in not-acid-producing rocks.	3
Figure 2: Map over South Norway, with a smaller map outcrop with the case area Lillesand. Source: kartverket.no	9
Figure 3: South Norway presented with the different geological sectors. The Bamble sector includes Kristiansand to approximately Porsgrunn (Oslo rift). Figure from Nijland, et al. (2014).	10
Figure 4: Bedrock map over Bamble sector. Lillesand is south on the map, and the dominant bedrock is gneiss. Map by Nijland et al. (2014). Note that the numbers in the map are related to the publication by Nijland et al. (2014) and are not relevant in this thesis.	11
Figure 5: Map of acid-producing gneiss from Lillesand to Risør. Note that the original map did not include a scalebar or legend, i.e. the scalebar is therefore an approximation. Map: Ånund Ættesatd, Lillesand municipality. The criteria used for identifying the rocks are unknown.	12
Figure 6: Stored samples at Lindum in Drammen.	19
Figure 7: Inside of the Los Angeles crusher. Steel balls that are rolled together with the gneiss sample.	20
Figure 8: Retsch agate mill used at NMBU.	20
Figure 9: Experimental design for single NAG test. The white buckets with beakers and temperature loggers are placed in a cardboard box. The cardboard box is closed during the experiment.	22
Figure 10: Setup for the Agder method. The sample reacted visibly as exemplified by the formation of bubbles (steel grey colour) and generation of heat.	25
Figure 11: Sample Eydehavn 1B.	27
Figure 12: Sample Tingsaker skole #1, grey surfaced samples. This sample did not show any sign of weathered surface.	27
Figure 13: Tingsaker skole #2, to the left the stone piece might be weathered as there is an orange colour in the outer corners.	28
Figure 14: Sample Tingsaker skole #2.	28
Figure 15: Sample Tingsaker skole #3. The piece to the left is fresh surface and has no sign of weathered surface. The piece to the right is rusty in the colour, and crumbles when touched.	29
Figure 16: Sample RV420 #1.	29
Figure 17: Sample Blakstad 3.	30
Figure 18: Birkland 5 had little variation in the sample. The sample itself are well weathered. This is the rusty yellow side.	31
Figure 19: The other side of Birkland 5. This is the rusty red surface.	31
Figure 20: Nordbø 1 has more weathered surface, but there are some spots inside the gneiss that is weathered.	32

Figure 21: Groos 1, the piece to the left shows the grey fresh surface colour and the orange weathered colour. The piece to the right shows piece with reddish colour.....	32
Figure 22: Rock sample Arendal legevakt 2. The piece to the left is less weathered and has the freshest surface that is grey. To the right is more weathered and are more rusty orange coloured. ...	33
Figure 23: Sample Arendal legevakt 4.	33
Figure 24: Rock sample from Arendal legevakt 5, three pieces to show the variation between the stones.	34
Figure 25: Manually temperature logging of sample Birkeland 5 during the 25 minutes. Maximum temperature is reached after 10 minutes. A temperature change of 21.3 °C was recorded after 25 minutes.....	39
Figure 26: Manually temperature logging of sample Tingsaker skole #3. The sample reaches the maximum temperature after 5 minutes. A temperature change at 1 °C was recorded after 25 minutes.	39
Figure 27: Manual temperature logging of sample Arendal legevakt 4 by the Agder method.....	40
Figure 28: Results from column experiment done at Lindum. Each pH measuring is done every 4 weeks and watered with deionised water once a week. Blue: Arendal legevakt 4, orange: Tingsaker skole #3, grey: Birkeland 5. Tingsaker skole #3 and Birkeland 5 started at a later time than Arendal legevakt 4, which explain why Arendal legevakt 4 has a longer pH logging time.	40
Figure 29: Arendal legevakt 4 presented as ΔT (°C) average from duplicates from each experiment type. Black is Arendal legevakt 4 done by AMIRA method. Green is Arendal legevakt 4 prepared by oxalate extraction before temperature logging by the AMIRA method.....	42
Figure 30: Tingsaker skole #3 presented as ΔT (°C) average from duplicates from each experiment. Black is done by the AMIRA method. Green is oxalate extraction prepared gneiss sample before AMIRA method.	42
Figure 31: Birkeland 5 presented as ΔT (°C) average from two experiments. Black represents the AMIRA test method, whereas green is the oxalated pre-treated gneiss sample before doing the AMIRA method.	43
Figure 32: Temperature evaluation in pyrite-quartz mixtures from the single NAG test. Results are presented as ΔT , i.e. the difference in temperature compared to the prior H_2O_2 addition. Different colours represent different amounts of pyrite, and therefore, variable amounts of S. Blue: 1 wt.% S, red: 0.75 wt.% S, black 0.50 wt.% S, pink: 0.25 wt.% S, yellow: 0 wt.% S. The blue curve with the highest S content reacts the most and fastest, a lower S content in the samples gives lower and slower reactions until zero S content where there is no reaction with the H_2O_2	46
Figure 33: Temperature evaluation in ferrihydrite-pyrite-quartz mixtures from the single NAG tests with fixed amount of ferrihydrite (0.5 g), and variable amount of pyrite and therefore variable S content. Green: 0 wt.% S, light blue: 0.12 wt.% S, yellow: 0.25 wt.% S, black: 0.50 wt.% S, red: 0.75 wt.% S, purple: 1 wt.% S.	47
Figure 34: Time and temperature for pyrite-quartz mixture equal to 0.75 wt.% S. Green: oxalate treated sample (single experiment), black: original pyrite and quartz mixture (average from duplicates).	47
Figure 35: Max ΔT reached during the experiment plotted against the S content. Pyrite-quartz (blue bullet points) and ferrihydrite-pyrite-quartz (red bullet points) compared to each other with the same amount of S in each sample and the samples temperature differences. Temperature differences is presented as ΔT_{max} (°C). Grey lines are drawn by hand to give an indication of the trend.	48

Figure 36: Max ΔT reached during the experiment for the different amounts of ferrihydrite in grams mixed with a fixed amount of pyrite (0.5 wt.% S) in the samples. The more ferrihydrite, the more temperature increases. Grey lines are drawn by hand to give an indication of the trend..... 49

Figure 37: NAG pH plotted against S content. Blue is pyrite-quartz, red is ferrihydrite-pyrite-quartz (same amount of ferrihydrite: 0.5 g). Black dotted line is the paste pH for ferrihydrite (pH 3.6). Grey lines are drawn by hand to give an indication of the trend..... 50

Figure 38: NAG pH plotted against the ferrihydrite-pyrite-quartz; pyrite fixed at 0.5 wt.% S. Grey lines are drawn by hand indicating the trend. 51

Figure 39: NAG plotted against S wt.% for pyrite-quartz (blue) and ferrihydrite-pyrite-quartz (red). The pyrite-quartz mixtures have higher NAG values, while ferrihydrite-pyrite-quartz mixtures have lower values of NAG. Grey lines are drawn by hand and indicates the trend. 52

Figure 40: NAG plotted against different amounts of ferrihydrite at the same S wt.% (0.5). The more ferrihydrite, the lower the NAG. Grey lines are drawn by hand to give an indication of the trend. 52

Figure 41: Reaction time and temperature increases for Fe(III)sulphate mixed with H₂O₂. 53

Figure 42: Pure LS-tailings done by the AMIRA single NAG method, including temperature logging. A small reaction is observed..... 54

Figure 43: Temperature logging of LS-tailings mixed with pyrite. Orange: LS-tailings with 0.75 wt.% S, green: LS-tailings with 0.5 wt.% S, blue: LS-tailings with 0.25 wt.% S and purple: LS-tailings with 0 wt.% S. 54

Figure 44: Decomposition of H₂O₂ (2%) in an acidic environment (pH = 3) with time. Figure from Teel Amy et al. (2007). Relevant for this section are the Mn-oxides pyrolusite and manganite, and the Fe oxides goethite, hematite..... 59

Figure 45: Max ΔT during the experiment for the sample mixes pyrite-quartz (blue points), ferrihydrite-pyrite-quartz, ferrihydrite fixed at 0.5 g (red points), LS-tailings-pyrite-quartz (black points). LS-tailings mixtures follow the reaction of the pyrite mixtures better than the ferrihydrite mixtures. Grey lines are drawn by hand to indicate the reaction trend. 63

Figure 46: Photos of Birkeland 5 during the titration in the single NAG test. The more yellow, the more precipitation of Fe in the solution. A, B and C are ordinary single NAG test, while D, E and F are modified single NAG test with pre-treated sample with oxalate extraction. A and D = before titration, B and E = pH 4.5, C and F = pH 7. The oxalate extraction had a visual effect on the sample Birkeland 5, F compared to C, where the less coloured picture F showed less precipitation of Fe in solution during titration..... 65

1 Introduction

Acid leaching or acid drainage is a significant problem for the environment. It is formed through the interaction of surface- or groundwater and oxygen with rocks that contain sulphide minerals, such as pyrite. The drainage water typically has a pH of less than 4 and often contains high metal concentrations, such as iron (Fe), copper (Cu), zinc (Zn) and aluminium (Al) (Nordstrom and Alpers, 1999). Acid drainage can occur under natural conditions, such as the Noguera de Vallferrar catchment in the Central Pyrenees (Zarroca *et al.*, 2021). However, in most cases, acid drainage is caused by human activities in which the rocks are exposed to surface water. This can specifically happen during mining activities in which rocks are removed to extract minerals (e.g., gold, copper, and graphite) or are used for energy production (i.e., coal). Under these circumstances, it is referred to as acid mine drainage (AMD). Consequently, AMD is typically a problem in mining countries, including, for example, Australia, Canada, China, the USA, and South Africa.

Typically, AMD is associated with the mine tailings (waste from extraction), which are exposed to both air and water, affecting surface- and groundwater for many years. In Norway, AMD is related to old mines. One example is the Follaldalen copper mine, where the tailings produce metal-enriched acid drainage flowing out into the river. This affects the river Folla, which is heavily polluted by metals such as Cu, Zn and Fe (Kampestuen, 2020). However, the most well-known acid drainage problem in Norway is related to the alum shale in the eastern part of Norway and the acid-producing gneiss in the southern part of Norway. This research project relates to the acid-producing gneisses in southern Norway. Acid leaching from gneiss goes back to the 1980s (Hagelia, 2023). This issue intensified as additional rocks were uncovered during infrastructure construction operations. At the end of the 1980s, there was a case of acidification of a lake that was a drinking water source and recreational area for fishing (Hagelia, 2023). Acidification results in high metal concentrations, such as Al, leading to fish die-offs (Hagelia, 2023). In recent times, during the construction of the E18 Grimstad-Kristiansand, the acid-producing gneiss was recognised as a potential environmental risk, which has resulted in the development of several tests to determine the acid-producing potential of these rocks (Hindar, 2012).

1.1 Why this study

Characterising acid rocks is essential for minimising environmental impacts. In Norway, there exist two guidelines regarding the characterisation of acid-producing rocks. The guideline "*Identifisering og karakterisering av syredannende bergarter*" written by the Norwegian Geotechnical Institute for the Norwegian Environment Agency, is developed for alum shale. Alum shale is obviously quite different from gneiss. Consequently, a specific guideline was developed for the acid-producing gneiss, called

“Retningslinjer for tiltak i områder med syredannende gneis» written by the Prosjektgruppen for kontroll av svovelholdig avrenning i Agder (Project group for control of sulphurs runoff in Agder). In this study, the guideline will be referred to as the Agder guideline. As shown by Lindum AS (2023) and Skjønborg (2023), the Agder method has numerous shortcomings and weaknesses, which in most cases will result in an incorrect characterisation of the acid gneiss.

Incorrect characterisations are described as false positives and false negatives. A false positive is defined as rocks being classified as acid-producing but are not acid-producing. In contrast, a false negative is defined as when rocks are classified as not acid-producing but are actually acid-producing. This incorrect characterisation leads to undesirable consequences. A consequence of a false negative is that those rocks are reused or placed in storage without any measures to prevent leaching. In addition, false positive leads to “clean” rocks being placed in approved landfills and occupying important space for acidic rocks, which is economically unfavourable for the developer.

1.2 Guidelines for characterisation of ARD

1.2.1 The Agder guideline

The Agder guideline recommends preliminary surveys of the planned action area; these recommendations include leaching test (Norwegian: ristetest), mineralogy and whole-rock geochemistry analysis, however, these are methods that are normally not applied during the investigation of the rocks due to the lack of recommended threshold values. Therefore, the three-step assessment is normally used for the characterisation of gneisses. The three-steps are the degree of weathering, sulphur (S) content, and temperature changes through H₂O₂.

The first step is to examine the degree of weathering on the rocks. If the rocks have a high degree of weathering they are automatically classified as acid-producing. If the degree of weathering is in the medium or low category, the rocks are supposed to be further assessed with S content and H₂O₂ test. A geologist decides on the degree of weathering, but no standardised methods exist (Prosjektgruppen for kontroll på svovelholdig avrenning i Agder, 2021). Therefore, any assessment is potentially an unreliable biased judgment call.

Further testing includes the determination of the total S content and H₂O₂ testing. The total S content is usually measured by using a handheld XRF on rock samples or its determination at an analytical laboratory. The following threshold values are used: low S (< 0.15 wt.%), medium S (0.15-0.8 wt.%) and high S (> 0.8 wt.%) contents (Prosjektgruppen for kontroll på svovelholdig avrenning i Agder, 2021). If the sample material belongs to the low or medium category, the sample will be tested with H₂O₂, and the final assessment will be seen in the context of the results from H₂O₂, where the H₂O₂ test becomes the deciding factor.

The H₂O₂ test is based on adding H₂O₂ to drilling dust and recording the temperature changes after 25 minutes. The following threshold values are used: low acid potential ($\Delta T < 0.7$ °C), medium acid potential ($\Delta T = 0.7-1.2$ °C) and high acid potential ($\Delta T > 1.2$ °C) (Prosjektgruppen for kontroll på svovelholdig avrenning i Agder, 2021). By using drilling dust for H₂O₂ testing, there is a risk that this could potentially give an unreliable result, considering the inverse correlation between reactivity and grain size and contamination with organic material, which can react exothermically with H₂O₂ (Xu *et al.*, 2022).

Figure 1 summarises the classification of the gneisses through the Agder method and illustrates the dependence between the steps: degree of weathering, S content and H₂O₂.

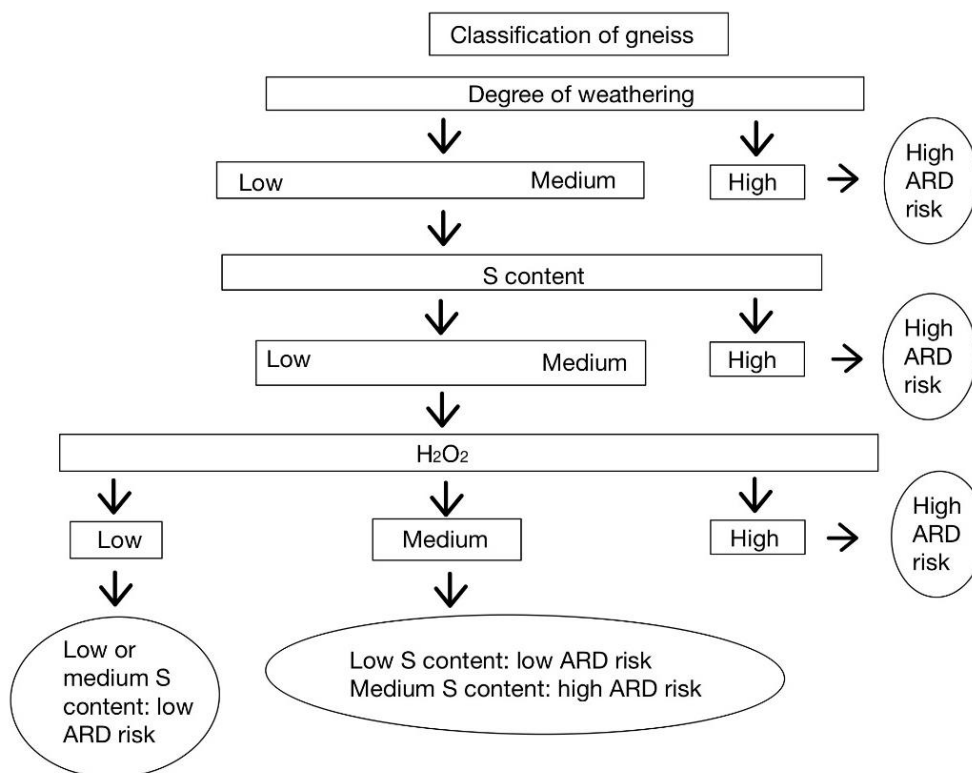


Figure 1: Flowchart of the three-step assessment of classification of gneiss. The figure is modified from Prosjektgruppen for kontroll på svovelholdig avrenning i Agder (2021). The degree of weathering decides whether the rock is further tested with S content and H₂O₂ test. If the rock has a high degree of weathering, the rocks are automatically acid-producing. If the rocks have a high S content, they are acid-producing, while the low and medium categories result in H₂O₂ testing. If the rock has a high temperature change, it is classified as acid-producing without taking S content into account. The medium is dependent on the S content, where low results are not acid-producing, and medium results are acid-producing. The low is also dependent on the S content, whereas the low and medium results in not-acid-producing rocks.

1.2.2 AMIRA guidelines

The AMIRA international ARD test handbook, written by Smart et al. (2002) at the Ian Wark Research Institute (University of South Australia), is used for acid rock drainage predictions. AMIRA describes a three-stage characterisation process of rocks or mining material. The first stage involves sample screening, which includes paste pH, electrical conductivity (EC), total sulphur determination, the calculation of net acid-producing potential (NAPP), neutralising capacity (ANC), and single addition net acid generation test (single NAG test) (Smart *et al.*, 2002). The paste pH is a test for assessing reactive minerals, i.e. the presence of stored acidity that is available in the sample, determined by mixing sample material with water. The EC is an indication of the salinity when the sample material is mixed with water. The single NAG test includes the use of H₂O₂ to accelerate the oxidation process of sulphur-containing minerals, which provides the net acid potential. The main objective of this test is to measure the NAG pH and titrate the solution with NaOH afterwards, where the amount of titrant is used to calculate the net acid generation (NAG). During the single NAG test, it is possible to add kinetic tests, such as recording the temperature, pH, and EC. The AMIRA handbook and single NAG test might be an inspiration for other handbooks worldwide.

Stage two involves further testing, including static tests and mineralogical characterisation (Smart *et al.*, 2002). Static tests could be sequential NAG, which is repeating the NAG test several times on the same sample material. Kinetic NAG tests are also included in stage two, this usually includes the single NAG test and recording of temperature, pH, or EC during the test. Mineralogical characterisation can give details of the composition of minerals in the material. An example is the detection of sulphide minerals and buffering minerals. There are several ways of characterising minerals, but typical methods include using X-ray diffraction (XRD), scanning electron microscopy (SEM), and geochemical analyses (Smart *et al.*, 2002).

Stage three is long-term testing, often involving leach column tests. Free-draining column tests are normally exposed to wetting and drying cycles in order to mimic a natural environment in which waste materials are exposed to water and oxygen. The pH and EC are determined after the water has flushed through the column. It is common to analyse these water samples for metals and ions (Smart *et al.*, 2002).

1.2.3 Summary of AMIRA method and Agder method

Table 1 shows an overview and a summary of the differences and similarities between the Agder guideline and AMIRA methods. Note that the Agder method includes fewer steps than the AMIRA method.

Table 1: Overview of the Agder method and AMIRA method, including similarities and differences.

Parameter	Agder guidelines	AMIRA method
Leaching tests	Leaching test, only at each 10 000 m ³	Leaching Column test
pH measurements	Leaching test, shake test	Paste pH
Weathering degree	Included, step 1 in characterisation	Not included
Total S content	Included, step 2 in characterisation	Included, usually uses XRF
H ₂ O ₂	Uses H ₂ O ₂ to oxidate S minerals and cause an exothermic reaction for temperature measurements	Uses H ₂ O ₂ to speed up oxidation reaction and then measures NAG pH
Mineralogy	Recommended, but normally not applied	Included in the guideline
ANC	Not included	Included in the guideline

Table 2 summarises the two different H₂O₂ methods used in the Agder and AMIRA methods. Note that there are some more considerable differences regarding the concentration and amount of H₂O₂ used and the amount of sample material.

Table 2: The main differences between the Agder and AMIRA guidelines for using the H₂O₂ test. Note that in the AMIRA method, it is possible to measure the temperature increase, but this is not used in the prediction of the acid-producing potential.

Parameter	Agder guidelines	AMIRA method
Mass sample	30 g, drilling dust	2.5 g, < 75 µm
H ₂ O ₂ strength	7%	15%
Liquid amount	200 mL	250 mL
Measurements	Starting temperature and temperature increase at 25 min are measured. The temperature increase is used to calculate ΔT_{25min} , which is used for deciding if the gneiss is acid-producing or not.	Measures NAG pH after reaction and heating the sample to decompose H ₂ O ₂ . After NAG pH, the solution is titrated to pH 4.5 and 7. Titration amount is used to calculate NAG. NAG pH and NAG are used to predict if the material is acid-producing or not.

1.3 Previous work done on acid-producing on gneiss in Norway

Table 3 presents work done on acid-producing gneiss, most of these reports are available from different organisations and are challenging to find. The overall language is Norwegian. Most of the reports have yet to be peer-reviewed.

The Geological Survey of Norway coordinates an ongoing mapping project on acid-producing gneiss in Kristiansand municipality (Marianne Bilksas, Kristiansand municipality, e-mail correspondence January 2024).

Table 3: Overview of previous work done on acid-producing gneiss in Norway.

Author	Title	Where to find
Adam Pearce	A Mineralogical and Geochemical Description of Potentially Acid-producing Gneisses from the Lillesand Area <i>Implications for Leaching Behaviour</i>	Master thesis University of Oslo http://urn.nb.no/URN:NBN:no-66959
Ingrid Skjønborg	An evaluation of methods for acid rock drainage prediction An assessment of short-term tests for prediction of long-term leaching behaviour	Master thesis University of Oslo https://www.duo.uio.no/handle/10852/105981
Prosjektgruppen for kontroll på svovelholdig avrenning i Agder.	Retningslinjer for tiltak i områder med syredannende gneis/ Guidelines for measures in areas with acid-forming gneiss	lillesand.kommune.no https://www.lillesand.kommune.no/forurensetgrunnbygging-og-graving.518415.no
Per Hagelia	Sur avrenning frå rusta svovelførande gneis/ Acid rock drainage from rusty sulphur-bearing gneiss	Statens vegvesens rapporter https://hdl.handle.net/11250/3083450
Lindum AS	Sluttrapport: Karakterisering av syredannende gneis - kunnskapsgrunnlag for utforming av retningslinjer / Final report: Characterisation of acid-forming gneiss - knowledge base for the development of guidelines	Unpublished. Contact person: Sandra Heldal at Lindum Sør
Lillesand kommune	Mapping gneiss of acid-producing gneiss	https://www.kommunekart.com/klient/lillesand/sitkart/

1.4 Aims of this study

Currently, the characteristic of gneiss is done by the Agder method, where H₂O₂ tests are one of three tests described in the method. The H₂O₂ test weighs heavily in the determination of whether a gneiss is acid-producing gneiss or not. Unfortunately, it appears that the H₂O₂ test has some problems, causing incorrect classification of the gneisses. This study aims to evaluate the Agder method H₂O₂ testing and assess sources for bias to temperature increases during the test and give recommendations for improvement. Consequently, this study has the following objectives:

- Investigate if secondary minerals may affect temperature changes during the H₂O₂ test and cause false negative or false positive results.
- Evaluate the AMIRA single NAG test, with kinetic test temperature logging.

1.5 Organisation of this thesis

This thesis is organised as follows:

- Chapter 2 presents a review of the geology in the area of southern Norway and Lillesand, where the gneisses are located.
- Chapter 3 introduces the concept of acid drainage, including the minerals that contribute to acid formation.
- Chapter 4 gives a description of the selected materials that were used in the experiments and a description of the methods used during the laboratory experiments.
- Chapter 5 presents the results, including a petrographic description of the gneiss samples, whole-rock geochemical analysis, and the Agder and AMIRA test data.
- Chapter 6 gives an interpretation and discussion of the results.
- Chapter 7: Concluding chapter.
- Chapter 8: Recommendation for future work.
- The appendix presents the raw data from the experiments and a summary of the results from the master thesis of Skjønborg (2023) and Pearce (2018).



Figure 3: South Norway presented with the different geological sectors. The Bamble sector includes Kristiansand to approximately Porsgrunn (Oslo rift). Figure from Nijland, et al. (2014).

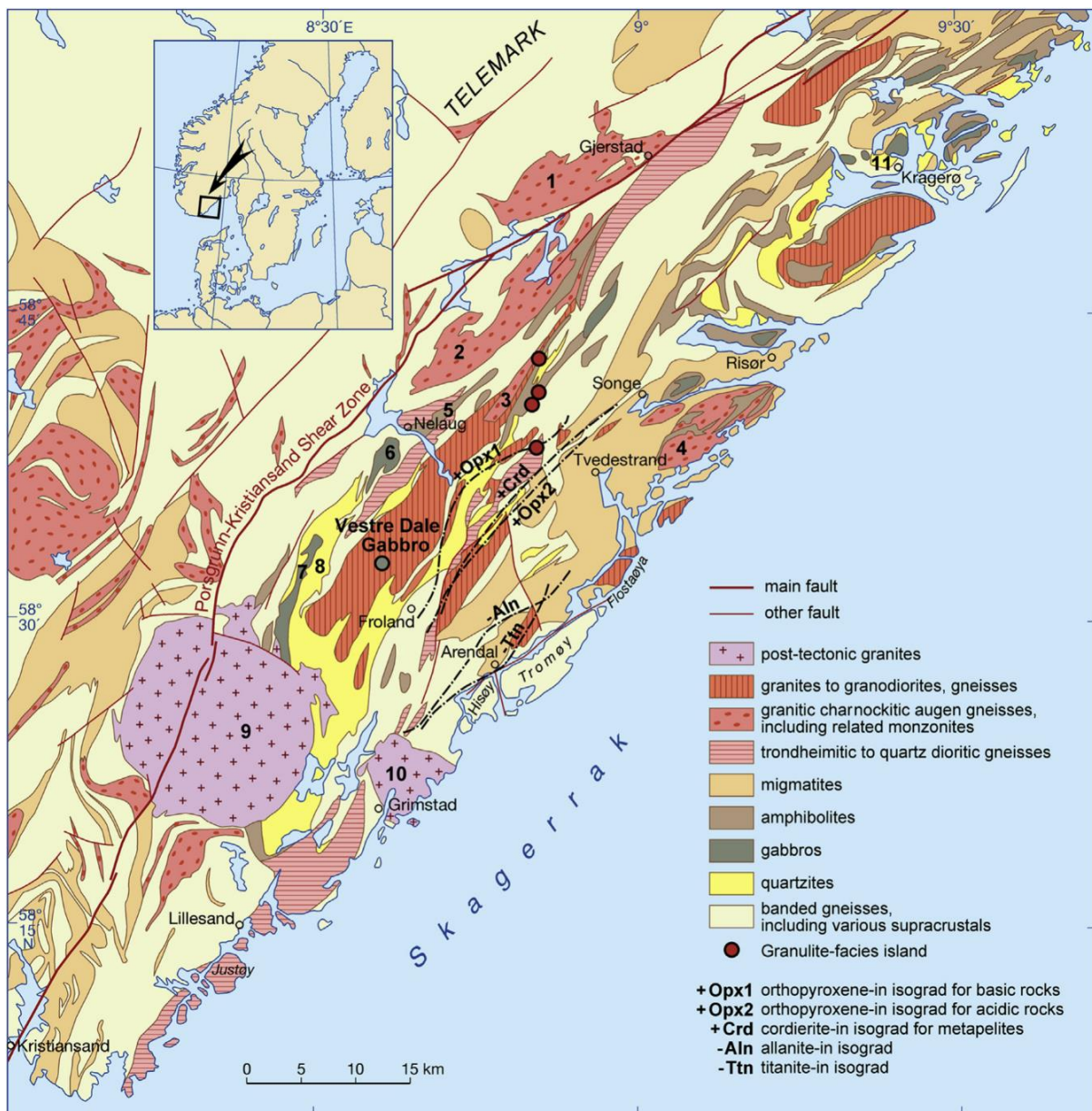


Figure 4: Bedrock map over Bamble sector. Lillesand is south on the map, and the dominant bedrock is gneiss. Map by Nijland et al. (2014). Note that the numbers in the map are related to the publication by Nijland et al. (2014) and are not relevant in this thesis.

The significant exposure of acid-producing gneiss in the Lillesand area resulted in funding for mapping these gneisses (Figure 5). Unfortunately, the Kristiansand municipality is not included in this map, and it is likely that acid-producing gneiss are also present in the Kristiansand municipality. In Lillesand, acid-producing gneiss are present in areas that are under consideration for development and construction work.

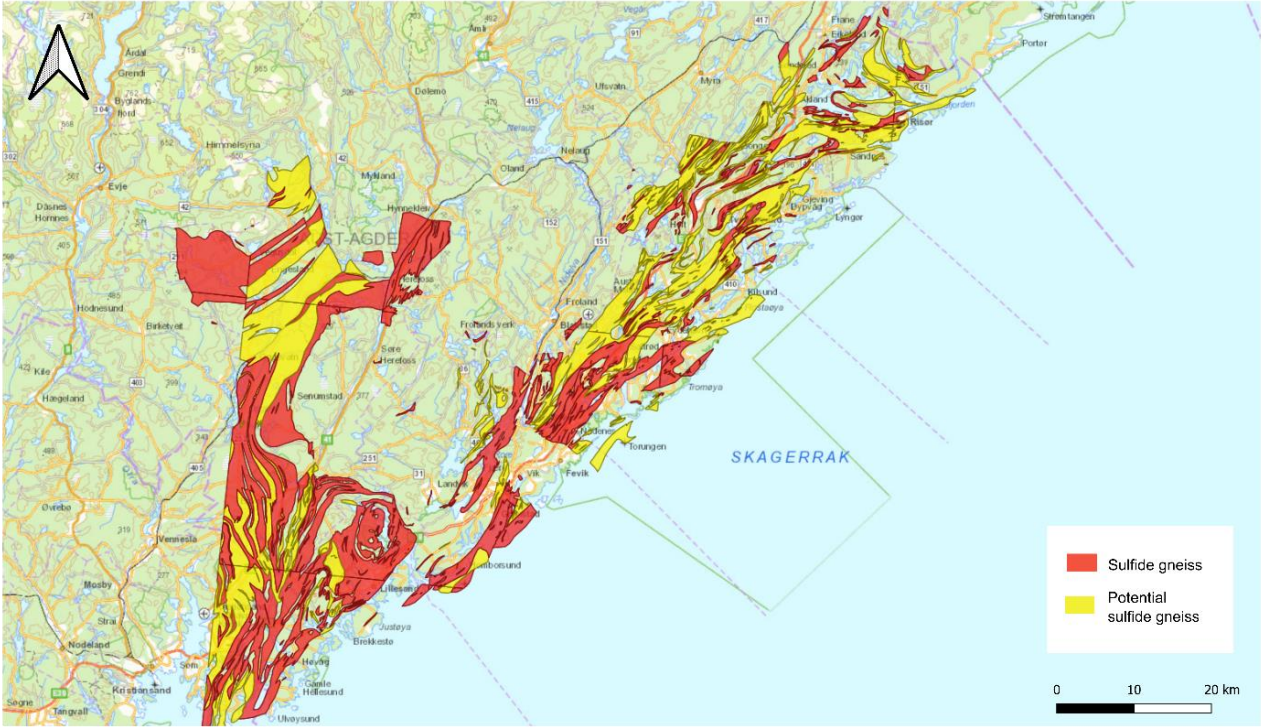


Figure 5: Map of acid-producing gneiss from Lillesand to Risør. Note that the original map did not include a scalebar or legend, i.e. the scalebar is therefore an approximation. Map: Ånund Ættesatd, Lillesand municipality. The criteria used for identifying the rocks are unknown.

3 Background

3.1 What is acid drainage?

As already mentioned in the first chapter, acid drainage is the process where rocks that are exposed to water and air and starts to produce a leachate with a low pH and relative enrichment of heavy metals, metals, and sulphate (Warren, 2011). Sulphur-rich minerals are typically the minerals that create acid drainage when exposed to water and air. There are several factors that are critical before acid drainage occurs (Akcil and Koldas, 2006):

1. Sulphide minerals must be or have been present.
2. Water/ precipitation/ humid atmosphere.
3. Oxidants, mainly oxygen and/or Fe(III) under acidic conditions.
4. Bacteria (not relevant in this thesis).

In general, a simplified equation can be used to describe acid drainage (Warren, 2011):



3.2 Environmental impact

A lowering of pH may lead to the release of heavy metals and metals such as nickel (Ni), cadmium (Cd), zinc (Zn), copper (Cu), lead (Pb) and aluminium (Al) (Hagelia, 2023). It is expected that in water systems with low pH, the metals are acting as dissolved ions, which is regarded as more bioavailable (Teien *et al.*, 2017). If the release of metals is in high concentrations it can be toxic for organisms, fish as an example are known to be sensitive to Al, and exposure to high concentrations could result in their death. For example, during the building of the new E18 Grimstad to Kristiansand, acid leaching affected the local rivers, resulting in high concentrations of Cu, Zn, Pb, Cd, Ni, Fe, and Al (Hagelia, 2023). This led to problems with fish dying, and in later times the Norwegian Public Roads Administration had to build cleaning systems for metals in the area around landfills and storage of acid gneiss.

3.3 Oxidation of sulphide minerals

Common iron sulphides include pyrite (FeS_2), pyrrhotite ($\text{Fe}_{(1-x)}\text{S}$), arsenopyrite (FeAsS), and chalcopyrite (CuFeS_2). However, other sulphides, such as sphalerite (ZnS) and galena (PbS) can contribute to acid drainage.

Pyrite is one of the most common sulphide minerals and is used here as an example to illustrate the acid-producing process. When pyrite is exposed to water and oxygen at a neutral pH (around 7) it will release H^+ according to the reaction:



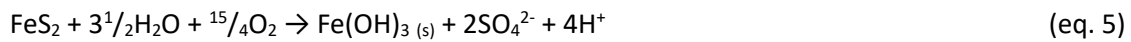
Furthermore, ferrous iron (Fe^{2+}) can be oxidised to ferric iron (Fe^{3+}).



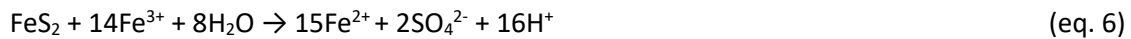
If the pH is above 4, this can cause precipitation of iron oxyhydroxide and release H^+ ions.



Therefore, the overall reaction can be described as:



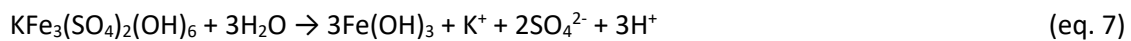
The release of H^+ will lower the pH in the environment, and when the pH is lower than 4 Fe^{3+} oxidises pyrite. This process will give negative feedback because oxidation by Fe^{3+} is faster than by oxygen:



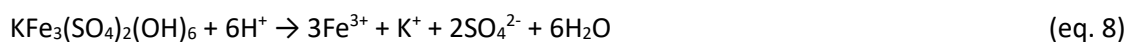
Inspection of eq. 3 and 6 illustrate the self-accelerating nature of these reactions.

3.4 The role of secondary minerals in acid drainage

It is not only primary minerals such as pyrite that can contribute to acid drainage, but also secondary minerals (e.g., jarosite, schwertmannite). Secondary minerals are usually formed by the chemical weathering of primary minerals (Raade, 2023) under acidic conditions. These secondary minerals can immobilise metals when they precipitate and release those metals, and increase the acidity when they dissolve (Hammarstrom *et al.*, 2005). Jarosite is an example of a secondary mineral that can contribute to acid drainage. Jarosite is usually formed by chemical weathering (oxidation) of pyrite (Welch *et al.*, 2008). Therefore, it is common in areas with acid mine drainage, but it also occurs in sulphide-rich rocks that have been weathered. Jarosite dissolves when it is in contact with H_2O :



If jarosite dissolves under acidic conditions (pH 2), the process will produce Fe^{3+} ions and consume H^+ . Eq. 8 shows the dissolution of jarosite at pH of 2 (Smith *et al.*, 2006). These Fe^{3+} ions can be used to oxidise pyrite as described in eq. 6.



3.5 Summary of produced H⁺ upon the oxidation of sulphides

To summarise and give an overview of the different minerals' release of H⁺ ions when they are oxidised is presented in Table 4. Sphalerite and galena do not produce any acidity when they are oxidised by oxygen and water. However, if they are oxidised by Fe³⁺ they will release H⁺ and contribute to acidity. Table 5 shows an overview of the same minerals, but Fe³⁺ oxidises them.

Table 4: Overview of released H⁺ ions by oxidation with oxygen. Sphalerite and galena are not producing any H⁺ during this reaction but are producing SO₄²⁻. Reaction equations are idealised reactions when the sulphide mineral is oxidised by oxygen. The table is modified from Dold (2017).

Mineral	Reaction	Release of H ⁺ to the environment when dissolved
Pyrite	$\text{FeS}_2 + 7/2\text{H}_2\text{O} + 15/4\text{O}_2 \rightarrow \text{Fe}(\text{OH})_3 (\text{s}) + 2\text{SO}_4^{2-} + 4\text{H}^+$	4
Pyrrhotite	$\text{Fe}_{(0.9)}\text{S} + 2.175 \text{O}_2 + 2.35\text{H}_2\text{O} \rightarrow 0.9\text{Fe}(\text{OH})_3 + \text{SO}_4^{2-} + 2\text{H}^+$	2
Arsenopyrite	$\text{FeAsS} + 2\text{O}_2 + 3\text{H}_2\text{O} \rightarrow \text{Fe}(\text{OH})_3 + \text{SO}_4^{2-} + \text{HAsO}_4^{2-} + 3\text{H}^+$	3
Chalcopyrite	$\text{CuFeS}_2 + 4\text{O}_2 + 3\text{H}_2\text{O} \rightarrow \text{Cu}^{2+} + \text{Fe}(\text{OH})_3 + 2\text{SO}_4^{2-} + 2\text{H}^+$	2
Sphalerite	$\text{ZnS} + 2\text{O}_2 \rightarrow \text{Zn}^{2+} + \text{SO}_4^{2-}$	0
Galena	$\text{PbS} + 2\text{O}_2 \rightarrow \text{Pb}^{2+} + \text{SO}_4^{2-}$	0

Minerals oxidised by Fe³⁺ release more H⁺ than if O₂ is the oxidising agent (Table 5). If oxidation with both Fe³⁺ and O₂ happens together, there will be an enrichment of H⁺ in the environment causing pH to lower. Different reactions are most likely to happen together, as the system is complex.

Table 5: An overview of minerals oxidised by Fe³⁺ and the corresponding release of H⁺. For using Fe³⁺ as an oxidant it needs to be produced in advance, and this reaction normally consumes H⁺, see eq. 3. The release of H⁺ indicated here is not corrected for the initial step of aqueous Fe³⁺ production. The table is modified from Dold (2017).

Mineral	Reaction	Release of H ⁺ to the environment when dissolved
Pyrite	$\text{FeS}_2 + 14\text{Fe}^{3+} + 8\text{H}_2\text{O} \rightarrow 15\text{Fe}^{2+} + 2\text{SO}_4^{2-} + 16\text{H}^+$	16
Pyrrhotite	$\text{Fe}_{(0.9)}\text{S} + 7.8 \text{Fe}^{3+} + 4\text{H}_2\text{O} \rightarrow 8.7\text{Fe}^{2+} + \text{SO}_4^{2-} + 8\text{H}^+$	8
Arsenopyrite	$\text{FeAsS} + 13\text{Fe}^{3+} + 8\text{H}_2\text{O} \rightarrow 14\text{Fe}^{2+} + \text{SO}_4^{2-} + \text{HAsO}_4^{2-} + 15\text{H}^+$	15
Chalcopyrite	$\text{CuFeS}_2 + 16\text{Fe}^{3+} + 8\text{H}_2\text{O} \rightarrow \text{Cu}^{2+} + 17\text{Fe}^{2+} + 2\text{SO}_4^{2-} + 16\text{H}^+$	16
Sphalerite	$\text{ZnS} + 8\text{Fe}^{3+} + 4\text{H}_2\text{O} \rightarrow \text{Zn}^{2+} + 8\text{Fe}^{2+} + \text{SO}_4^{2-} + 8\text{H}^+$	8
Galena	$\text{PbS} + 8\text{Fe}^{3+} + 4\text{H}_2\text{O} \rightarrow \text{Pb}^{2+} + 8\text{Fe}^{2+} + \text{SO}_4^{2-} + 8\text{H}^+$	8

Secondary minerals dissolution can contribute to releasing H⁺ into the environment when they dissolve (Dold, 2017), shown in Table 6.

Table 6: Dissolution of secondary minerals and their release of H⁺. The table is modified from Dold (2017).

Mineral	Reaction	Release of H ⁺ to the environment
Jarosite	$\text{KFe}_3(\text{SO}_4)_2(\text{OH})_6 + 3\text{H}_2\text{O} \rightarrow 3\text{Fe}(\text{OH})_3 + \text{K}^+ + 2\text{SO}_4^{2-} + 3\text{H}^+$	3
Schwertmannite	$\text{Fe}_{16}\text{O}_{16}(\text{OH})_{10}(\text{SO}_4)_3 + 6\text{H}_2\text{O} \rightarrow 16\text{FeO}(\text{OH}) + 3\text{SO}_4^{2-} + 6\text{H}^+$	6

4 Material and method

4.1 Samples

4.1.1 Selection of the gneiss samples for petrographic description, mineralogy, and whole-rock geochemical analysis

The sample selection of the gneisses is based on the results from Lindum's "Sluttrapport: karakterisering av syredannende gneis – kunnskapsgrunnlag for utforming av retningslinjer». In this report, H₂O₂ tests were compared with results from the column test. After comparison, it was discovered that there were false negative and false positive results (see section 1.1 for definition of false negative and false positive). Consequently, samples that show false negatives (five samples), false positives (four samples), and three correct samples were selected to address the aims of this study. The samples are presented in Table 7.

Table 7: Chosen samples based on Sluttrapport from Lindum and the following sample sites (Lindum AS, 2023). The highlighted samples are further investigated with H₂O₂ tests using both the AMIRA single NAG test and the Agder method in this study.

Sample	Result	Sample site	
		Latitude (°N)	Longitude (°E)
Tingsaker skole 1	False negative	58.260921	8.399565
Tingsaker skole 2	False negative	58.260921	8.399565
Tingsaker skole 3	False negative	58.260921	8.399565
Blakstad 3	False negative	58.503258	8.645421
Nordbø 1	False negative	58.243479	8.287549
Eydehavn 1B	False positive	58.499307	8.876161
Arendal legevakt 2	False positive	58.467843	8.755674
Arendal legevakt 5	False positive	58.467843	8.755674
Arendal legevakt 4	False positive	58.467843	8.755674
RV420#1	Correct	58.232812	8.317284
Birkeland 5	Correct	58.310679	8.25182
Gross 1	Correct	58.324626	8.577991

4.1.2 Selection of gneiss samples for single NAG test

For single NAG tests, three samples from gneiss. The details of the gneiss samples are shown in Table 8. Birkeland 5 is chosen due to its correctly characterisation as acid-producing by the Agder method (Table 8). It reacts well with H₂O₂ and has a low column pH. Meanwhile, Arendal legevakt 4 is characterised as false positive and has a column pH of 6.7. The Lindum results of Arendal legevakt 4 (Table 8) show high reactivity with H₂O₂, but the sample is not acid-producing. Since it is incorrectly characterised as acid-producing and reacts with H₂O₂, Arendal legevakt 4 was selected. The false negative sample Tingsaker skole #3 weakly reacted with H₂O₂ but is acid-producing with a column pH of 3.2.

Table 8: Overview of selected gneiss sample for further testing with H₂O₂. Sample information is from Lindum Skattefunnsluttrapport, and the samples were tested by the Agder method. Table modified from Lindum AS (2023).

Sample name	Consistency with column test	Weathering	wt.% S (category)	H ₂ O ₂ test ΔT _{25 min} (category)	pH from column test at Lindum
Birkeland 5	Correct	High	1.01 (high)	32.1 °C (high)	2.3
Arendal legevakt 4	False positive	Low	0.05 (low)	1.7 °C (high)	6.7
Tingsaker skole #3	False negative	Medium	0.005 (low)	1.1 °C (medium)	3.2

4.1.3 Selection of pure mineral phases for single NAG test

Other samples, such as ferrihydrite, pyrite, and quartz were selected with the purpose of testing their reaction with H₂O₂ (Table 9). This makes it easier to evaluate the effect and influence from other unknown minerals and amorphous content that could potentially react with H₂O₂, such as in the gneisses. Pyrite is used because it reacts with H₂O₂ and produces acid. Ferrihydrite is selected as a model for Fe(III) secondary phase, with the expectation that it will react with H₂O₂. LS-tailings are chosen as it is a weathered waste material from the Folldalen mines and are containing Fe oxides with no sulphides with the expectation that it will react with H₂O₂. Quartz does not react with H₂O₂, i.e. it is used as a blank sample, and additional material in the sample mixtures between pyrite, ferrihydrite-pyrite, and pyrite-LS-tailings mixtures. Sample mixtures are described in Table 10 for pyrite-quartz mixtures, Tables 11 and 12 for ferrihydrite-pyrite-quartz mixtures, and Table 13 for LS-tailings-pyrite-quartz mixtures.

Table 9: Selection of samples from other sources than gneiss. Purity results by XRD are provided by NGI.

Sample	Source	Purity (XRD)	Comments
Ferrihydrite	Synthesised (Dublet <i>et al.</i> , 2017)	100%	Amorphous Fe oxide
Pure pyrite	NMBU collection	100%	Acid-producing
Quartz	Commercial	100%	Not acid-producing or reactive
LS-tailings	Mine tailing form Folldalen		Weathered mine tailing, containing Fe oxides without sulphides

Table 10: Pyrite-quartz mixtures.

wt.% S	Pyrite (g)	Ferrihydrite (g)	Quartz (g)	SUM (g)
1.000	0.050	0.000	2.450	2.500
0.750	0.038	0.000	2.462	2.500
0.500	0.025	0.000	2.475	2.500
0.250	0.013	0.000	2.487	2.500
0.000	0.00	0.000	2.500	2.500

Table 11: Pyrite, ferrihydrite, quartz mixtures. Ferrihydrite amount is fixed at 0.5 g.

wt.% S	Pyrite (g)	Ferrihydrite (g)	Quartz (g)	SUM (g)
1.000	0.050	0.500	1.950	2.500
0.750	0.038	0.500	1.963	2.500
0.500	0.025	0.500	1.975	2.500
0.250	0.013	0.500	1.988	2.500
0.120	0.006	0.500	1.994	2.500
0.000	0.000	0.500	2.450	2.500

Table 12: Pyrite-ferrihydrate-quartz mixtures. Pyrite amount is fixed at 0.25 g.

wt.% S	Pyrite (g)	Ferrihydrate (g)	Quartz (g)	SUM (g)
0.500	0.025	0.050	2.425	2.500
0.500	0.025	0.250	2.225	2.500
0.500	0.025	0.400	2.075	2.500
0.500	0.025	0.500	1.975	2.500
0.500	0.025	0.700	1.775	2.500

Table 13: Pyrite – LS-tailings – quartz mixtures.

wt.% S	Pyrite (g)	LS-tailings (g)	Quartz (g)	SUM (g)
1.000	0.050	0.000	2.450	2.500
0.750	0.038	0.625	1.838	2.500
0.500	0.025	1.250	1.225	2.500
0.250	0.013	1.875	0.613	2.500
0.000	0.00	2.500	0.000	2.500

4.2 Sample collection, crushing and milling

4.2.1 Sample collection

Gneiss samples were already collected from the field or at the landfill in Lillesand and stored in buckets at Lindum in Drammen (Figure 6). The sample collector and date of collection are unknown. About 3 kg of sample material was taken from the buckets and put in plastic bags for transport to Feiring AS for crushing.



Figure 6: Stored samples at Lindum in Drammen.

4.2.2 Sample crushing

Gneiss samples were crushed by Feiring AS, using a Matest A075N Los Angeles crusher with 13 steel balls with a rotation at 1200 rpm. A painting brush was used to clean between each sample. Approximately 3 kg of material was crushed to a grain size less than 2 mm.



Figure 7: Inside of the Los Angeles crusher. Steel balls that are rolled together with the gneiss sample.

4.2.3 Agat milling and sieving

Approximately 250-300 g of the crushed material was sieved by using a 75 μm sieve. Material greater than 75 μm was milled on the Retch Agat mill at NMBU, where the material was milled for 3-4 min each time between sieving. This was repeated until 200 g of sieved material was collected. For cleaning, the mill was brushed with a brush and vacuumed. To minimise contamination, material of the same sample was used for pre-treatment of the mill.

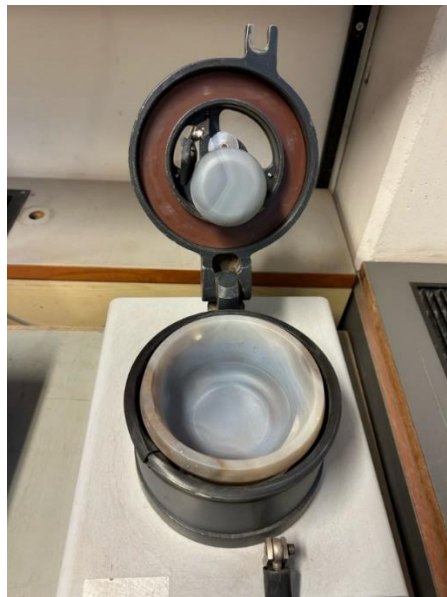


Figure 8: Retsch agate mill used at NMBU.

4.3 Mineralogy and geochemistry of gneiss samples

4.3.1 X-ray diffraction

Approximately 30 g of crushed material (< 2 mm) was put in small paper bags for X-ray analysis at *X-Ray Mineral Service UK* (<https://www.xrayminerals.co.uk/en/home/>) for XRD analysis.

X-ray diffraction (XRD) mineral quantification was done by the Rietveld refinement method. The method used Cu as the x-ray source, and the range of angle is from 4.5 to 75 presented in 2-theta. The quantification limit is < 0.5 wt.% for most minerals, but the limit can vary as it is a function of the matrix type. Lower values than the quantification limit are presented as trace amounts.

Analysis done on the samples is quantification of mineralogy, and amorphous content. Analysis of clay minerals was not performed, as it is expected to not be present in the rocks.

4.3.2 Whole-rock geochemical analysis

100 g of < 2 mm material was transported to ALS Global for chemical analysis in sealed allophane bags. Chemical analysis was done at ALS Czech Republic and ALS Scandinavia AB Luleå.

The gneiss samples were prepared for analysis by ALS, which included crushing and milling, and preparing of the samples for metal analysis by digestion HNO₃/HCl/HF in heat block and merger and support of the sample.

Analysis performed was drying (50 °C), dry matter content (105 °C), and loss on ignition (1000 °C), which are used for calculations of the water content and dry matter content in the rocks. Metal analysis was performed through ICP-SFMS using the US EPA method.

4.4 Paste pH and electric conductivity test

Two types of paste pH tests were done, one as defined by AMIRA and one with the same material amount as used in the H₂O₂ test.

Following the AMIRA method (Smart *et al.*, 2002), 5 g of rock material (< 75 µm) was transferred to 50 mL centrifuge tubes, and adding 10 mL milli-Q water until the ratio between sample and milli-Q was 1:2. The centrifuge tubes were placed on Heidolph REAX20 overhead shaker for 10 minutes at 13 rpm. Samples were set away for settling for 24 hours before measuring pH and EC. The pH meter was calibrated by a standard solution at pH values of 4.0, 7.0 and 10.0.

Inspired by the H₂O₂ test by AMIRA, 2.5 g material was mixed with 25 0mL milli-Q water with a magnetic stirrer, fulfilling the ratio 1:10. Magnetic stirring was done for 10 minutes at 200 rpm before the sample was stored for 24 hours. After 24 hours, the pH and EC were measured. This method was used on 2.5 g of pure quartz and ferrihydrite.

4.5 AMIRA single NAG tests

Samples that are selected and used during the Single NAG tests are described in sections 4.1.2 and 4.1.3. Samples involve the three selected gneisses and mixtures between pure mineral phases.

4.5.1 Single NAG test

Preparing for the single NAG tests, 30% H_2O_2 and milli-Q water were stored in the same fume hood as the tests. This was to reduce temperature differences in the beginning, as the temperature in the room was 16-17 °C, and the storing room had approximately 20 °C. During the test 900 mL beakers were placed in plastic buckets with a loose lid on top. The buckets were placed in a bigger cardboard box that was closed during the test by using a bigger plastic lid. This was done to reduce the influence of light on the experiments. During the experiments, the lights were switched off because H_2O_2 is light sensitive, as it decomposes in light (Roth, 2023).



Figure 9: Experimental design for single NAG test. The white buckets with beakers and temperature loggers are placed in a cardboard box. The cardboard box is closed during the experiment.

The single NAG test is done by the method from AMIRA (Smart *et al.*, 2002). 2.5 g of sample (< 75 μm) and temperature loggers from HBOB TidbiT MX Temp 400 were put in a 900 mL beaker. Temperature loggers were, in advance, covered in a thin layer of cling film and tape to protect the loggers. Subsequently, 250 mL of 15% H_2O_2 was added. The H_2O_2 was diluted to 15% from 30% with a ratio of 1:1 with milli-Q water. Temperature logging was done every 5 minutes for approximately 20 hours.

After the reaction was completed, the sample was heated to a maximum of 80 °C until the effervescence stopped. If the sample does not show any sign of effervescence on the hotplate after placing it on the hotplate, it was left on the hotplate for 2 hours to ensure that potential H₂O₂ residues are removed. The solution should have a final volume of 250 mL; therefore, it was added milli-Q water as needed.

After cooling down the solution, the NAG pH and EC were measured. After pH measurement, the suspension was filtered by using Pall Corporation 0.45 µm filter. After filtration 50 mL of gneiss samples solution were set away for metal analysis. 200 mL was used for titration with NaOH. Depending on the NAG pH, the choice of NaOH solution was made. According to AMIRA, 0.1 M NaOH should be used for titration if the NAG pH > 2, and 0.5 M NaOH should be used for titration if the NAG pH = 2. As most of the samples had a NAG pH over 2, 0.1 M NaOH was used. The solution was titrated to a pH of 4.5 and 7.

4.6 Oxalate extraction for removal of Fe(III)

4.6.1 Oxalate extraction of Fe and Al oxide procedure

The extraction solution is a mixture of 5 L milli-Q water, 81 g of ammonium oxalate ((NH₄)₂C₂O₄), and 54 g of oxalic acid (C₂H₂O₄). The pH in the extraction solution is, if necessary, adjusted with oxalic acid to a pH of 3. The extraction solution is durable for one week.

Oxalate extraction is done by adding 2.5 g of the sample material of gneiss, one pyrite-quartz mixture, and one ferrihydrite-pyrite-quartz mixture into 200 mL glass bottles, together with 125 mL of the oxalic extraction solution. The ratio between the sample material and extraction solution should be 1:50. The mixture needs to be shaken for 4 hours in the dark. Glass bottles were placed in a small cardboard box to give the samples a dark atmosphere. The extracted solution is stored in 50 mL centrifuge tubes for chemical analyses.

4.6.2 Preparing material for single NAG test

After oxalate extraction, the gneiss samples were washed with milli-Q water to remove the oxalate extraction solution. For that, the samples were washed repetitively (3-5 times) until the EC was below 26 µS/cm. The gneiss material was subsequently placed overnight in a drying cabin at 105 °C. The dried gneiss samples were weighted to determine the loss of material before the single NAG H₂O₂ test was done (as described in section 4.5.1).

4.7 NAG calculation in AMIRA single NAG test

The NAG is calculated by using this equation:

$$\text{NAG (kg H}_2\text{SO}_4\text{/t)} = (49 \times V \times M)/W \quad (\text{eq. 9})$$

where V denotes the total volume (L) used of NaOH during titration, M denotes the concentration of NaOH used (mol/L) for titration, and W is the sample mass in grams used during the H_2O_2 test. The constant 49 is a conversion factor to calculate $\text{kg H}_2\text{SO}_4\text{/t}$ (Smart *et al.*, 2002).

All samples were titrated with 0.1 M NaOH as the pH was higher than 2 (Smart *et al.*, 2002).

4.8 Water analyses of extracted solution and supernatants

In total 11 water samples were stored in centrifuge tubes and analysed at NMBU using an Agilent 5110 ICP-OES for Al, Fe, K, Mn, Na, S, Cu, and Zn. Table 14 gives an overview of the selected samples and the treatment before water chemistry analysis.

The metals Fe and Al are chosen because oxalate extraction extracts for Fe and Al oxides. Iron was also chosen due to the interest in the Fe-oxides, and S was selected as it causes acid leaching in the rocks. Therefore, it was of special interest to see if it occurs together with amorphous bounded Fe or in crystalline Fe. The metals K, Mn, Na, Cu and Zn are selected as there is an expectation that they are released from jarosite in the oxalate extraction and from sulphide minerals during the oxidation through the H_2O_2 test.

Table 14: Overview of selected extraction solutions for water analysis for samples Birkeland 5, Tingsaker skole #3, Arendal legevakt 4, and the pure mineral phases mixtures between ferrihydrite-pyrite-quartz and pyrite-quartz. The mark "X" marks the treatment before water analysis.

Sample	Treatment		
	Supernatant after H_2O_2	Oxalate extraction extract	Supernatant after H_2O_2 test on oxalate extracted material
Birkeland 5	X	X	X
Arendal legevakt 4	X	X	X
Tingsaker skole #3	X	X	X
Ferrihydrite 0.5 g - pyrite 0.5 wt.% S - quartz		X	
Pyrite, 0.75 wt.% S - quartz		X	

4.9 Agder method

30% H₂O₂ was diluted to 7% H₂O₂ by adding 46.6 mL 30% H₂O₂ to 153.4 mL milli-Q water. The initial temperature of this solution was measured before adding it into a 1000 mL beaker with 30 g of gneiss material (< 75 µm). Subsequently, the temperature was manually registered every 5 minutes for 25 minutes.

The room temperature during the test was 16-17 °C. The test was exposed to light and done in a fume hood.



Figure 10: Setup for the Agder method. The sample reacted visibly as exemplified by the formation of bubbles (steel grey colour) and generation of heat.

5 Results

5.1 Petrographic description of gneiss samples

Eydehavn 1B

The fresh surface colour of Eydehavn 1B is dark grey, almost black. The weathered surface has rust colour. It has a fine to medium grain size without foliation. The sample comprises quartz, feldspar, biotite, and pyroxene/amphibole.



Figure 11: Sample Eydehavn 1B.

Tingsaker skole #1

Tingsaker skole #1 (Figure 12) has a grey fresh-surface colour. It has a fine to medium grain size without foliation. The sample includes quartz, biotite, feldspar, and pyrite/pyrrhotite.



Figure 12: Sample Tingsaker skole #1, grey surfaced samples. This sample did not show any sign of weathered surface.

Tingsaker skole #2

Tingsaker skole #2 has a grey fresh-surface colour and a rust colour on the weathered surface (Figures 13, 14). It has a fine to medium grain size without foliation. The minerals include quartz, biotite, feldspar, and Fe oxides and possibly jarosite in the more weathered sample. Jarosite is suggested since the colour of the Fe oxides is yellow-dark brown-red and has a sandy characteristic, which is something that is pointed out in the report from Hagelia (2023).



Figure 13: Tingsaker skole #2, to the left the stone piece might be weathered as there is an orange colour in the outer corners.



Figure 14: Sample Tingsaker skole #2.

Tingsaker skole #3

Tingsaker skole #3 is a grey coloured rock on the fresh surface, the weathered surface is rusty orange-red. The sample to the right in Figure 15 is so weathered that it crumbles when touched. The sample has a medium grain size. It is not possible to see any foliation in the hand specimen. The sample comprises quartz, biotite, feldspar, and small amounts of pyrite or pyrrhotite. In the weathered

sample, there are Fe oxide minerals, and possibly jarosite due to the colour yellowish dark brown-red, and the weathered piece crumbles and has a sandy characteristic (Hagelia, 2023).



Figure 15: Sample Tingsaker skole #3. The piece to the left is fresh surface and has no sign of weathered surface. The piece to the right is rusty in the colour, and crumbles when touched.

RV420 #1

The surface colour of sample RV420#1 is grey, and the weathered surface has an orange-red rust colour. The sample has a fine to medium grain size without foliation. The sample comprises quartz, biotite, muscovite, feldspar, and pyrite or pyrrhotite. On the weathered surface Fe oxide minerals are present.



Figure 16: Sample RV420 #1.

Blakstad 3

The sample Blakstad 3 has a grey coloured fresh surface, with a more metallic look. The weathered surface is rusty orange in colour. The sample is fine to medium grain size without foliation. Minerals include quartz, biotite, feldspar, Fe oxides, and possibly jarosite due to yellowish dark brown-red colour.



Figure 17: Sample Blakstad 3.

Birkeland 5

Birkeland 5 did not have any fresh surface, but the weathered surface has a rusty yellow colour and rusty red colour, Figures 18 and 19. Birkeland 5 had a fine to medium grain size. It is not possible to see any sign of orientation or foliation in the sample. It was hard to see the mineralogy since it intensely weathered, but there is Fe oxide mineral (redish rust brown) present together with muscovite and quartz. This sample has a sulfuric smell and crumbles easily.



Figure 18: Birkland 5 had little variation in the sample. The sample itself are well weathered. This is the rusty yellow side.



Figure 19: The other side of Birkland 5. This is the rusty red surface.

Nordbø 1

Nordbø 1 (Figure 20) has a grey fresh surface, the weathered surface is rust yellow, with small amounts of rusty red. The grains are fine to medium, and a foliation is visible. The sample comprises quartz, biotite, muscovite, feldspar, and Fe oxide minerals.



Figure 20: Nordbø 1 has more weathered surface, but there are some spots inside the gneiss that is weathered.

Groos 1

Groos 1 (Figure 21) is a grey coloured rock on the fresh surface. The more weathered surface has a rusty red and orange colour. The grains are fine to medium; a foliation is not visible. Minerals comprises quartz, biotite, muscovite, feldspar, and possibly pyrite or pyrrhotite.



Figure 21: Groos 1, the piece to the left shows the grey fresh surface colour and the orange weathered colour. The piece to the right shows piece with reddish colour.

Arendal legevakt 2

Arendal legevakt 2 has a grey coloured fresh surface, whereas the weathered surface is rusty orange (Figure 22). The grain size is fine to medium, but foliation is not visible. The sample comprises biotite, pyroxene, quartz, feldspar, magnetite, and Fe oxide minerals.



Figure 22: Rock sample Arendal legevakt 2. The piece to the left is less weathered and has the freshest surface that is grey. To the right is more weathered and are more rusty orange coloured.

Arendal legevakt 4

The colour of the fresh surface of Arendal legevakt 4 is dark grey, with a metallic lustre. The weathered surface has a rust colour. The sample has a fine to medium grain size without foliation. The sample comprises quartz, biotite, pyroxene, feldspar, and Fe-oxides minerals on the weathered surface.



Figure 23: Sample Arendal legevakt 4.

Arendal legevakt 5

Arendal legevakt 5 is a grey coloured rock with a weathering colour with rusty yellow/orange grade. The sample is medium grained without foliation. Minerals include quartz, biotite, pyroxene, feldspar, and magnetite, while the weathered parts contain Fe oxide minerals. Some of the sample pieces are more weathered (Figure 24).



Figure 24: Rock sample from Arendal legevakt 5, three pieces to show the variation between the stones.

5.2 Mineralogical and geochemical characteristics of the gneisses of diverse response to H₂O₂ test

5.2.1 Major and trace element geochemistry

Major elements are presented in Table 15, where the results are divided into major oxides, total carbon (TC), total inorganic carbon (TIC), total organic carbon (TOC) and major elements calculated from the oxides. Fe₂O₃ ranges from 4.49 wt.% (Blakstad 3) to 10.70 wt.% (Birkeland 5). Note that for samples Eydehavn 1B and Arendal legevakt 4, the TC are lower than the TIC due to analytical error. The TIC is below the detection limit in the other gneiss samples and the TOC is only abundant in five of the gneiss samples. Loss on ignition (LOI) is an indication of the organic matter content in the rocks, and the dry matter indicates the amount of water in the rocks.

Table 15: Major element geochemistry of gneiss samples in wt.%. Elemental concentrations are calculated from the oxides. bdl stands for below detection limit.

Major elements	Eydehavn 1B	Tingsaker skole #1	Tingsaker skole #2	Tingsaker skole #3	RV 420#1	Blakstad 3	Birkeland 5	Nordbø 1	Groos 1	Arendal legevakt 2	Arendal legevakt 4	Arendal legevakt 5
Al ₂ O ₃	15.00	15.40	15.80	16.00	15.40	12.20	14.10	17.90	14.10	13.50	13.60	12.20
P ₂ O ₅	0.13	0.15	0.16	0.15	0.13	0.13	0.19	0.19	0.18	0.10	0.23	0.09
Fe ₂ O ₃	10.60	6.64	6.66	6.27	5.04	4.49	10.70	6.85	6.59	6.61	9.42	6.84
K ₂ O	0.90	2.06	2.17	2.04	2.16	2.75	2.02	1.41	2.51	1.09	0.82	0.81
CaO	9.19	3.14	2.96	3.26	2.44	0.62	4.09	5.40	1.22	1.20	4.51	1.56
MgO	7.93	2.22	1.88	2.04	1.50	2.14	3.11	2.40	1.60	1.94	3.15	2.05
MnO	0.15	0.08	0.08	0.08	0.06	0.03	0.12	0.09	0.04	0.11	0.20	0.15
Na ₂ O	2.56	3.06	2.92	3.13	3.06	0.71	1.93	4.55	2.55	5.88	4.92	5.05
SiO ₂	51.60	63.80	67.10	65.40	65.10	72.70	60.00	58.40	65.40	68.70	59.20	67.70
TiO ₂	0.90	0.72	0.70	0.68	0.57	0.62	1.18	0.58	0.66	0.45	0.78	0.46
Total	99.00	97.30	100.00	99.10	95.50	96.40	97.40	97.80	94.80	99.60	96.80	96.90
TC	0.07	0.08	0.13	0.07	0.04	0.11	0.23	0.26	0.43	0.06	0.05	0.05
TIC	0.09	bdl	bdl	bdl	bdl	bdl	bdl	bdl	bdl	bdl	0.06	bdl
TOC	bdl	bdl	0.13	bdl	bdl	0.11	0.23	0.26	0.43	bdl	bdl	bdl
Al	7.94	8.15	8.36	8.47	8.15	6.46	7.46	9.47	7.46	7.14	7.20	6.46
P	0.06	0.07	0.07	0.07	0.06	0.06	0.08	0.08	0.08	0.04	0.10	0.04
Fe	7.41	4.64	4.66	4.38	3.52	3.14	7.48	4.79	4.61	4.62	6.59	4.78
K	0.75	1.71	1.80	1.69	1.79	2.28	1.68	1.17	2.08	0.90	0.68	0.67
Ca	6.56	2.24	2.11	2.33	1.74	0.44	2.92	3.86	0.87	0.86	3.22	1.11
Mg	4.78	1.34	1.13	1.23	0.90	1.29	1.88	1.45	0.96	1.17	1.90	1.24
Mn	0.11	0.06	0.06	0.06	0.05	0.02	0.09	0.07	0.03	0.09	0.16	0.11
Na	1.90	2.27	2.17	2.32	2.27	0.53	1.43	3.38	1.89	4.36	3.65	3.75
Si	24.12	29.82	31.36	30.57	30.43	33.98	28.04	27.29	30.57	32.11	27.67	31.64
Ti	0.54	0.43	0.42	0.41	0.34	0.37	0.71	0.35	0.39	0.27	0.47	0.28
LOI (1000 °C) Dry material at 105 °C	0.49	1.13	0.95	0.91	0.98	1.86	3.13	0.80	2.64	0.04	0.34	0.10

Table 15 and 16 present the whole-rock geochemistry showing that the most abundant elements are Fe and S. The abundance of S in the samples ranges from 13000 ppm (Birkeland 5) to 125 ppm (Arendal legevakt 5). Arendal legevakt 2 is the only sample where S was not detected. Iron ranges from 3.52 wt.% (Blakstad 3) to 7.48 wt.% (Birkeland 5).

Using the S content characterisation of the samples (low: S < 1500 ppm, medium: S = 1500-8000 ppm, high: S > 8000 ppm) from "Retningslinjer for tiltak i områder med syredannende gneiss (Prosjektgruppen for kontroll på svovelholdig avrenning i Agder, 2021), there are four samples that are in the category low (Eydehavn 1B, Arendal legevakt 4, Arendal legevakt 5, Nordbø 1), five samples (RV420#1, Blakstad 3, Tingsaker skole #2, Tingsaker skole #1, Tingsaker skole #3) are in the medium group, and two samples (Birkeland 5 and Groos 1) have a high S content.

Table 16: Trace element contents in ppm. bdl stands for below detection limit.

Trace elements	Eydehavn 1B	Tingsaker skole #1	Tingsaker skole #2	Tingsaker skole #3	RV420#1	Blakstad 3	Birkeland 5	Nordbø 1	Groos 1	Arendal legevakt 2	Arendal legevakt 4	Arendal legevakt 5
As	bdl	bdl	bdl	bdl	4.59	bdl	bdl	bdl	bdl	bdl	bdl	bdl
Ba	283	349	379	332	353	484	576	313	447	211	135	195
Be	0.865	1.54	1.84	2.23	1.42	0.906	1.17	1.45	1.15	bdl	bdl	bdl
Cd	0.15	0.146	0.126	0.105	bdl	bdl	1.83	bdl	bdl	bdl	0.181	0.102
Co	44.7	16.7	13.5	15.4	6.52	8.69	18.6	13.8	14.5	7.33	18.3	10.5
Cr	386	45.8	58.5	46.4	41.4	54.9	69.8	39.7	67.1	15.9	33	11.8
Cu	62.8	33.4	40.2	43.2	26.5	57.5	68.5	51.2	103	9.13	34.7	16.5
Fe	74500	46500	46600	43800	35300	31400	74800	47900	46100	46300	65900	47900
Hg	bdl	bdl	bdl	bdl	bdl	bdl	bdl	bdl	bdl	bdl	bdl	bdl
Mo	bdl	bdl	bdl	bdl	bdl	bdl	bdl	bdl	bdl	bdl	bdl	bdl
Nb	5.84	9.2	9.67	8.41	9.01	12.9	7.01	bdl	10.3	bdl	bdl	bdl
Ni	141	29	25	29.8	10.1	13.5	31.8	12.9	32.7	3.1	16.7	6.46
Pb	4.24	11.9	10.7	11.1	14.6	4.72	11	7.71	14.5	5.9	8.15	7.07
S	1110	7330	7120	5160	2190	1980	13000	531	11400	bdl	559	125
Sc	31.7	14.2	15	12.3	11.7	11.3	25.5	14.7	15.6	16.7	26.3	16.1
Sn	bdl	bdl	bdl	bdl	bdl	bdl	bdl	bdl	bdl	bdl	bdl	bdl
Sr	177	280	263	307	249	48.7	145	720	99.6	70.9	165	94.8
Th	2.13	7.42	7.62	6.2	6.25	12.9	4.02	3.59	10.3	1.91	1.15	2.51
U	0.42	2.2	2.35	2.11	2.03	2.53	2.67	1.14	3.93	0.293	0.365	0.347
V	184	122	92.4	96.6	69.7	60.5	232	113	80.4	55.5	155	79.6
W	bdl	bdl	bdl	bdl	bdl	bdl	bdl	bdl	bdl	bdl	bdl	bdl
Y	33.4	27.9	25.9	21.5	27.9	28.8	29	12.7	36.9	22.6	22.2	20.5
Zn	95.7	96.7	80.6	89.9	89.2	40.1	291	87.6	78.9	74.6	205	97.8
Zr	114	160	171	157	160	363	130	97.9	207	70.4	64.9	70.8

5.2.2 Mineralogy of gneiss samples

The mineralogy determined by XRD is presented in Tables 17 and 18. The minerals that normally contributes to ARD is sulphide minerals, such as pyrite, which is only detected in samples Groos 1, Birkeland 5 and Tingsaker skole 1, and in trace amounts in Tingsaker skole 3. Birkeland 5 is the only sample with detected jarosite and goethite. Magnetite is detected in the samples Arendal legevakt 2, 4 and 5. Amorphous content is detected in six of the samples, where the highest values are found in Eydehavn 1B. Dolomite was detected in the samples Eydehavn 1B, Arendal legevakt 2 and Arendal legevakt 4. Calcite, on the other hand, was not detected in any of the samples. Note that the XRD analyses presented in Table 17 were done in context of this report, whereas Table 18 presents the XRD results obtained from NGI.

Table 17: XRD mineralogy presented in wt.%. The abbreviation TR stands for trace. Bold black are minerals that contain Fe(II), red are minerals with Fe(III), and purple are minerals with Fe(II/III).

Mineral	Eydehavn 1B	Tingsaker skole #2	RV420#1	Blakstad 3	Nordbø 1	Groos 1	Arendal legevakt 2	Arendal legevakt 4	Arendal legevakt 5
Biotite	6	19	15	11	11	6	4	4	8
Muscovite	0	3	5	19	0	13	0	0	0
Chlorite	TR	3	5	5	3	7	0	0	TR
Quartz	4	35	31	57	16	35	24	31	17
K Feldspar	0	4	4	0	0	8	6	TR	0
Plagioclase	40	37	41	8	45	20	53	45	38
Pyroxene	12	0	0	0	0	0	5	5	3
Amphibole	16	0	TR	0	9	0	0	1	12
Dolomite	3	0	0	0	0	0	1	1	0
Pyrite	0	0	0	0	0	1	0	0	0
Magnetite	0	0	0	0	0	0	2	2	3
Ilmenite	0	0	0	0	0	0	0	1	1
Rutile	0	0	0	0	0	0	TR	TR	0
Amorphous	20	0	0	0	16	10	6	11	18
Total	100	100	100	100	100	100	100	100	100

Table 18: XRD mineralogy of gneiss samples Tingsaker skole #1, Tingsaker skole #3 and Birkeland 5 in wt. %. Results are obtained from NGI. The amorphous content was not measured. Bold black are minerals that contain Fe(II), red are minerals with Fe(III).

Mineral	Tingsaker skole #1	Tingsaker skole #3	Birkeland 5
Illite+mica	9	14	7
Chlorite	4	4	5
Quartz	33	28	39
K Feldspar	7	5	6
Plagioclase	37	42	32
Amphibole	9	7	5
Pyrite	0.4	TR	2
Jarosite	0	0	1
Goethite	0	0	4
Total	100	100	100

5.3 Classification according to the Agder method

5.3.1 Classification of the gneisses by the Agder method

Results of the selected gneiss samples from the Agder guidelines are presented in Table 19 (Lindum AS, 2023). This table indicates several characterisations that are false, and there are only a few that are correctly characterised. The criteria for the assessment of the degree of weathering were based on the colour of the sample (Adam Pearce, e-mail correspondence, March 2024) (Table 19).

Table 19: Overview of gneiss samples and their properties, modified from Lindum AS (2023). pH from the column test is presented as pH (weeks). pH was measured in the column leachate, and “weeks” stands for the number of weeks since the experiment started. The criteria for the degree of weathering were based on the colour of the samples (Adam Pearce, e-mail correspondence, March 2024). ARD stands for acid rock drainage. The colours are organised as follows: red colour means high value (S content: > 0.8 wt.%, ΔT_{25min} : > 1.2 °C), orange is medium (S content: 0.15-0.8 wt.%, ΔT_{25min} : 0.7-1.2 °C), and green is low (S content: < 0.15 wt.%, ΔT_{25min} : < 0.7 °C). Threshold values are from the Agder guideline (Prosjektgruppen for kontroll på svovelholdig avrenning i Agder, 2021).

Sample	Weathering	wt.% S	H ₂ O ₂ test (ΔT_{25min})	Characterisation	pH from column test	Consistency with pH and characterisation
Eydehavn 1B	Medium	0.004	3.8	High ARD risk	7.8 (32w)	False positive
Tingsaker skole #1	Medium	0.006	0.8	Low ARD risk	3.6 (22w)	False negative
Tingsaker skole #2	Medium	0.01	0.8	Low ARD risk	3.5 (22w)	False negative
Tingsaker skole #3	Medium	0.005	1.1	Low ARD risk	3.2 (22w)	False negative
RV420#1	High	0.008	0.6	High ARD risk	2.6 (32w)	Correct
Blakstad 3	Medium	0.015	1.0	Low ARD risk	3.2 (32w)	False negative
Birkland 5	High	1.01	32.1	High ARD risk	2.3 (32w)	Correct
Nordbø 1	Medium	0.004	0.45	Low ARD risk	4.3 (32w)	False negative
Gross 1	High	0.008	1.25	High ARD risk	2.5 (32w)	Correct
Arendal legevakt 2	Medium	0.05	1.8	High ARD risk	6.6 (42w)	False positive
Arendal legevakt 4	Low	0.051	1.7	High ARD risk	6.7 (42w)	False positive
Arendal legevakt 5	Medium	0.051	2.1	High ARD risk	6.4 (42w)	False positive

The results of the Agder method provided in the context of this thesis for the selected gneiss samples are presented in Table 20. While doing this characterisation, the degree of weathering of the samples was used from Table 19, S content is from Table 16, and temperature changes are results in the context of this thesis done by the Agder method. Note that the Arendal legevakt 4 was tested twice with different light conditions in the room, one with light and one without light. The two different light conditions gave different ΔT_{25min} results.

Table 20: Categorising selected gneiss samples using the Agder method by the results from this thesis. The degree of weathering is provided by Lindum AS (2023). S content is the result from whole-rock geochemistry, and ΔT_{25min} is the results from the Agder H₂O₂ test performed by the author. Red colour means high value (S content: > 0.8 wt.%, ΔT_{25min} : > 1.2 °C), orange is medium (S content: 0.15-0.8 wt.%, ΔT_{25min} : 0.7-1.2 °C), and green is low (S content: < 0.15 wt.%, ΔT_{25min} : < 0.7 °C). Threshold values are from the Agder guideline (Prosjektgruppen for kontroll på svovelholdig avrenning i Agder, 2021). The criteria for the degree of weathering were based on the colour of the samples (Adam Pearce, e-mail correspondence, March 2024). ARD stands for acid rock drainage. The column exposure to light describes the light conditions in the room during the experiment.

Sample	Weathering	S content [wt.%]	ΔT_{25min} [°C]	Characterisation	Exposure to light during the experiment
Tingsaker skole #3	Medium	0.52	1.0	High ARD risk	Exposed to light
Birkland 5	High	1.3	21.3	High ARD risk	Exposed to light
Arendal legevakt 4	Medium	0.056	0.22	Low ARD risk	Not exposed to light
Arendal legevakt 4	Medium	0.056	1.0	Low ARD risk	Exposed to light

5.3.2 Manual temperature logging during the Agder method H₂O₂ test

The $\Delta T_{25\text{min}}$ manual temperature logging results are illustrated in Figure 25 (Birkeland 5), Figure 26 (Tingsaker skole #3), and Figure 27 (Arendal legevakt 4). During the test, temperature changes were logged every 5 minutes throughout the 25-minute test. As presented in Figure 25, sample Birkeland 5 reached its maximum temperature after 10 minutes. Tingsaker skole #3 reached the maximum temperature after 5 minutes and, surprisingly, cooled before it reacted again. Arendal legevakt 4 (Figure 27) shows a temperature increase during the first 15 minutes.

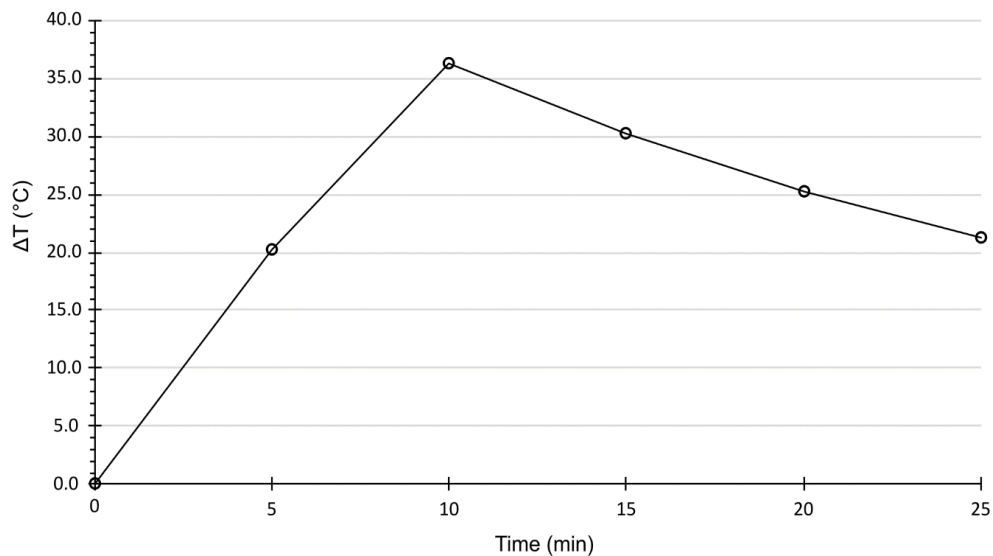


Figure 25: Manually temperature logging of sample Birkeland 5 during the 25 minutes. Maximum temperature is reached after 10 minutes. A temperature change of 21.3 °C was recorded after 25 minutes.

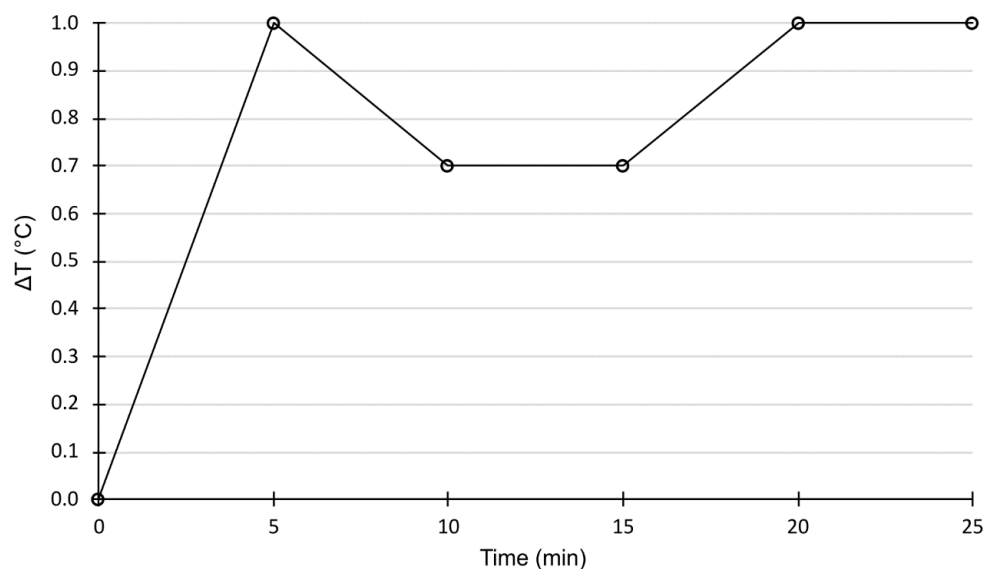


Figure 26: Manually temperature logging of sample Tingsaker skole #3. The sample reaches the maximum temperature after 5 minutes. A temperature change at 1 °C was recorded after 25 minutes.

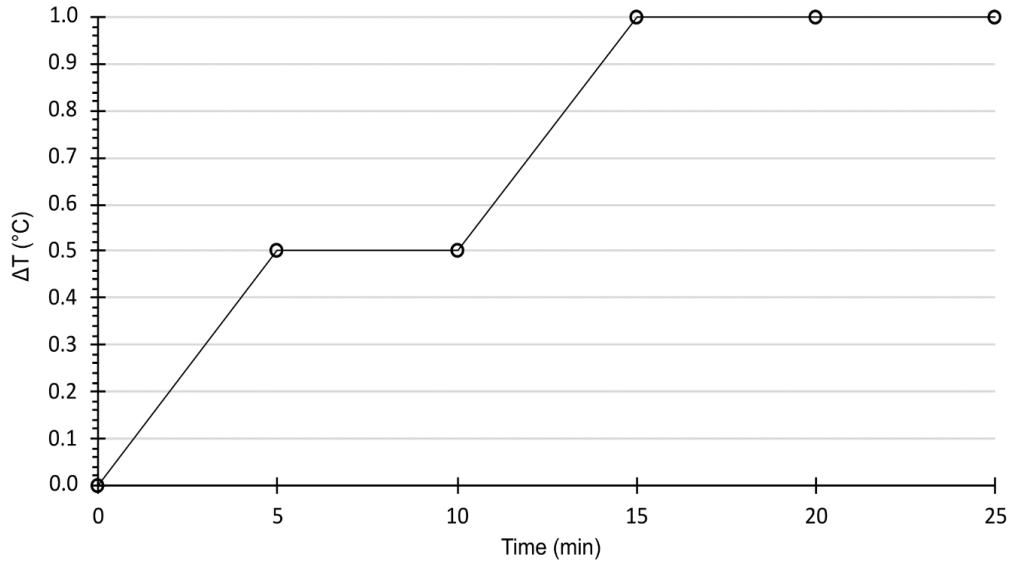


Figure 27: Manual temperature logging of sample Arendal legevakt 4 by the Agder method.

5.3.3 Column experiment at Lindum

Figure 28 shows pH measurements over a 1.5-year period for gneiss samples Arendal legevakt 4, Tingsaker skole #3 and a two-year period for Birkeland 5. The pH measurements illustrate that the pH stabilises around pH 3 after 24 weeks for the samples Tingsaker skole #3 and Birkeland 5, while Arendal legevakt 4 stabilises around pH between 7 to 8 after 80 weeks. The column test has been going on for 120 weeks for sample Arendal legevakt 4, and approximately 75 weeks for the samples Tingsaker skole #3 and Birkeland 5.

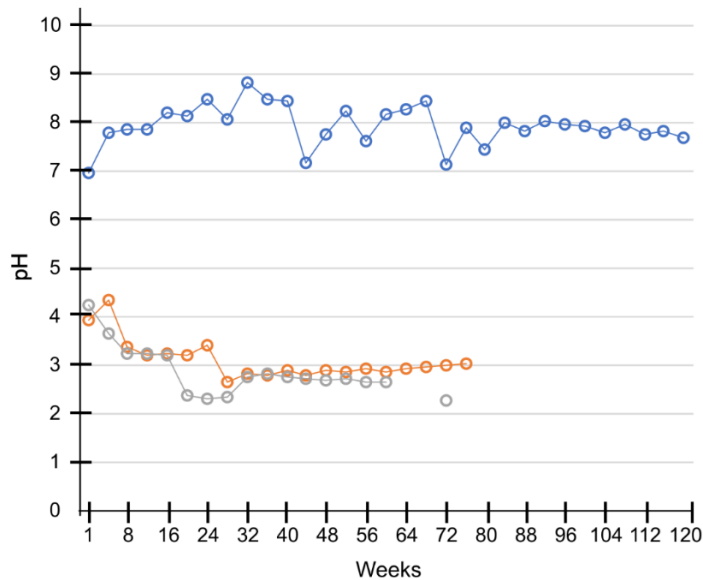


Figure 28: Results from column experiment done at Lindum. Each pH measuring is done every 4 weeks and watered with deionised water once a week. Blue: Arendal legevakt 4, orange: Tingsaker skole #3, grey: Birkeland 5. Tingsaker skole #3 and Birkeland 5 started at a later time than Arendal legevakt 4, which explain why Arendal legevakt 4 has a longer pH logging time.

5.4 Single NAG test on gneiss samples

5.4.1 Net acid generation characterisation of the gneisses

Table 21 presents the paste pH, NAG pH, NAG, and acid potential results. Tingsaker skole #3 and Arendal legevakt 4 have a paste pH over 7. For Tingsaker skole #3 this was unexpected as the column test had a pH below 4 (Figure 28). Arendal legevakt 4 was expected to have a pH around 7 as the column experiment has a pH around 7. Birkeland 5 has a pH around 4, which was expected as the sample is weathered.

The paste pH is calculated as an average from triplicates presented in Appendix A. Duplicate NAG pH and NAG test results (AMIRA method) of the gneiss samples (Table 21). Both the NAG pH and NAG (kg H₂SO₄/t) results give the same characterisation of the samples.

Table 21: Acid potential of selected gneiss sample. Paste pH is calculated from triplicates, presented in Appendix A. NAG pH and NAG are used to determine the acid potential of the samples. Red colour means that the values are below the acid potential limits, where NAG pH < 4.5 and NAG > 5 are coloured red (Smart et al., 2002). NAF: Non-acid-forming, PAF: potentially acid-forming.

Sample	Paste pH	NAG pH	NAG (kg H ₂ SO ₄ /t)	Acid potential of sample
Birkeland 5	4.2	2.4	27.3	PAF
Birkeland 5		2.5	26.4	PAF
Arendal legevakt 4	7.8	6.9	0.18	NAF
Arendal legevakt 4		6.8	0.21	NAF
Tingsaker skole #3	7.3	3.0	10.8	PAF
Tingsaker skole #3		2.9	13.4	PAF

Table 22 presents the NAG pH and NAG of the pre-treated gneiss sample with oxalate extraction. Although the gneiss samples are pre-treated, the NAG pH is similar for the untreated gneiss samples (Table 21). Net acid generation (NAG) values are lower for both Birkeland 5 and Tingsaker skole #3, whereas Arendal legevakt 4 has higher NAG values in pre-treated material. The NAG calculations are adjusted for the amount of sample material, as some material was lost during the oxalate extraction procedure (see Appendix D for material loss).

Table 22: Pre-treated gneiss samples with oxalate extraction and the acid potential. NAG pH and NAG are used to determine the acid potential of the samples. Red colour means that the values are below the acid potential limits, where NAG pH < 4.5 and NAG > 5 are coloured red (Smart et al., 2002). NAF: Non-acid-forming, PAF: potentially acid-forming.

Sample	Paste pH	NAG pH	NAG (kg H ₂ SO ₄ /t)	Acid potential of sample
Birkeland 5	-	2.7	17.0	PAF
Birkeland 5		2.8	19.5	PAF
Arendal legevakt 4	-	6.6	0.7	NAF
Arendal legevakt 4		6.6	0.6	NAF
Tingsaker skole #3	-	3.0	7.4	PAF
Tingsaker skole #3		2.9	11.5	PAF

5.4.2 Temperature logging during the single NAG test of the gneisses

Temperature logging of Arendal legevakt 4 of both original gneiss powder (black) and oxalate extracted powder (green) is presented in Figure 29. The original sample reaches maximum temperature after 1.5 hours and starts cooling after 2.5 hours. ΔT is approximately 0.22 °C by using the AMIRA method. Oxalate treated material has no temperature increases.

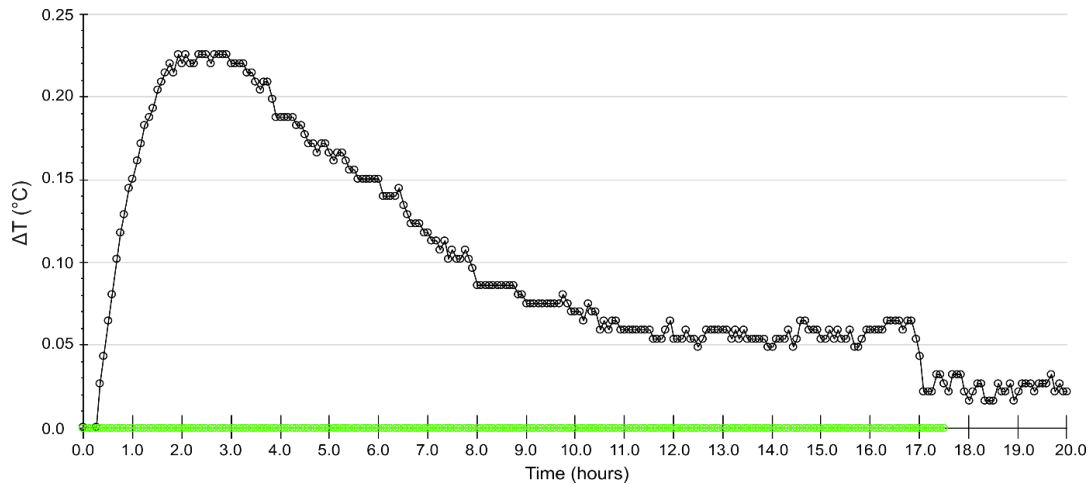


Figure 29: Arendal legevakt 4 presented as ΔT (°C) average from duplicates from each experiment type. Black is Arendal legevakt 4 done by AMIRA method. Green is Arendal legevakt 4 prepared by oxalate extraction before temperature logging by the AMIRA method.

By the AMIRA method (black) Tingsaker skole #3 has a fast increase at the beginning of the tests before it slows down and then accelerates again (Figure 30). Tingsaker skole #3 needs a longer time to react and has the maximum temperature at approximately 33 hours after the addition of H_2O_2 . Oxalate extracted material (green) has a faster increase in the beginning after adding H_2O_2 before it cools off and shows small changes after 24 hours. Overall, the ΔT is smaller in the oxalate treated material than the temperature increases by AMIRA (black).

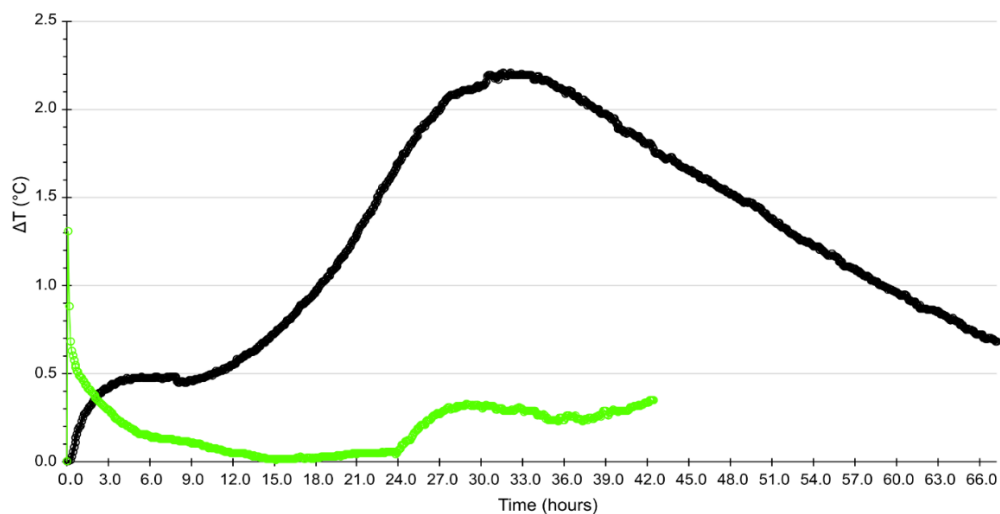


Figure 30: Tingsaker skole #3 presented as ΔT (°C) average from duplicates from each experiment. Black is done by the AMIRA method. Green is oxalate extraction prepared gneiss sample before AMIRA method.

By the AMIRA method (black) Birkeland 5 is the most reactive of the sample, it reacts fast and strongly. Figure 31 presents Birkeland 5 by AMIRA and oxalated treated material (green). By using AMIRA, the sample has a ΔT_{max} of 46 °C after approximately 2.5 hours, compared to oxalate treated material that has a lower ΔT_{max} of approximately 8 °C after 7 hours, and needs longer time to react.

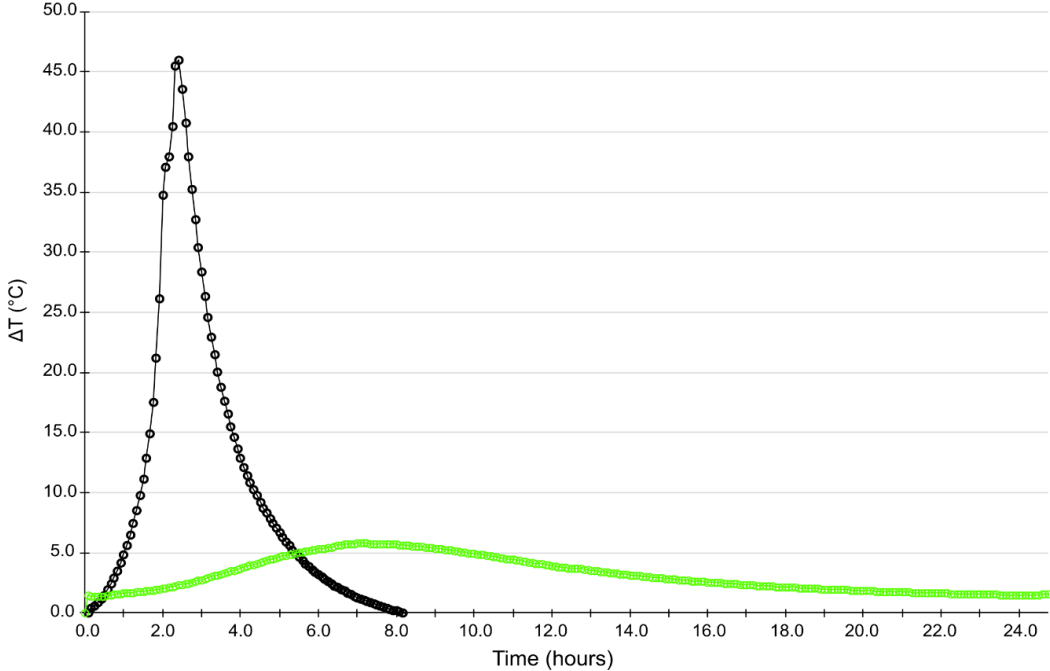


Figure 31: Birkeland 5 presented as ΔT (°C) average from two experiments. Black represents the AMIRA test method, whereas green is the oxalated pre-treated gneiss sample before doing the AMIRA method.

5.4.3 Summary of gneiss characteristics by AMIRA method

A comparison of the standard AMIRA single NAG test and modified single NAG test by pre-treatment with oxalate extraction is presented in Table 23.

Table 23: A summary of the standard AMIRA single NAG test and the modified single NAG test with pre-treated oxalate extracted samples material. Paste pH is presented as an average from triplicates, and NAG pH, NAG, ΔT_{max} and ΔT_{25min} are presented as an average from duplicates. Red colour means that the values are below the acid potential limits, where NAG pH < 4.5 and NAG > 5 are coloured red (Smart et al., 2002). NAF: Non-acid-forming, PAF: potentially acid-forming.

Sample	Standard AMIRA H ₂ O ₂ test						Modified AMIRA by oxalate extracted sample H ₂ O ₂ test				
	Paste pH	NAG pH	NAG (kg H ₂ SO ₄ /t)	Acid potential of sample	ΔT_{max} [°C] (time reached)	ΔT_{25min} [°C]	NAG pH	NAG (kg H ₂ SO ₄ /t)	Acid potential of sample	ΔT_{max} [°C] (time reached)	ΔT_{25min} [°C]
Tingsaker skole #3	7.3	3.0	12.1	PAF	2.2 (30hr 18 min)	0.1	3.0	9.5	PAF	1.3 (5min)	1.2
Birkeland 5	4.2	2.5	26.9	PAF	46.0 (2hr 24min)	1.2	2.8	18.3	PAF	5.8 (6hr 45min)	1.4
Arendal legevakt 4	7.8	6.9	0.2	NAF	0.23 (2hr 18min)	0	6.6	0.7	NAF	0	0

5.5 Single NAG test of mixtures of known proportions of pyrite and ferrihydrite

5.5.1 Classification of pyrite-ferrihydrite-quartz mixtures

Table 24 presents NAG pH and NAG of the different mixes between pyrite-quartz, pyrite-ferrihydrite-quartz with ferrihydrite fixed at 0.5 g and ferrihydrite-pyrite-quartz, with pyrite fixed at 0.025 g (0.5 wt.% S). The pyrite mixtures are characterised as potential acid-forming (PAF), while pure quartz is non-acid-forming (NAF). Ferrihydrite mixtures are characterised as PAF if the S wt.% content is 0.75 and 1 and low capacity PAF (PAF-LC) if the S content is 0.5 to 0.12 wt.%. Pure ferrihydrite, on the other hand, is characterised as NAF and PAF, depending on the duplicate, the deciding factor for the assessment was NAG pH.

Table 24 present NAG pH and NAG of selected samples that have been through oxalate extraction. The sample has a NAG pH at 2.8, while NAG pH for normal treatment is in the range between 2.6-2.5. This is a slightly change in the NAG pH, but the NAG calculation and the acid potential of the sample is still acid-producing.

Table 24: Acid potential of the mixed samples from pyrite and ferrihydrite (duplicate tests). Paste pH is done on pure quartz and pure ferrihydrite. NAG pH and NAG are used to determine the acid potential of the mixtures. Red colour indicates values below the acid potential limits, where NAG pH < 4.5 is coloured red, and NAG > 5 is coloured red (Smart et al., 2002). NAF: non-acid-forming, PAF: potentially acid-forming, PAF-LC: potential acid-forming – lower capacity. PAF-LC is described as material that may be able to treat with lime or other NAF material (Smart et al., 2002). ΔT_{max} is the average from the duplicates of samples.

Sample	Paste pH	NAG pH	NAG (kg H ₂ SO ₄ /t)	Acid potential of sample	ΔT_{max} [°C]
<i>Pyrite-quartz</i>					
Pyrite, 1 wt.% S		2.3	24.7	PAF	22.3 (5hr 40min)
Pyrite, 1 wt.% S		2.3	25.9	PAF	
Pyrite, 0.75 wt.% S		2.6	16.1	PAF	8.1 (6hr 35min)
Pyrite, 0.75 wt.% S		2.5	19.1	PAF	
Pyrite, 0.5 wt.% S		2.6	14.3	PAF	1.5 (8hr 15min)
Pyrite, 0.5 wt.% S		2.3	10.5	PAF	
Pyrite, 0.25 wt.% S		2.9	5.1	PAF	0.2 (2hr 20min)
Pyrite, 0.25 wt.% S		2.9	6.3	PAF	
Quartz, 0 wt.% S	8.1	3.8	1.9	NAF	0
<i>Ferrihydrite-pyrite-quartz, ferrihydrite fixed at 0.5 g</i>					
Ferrihydrite 0.5 g, 1 wt.% S		2.6	11.5	PAF	6.2 (2hr 5min)
Ferrihydrite 0.5 g, 1 wt.% S		2.7	14.7	PAF	
Ferrihydrite 0.5 g, 0.75 wt.% S		2.8	9.5	PAF	8.9 (2hr 5min)
Ferrihydrite 0.5 g, 0.75 wt.% S		2.7	9.4	PAF	
Ferrihydrite 0.5 g, 0.5 wt.% S		3.0	4.6	PAF-LC	12.6 (2hr 15min)
Ferrihydrite 0.5 g, 0.5 wt.% S		3.0	4.9	PAF-LC	
Ferrihydrite 0.5 g, 0.25 wt.% S		3.7	2.9	PAF-LC	36.8 (2hr 35min)
Ferrihydrite 0.5 g, 0.25 wt.% S		3.8	1.2	PAF-LC	
Ferrihydrite 0.5 g, 0.12 wt.% S		4.1	0.9	PAF-LC	43.7 (2hr 5min)
Ferrihydrite 0.5 g, 0.12 wt.% S		4.2	0.6	PAF-LC	
Ferrihydrite 0.5 g, 0 wt.% S	3.6	4.7	0.2	NAF	34.0 (1hr 55min)
Ferrihydrite 0.5 g, 0 wt.% S	3.6	4.4	0.5	PAF-LC	
<i>Ferrihydrite-pyrite-quartz, pyrite fixed at 0.025g (0.5 wt.% S)</i>					
Ferrihydrite 0.05 g, 0.5 wt.% S		2.6	10.8	PAF	0.4 (1hr 55min)
Ferrihydrite 0.25 g, 0.5 wt.% S		2.8	8.7	PAF	2.0 (1hr 45min)
Ferrihydrite 0.4 g, 0.5 wt.% S		3.0	5.3	PAF	7.9 (5hr 35min)
Ferrihydrite 0.7 g, 0.5 wt.% S		3.4	2.9	PAF-LC	53.6 (1hr 10min)
<i>Pretreated with oxalate extraction: pyrite-quartz</i>					
Pyrite, 0.75 wt.% S		2.8	9.9	PAF	0

5.5.2 Temperature logging during the single NAG test for pyrite-quartz and ferrihydrite-pyrite-quartz mixtures

Figure 32 presents ΔT of pyrite-quartz mixtures at different S content. This gives an indication of how the different amounts of S content in the samples will influence the reactivity towards H_2O_2 . The blue curve has the steepest and highest temperature increases, which is expected as the S content is 1 wt.%. As expected, lower S content results in a lower and slower temperature increase in the samples.

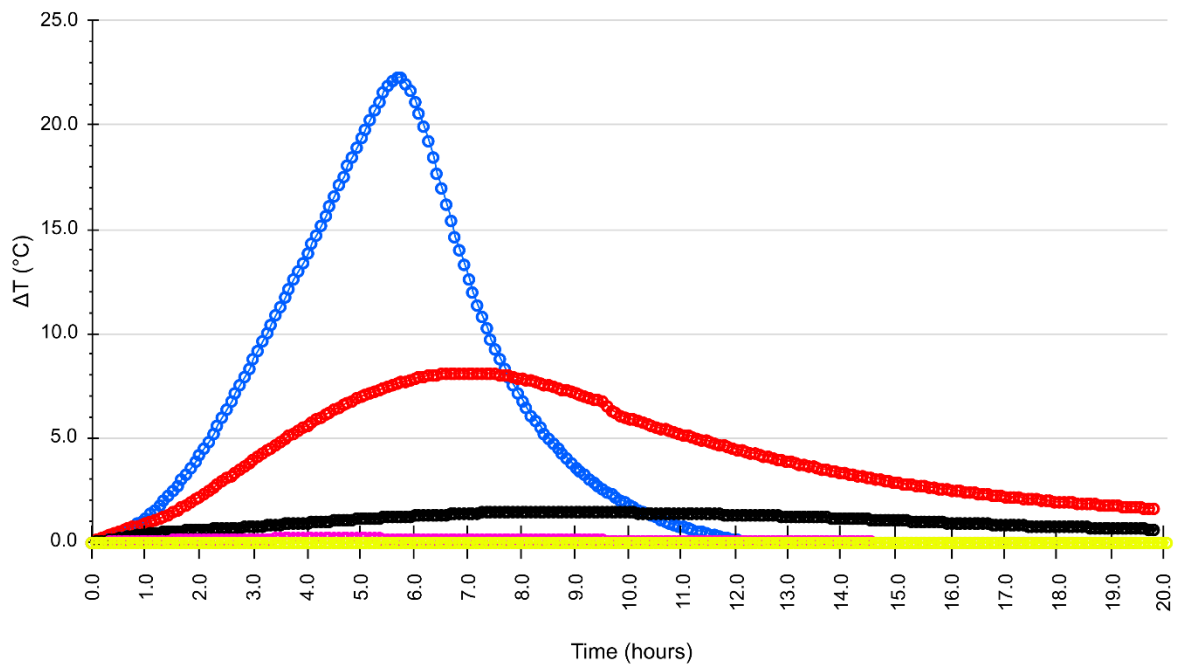


Figure 32: Temperature evaluation in pyrite-quartz mixtures from the single NAG test. Results are presented as ΔT , i.e. the difference in temperature compared to the prior H_2O_2 addition. Different colours represent different amounts of pyrite, and therefore, variable amounts of S. Blue: 1 wt.% S, red: 0.75 wt.% S, black 0.50 wt.% S, pink: 0.25 wt.% S, yellow: 0 wt.% S. The blue curve with the highest S content reacts the most and fastest, a lower S content in the samples gives lower and slower reactions until zero S content where there is no reaction with the H_2O_2 .

Ferrihydrite-pyrite-quartz (ferrihydrite fixed at 0.5 g) mixtures shows the opposite trend with temperature increases than in the pyrite-quartz mixtures (Figure 33). The lower the S content, the higher the temperature increase. However, pure ferrihydrite (0 wt.% S, without pyrite content) reacts faster but gives a lower ΔT than ferrihydrite-pyrite-quartz mixture of 0.12 wt.% and 0.25 wt.% S.

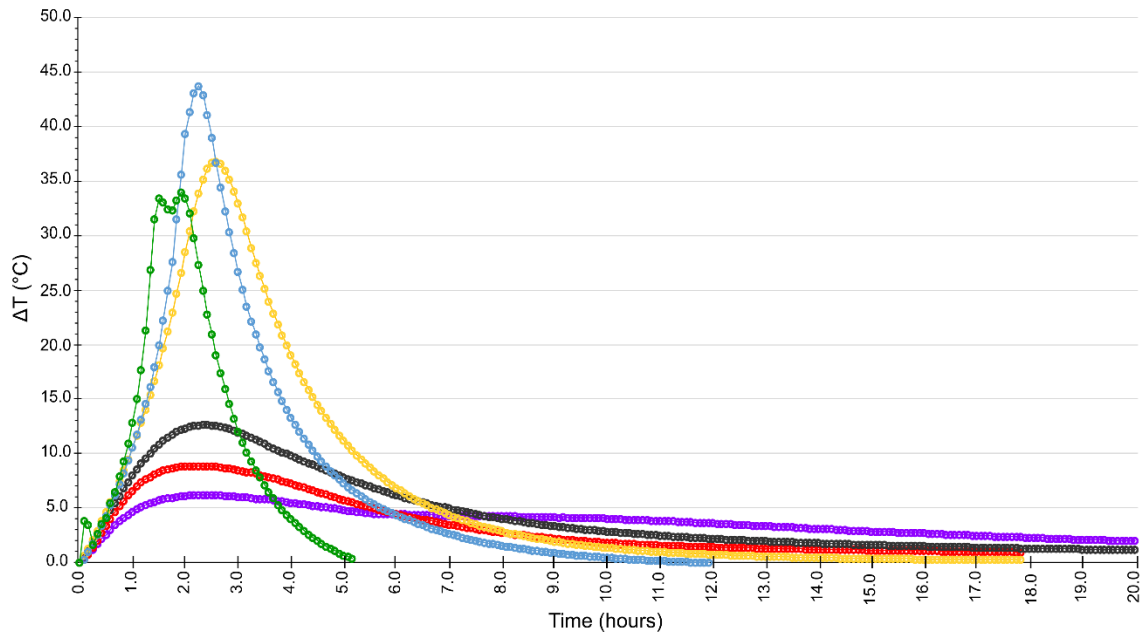


Figure 33: Temperature evaluation in ferrihydrite-pyrite-quartz mixtures from the single NAG tests with fixed amount of ferrihydrite (0.5 g), and variable amount of pyrite and therefore variable S content. Green: 0 wt.% S, light blue: 0.12 wt.% S, yellow: 0.25 wt.% S, black: 0.50 wt.% S, red: 0.75 wt.% S, purple: 1 wt.% S.

Time and ΔT for a selected sample of pyrite (0.75 wt.% S) that were pre-treated with oxalate extraction (green line) is presented in Figure 34. The original sample (black circles in Figure 34), without oxalate pre-treatment, reacts as expected during the temperature logging. Surprisingly, the pyrite-quartz sample treated with oxalate extraction (green line in Figure 34) shows no temperature change. This was not expected as oxalate extraction is not supposed to attack pyrite.

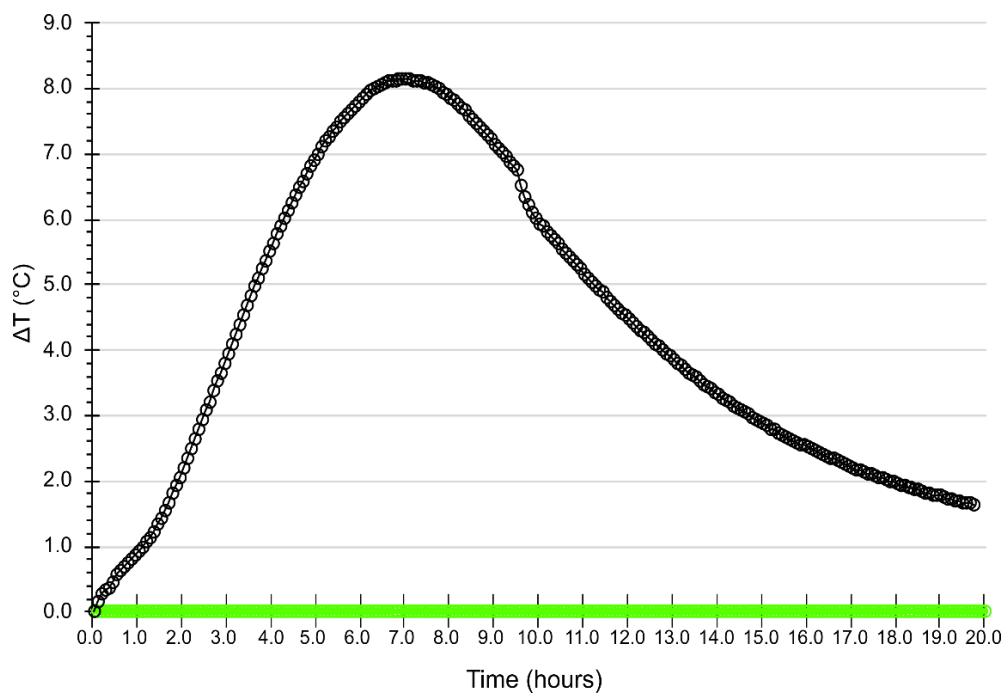


Figure 34: Time and temperature for pyrite-quartz mixture equal to 0.75 wt.% S. Green: oxalate treated sample (single experiment), black: original pyrite and quartz mixture (average from duplicates).

5.6 Comparison of pyrite-quartz and ferrihydrite-pyrite-quartz mixtures

5.6.1 Maximum temperature change compared with the S content in the samples

As expected, more pyrite (thus higher S wt.%) results in greater temperature changes (Figure 35). Surprisingly, ferrihydrite-pyrite-quartz (ferrihydrite fixed at 0.5 g) mixtures do not show the same trend as pyrite-quartz mixtures. Ferrihydrite alone (0 wt.% S) reacts excessively with H_2O_2 and gives a high temperature change. The ferrihydrite-pyrite-quartz mixture was expected to follow the same trend as the pyrite-quartz mixture, i.e. increasing pyrite amounts in the ferrihydrite-pyrite-quartz mixture would result in a greater temperature increase. However, this is not the case, as ferrihydrite-pyrite-quartz mixtures show a downward ΔT trend with increasing amounts of pyrite in the mixture.

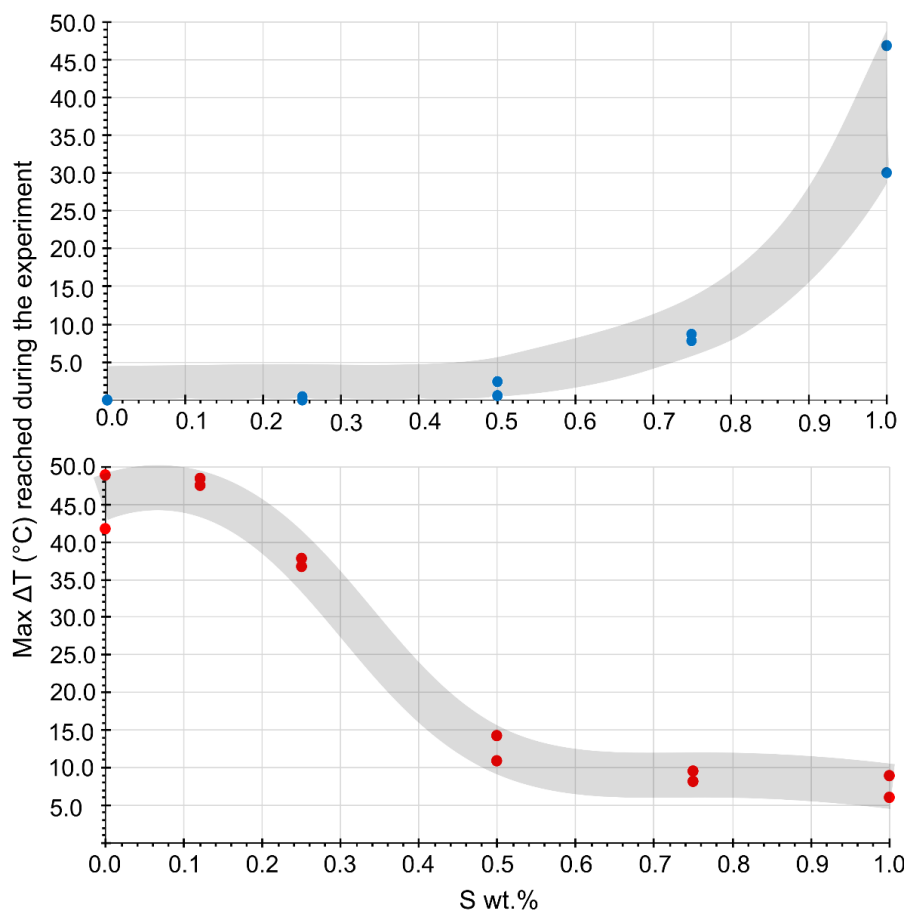


Figure 35: Max ΔT reached during the experiment plotted against the S content. Pyrite-quartz (blue bullet points) and ferrihydrite-pyrite-quartz (red bullet points) compared to each other with the same amount of S in each sample and the samples temperature differences. Temperature differences is presented as ΔT_{max} (°C). Grey lines are drawn by hand to give an indication of the trend.

It may appear that there is a trend where the more ferrihydrite, the more reaction and higher temperature changes, presented in Figure 36. However, it is important to note that these results represent a single experiment, except for 0.5 g ferrihydrite which was done twice. Optimally, the experiments should have been done several times and at several concentrations of S wt.% to know the trend. However, time and material quantity were limiting factors in this study.

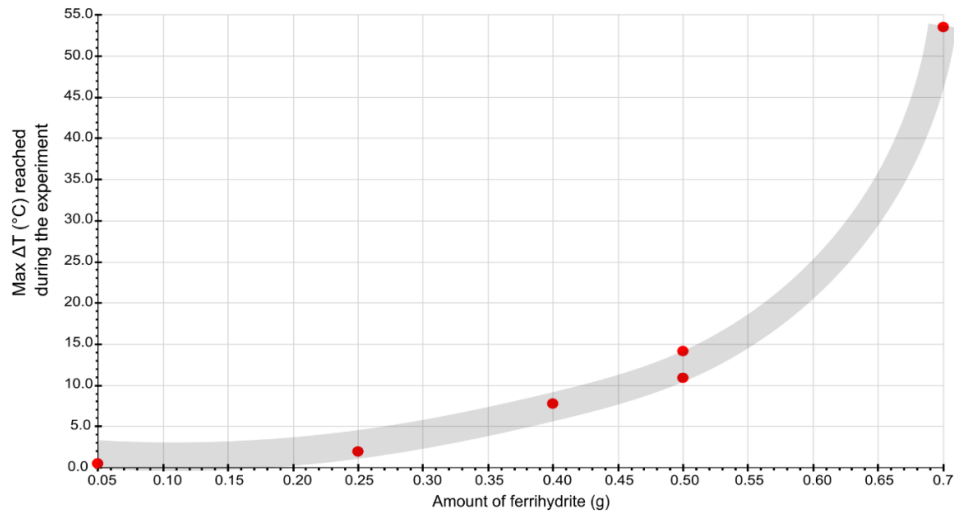


Figure 36: Max ΔT reached during the experiment for the different amounts of ferrihydrite in grams mixed with a fixed amount of pyrite (0.5 wt.% S) in the samples. The more ferrihydrite, the more temperature increases. Grey lines are drawn by hand to give an indication of the trend.

5.6.2 Net acid generation pH and S content

The net acid generation pH (NAG pH) for both pyrite-quartz and ferrihydrite-pyrite-quartz with ferrihydrite fixed at 0.5 g is presented in Figure 37. As expected, pyrite indicates a downward trend. This means that with more pyrite, a lower NAG pH is expected. Ferrihydrite also indicates a downward trend, but it appears that ferrihydrite contributes to the inhibition of the effect of pyrite on pH.

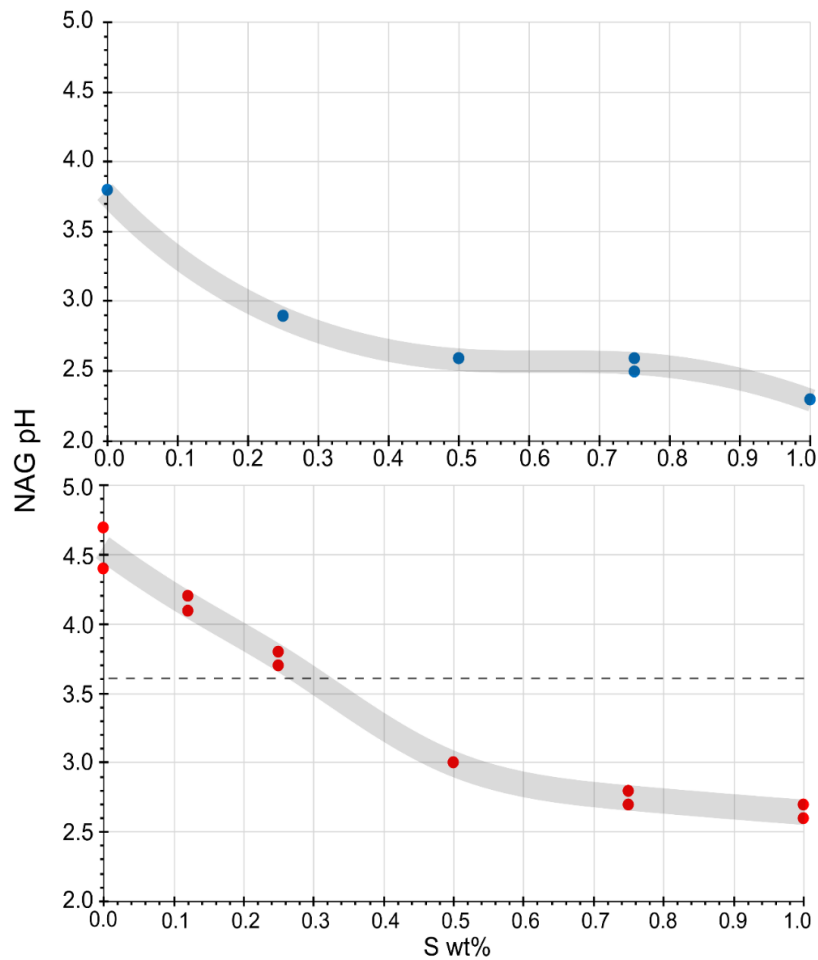


Figure 37: NAG pH plotted against S content. Blue is pyrite-quartz, red is ferrihydrite-pyrite-quartz (same amount of ferrihydrite: 0.5 g). Black dotted line is the paste pH for ferrihydrite (pH 3.6). Grey lines are drawn by hand to give an indication of the trend.

The amount of ferrihydrite in a sample will affect the NAG pH (Figure 38). The samples have a fixed amount of pyrite (0.5 wt.% S) but are mixed with different amounts of ferrihydrite. It appears that the ferrihydrite amount in a sample correlate positively with the NAG pH.

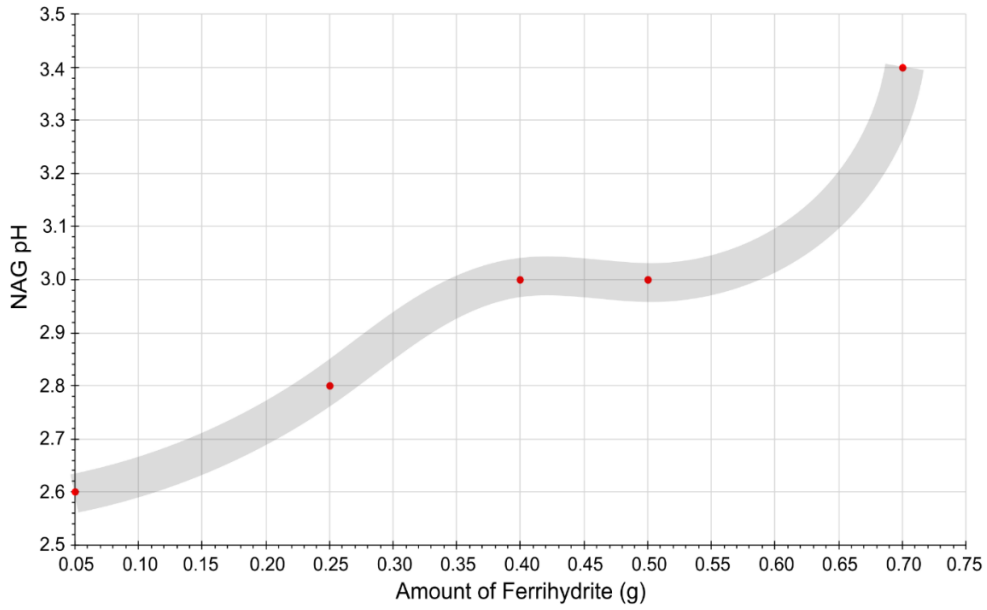


Figure 38: NAG pH plotted against the ferrihydrite-pyrite-quartz; pyrite fixed at 0.5 wt.% S. Grey lines are drawn by hand indicating the trend.

5.6.3 Net acid generation and S content

Figure 39 presents the NAG vs. pyrite-quartz and ferrihydrite-pyrite-quartz (ferrihydrite fixed at 0.5 g). Pyrite-quartz shows an increasing trend, where more S wt.% in the sample gives higher NAG values. This is expected as pyrite is acid-producing. However, the ferrihydrite-pyrite-quartz mixture gives lower NAG values.

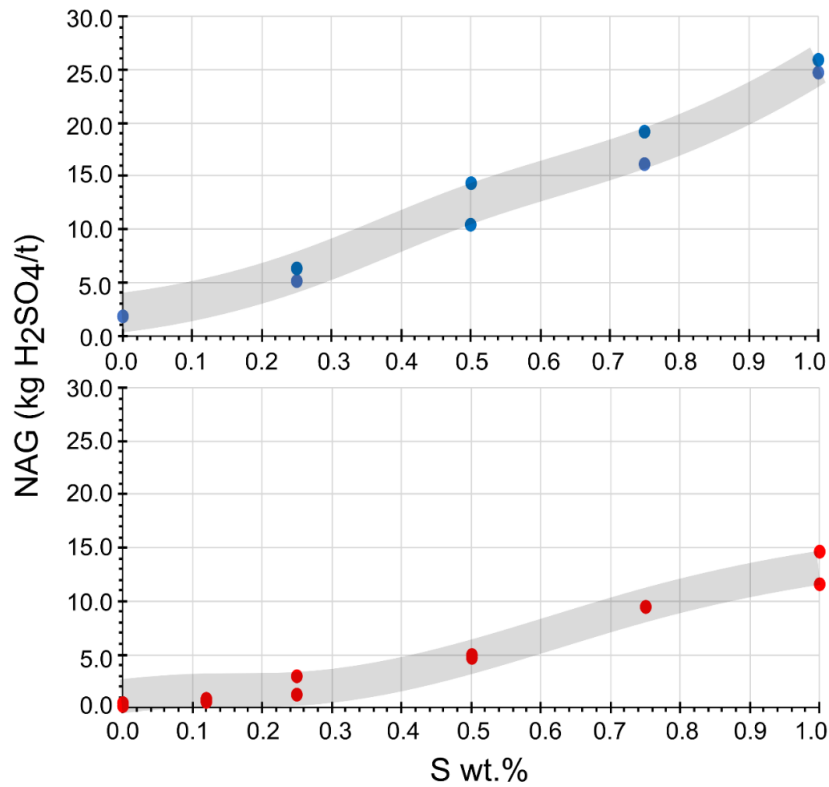


Figure 39: NAG plotted against S wt.% for pyrite-quartz (blue) and ferrihydrite-pyrite-quartz (red). The pyrite-quartz mixtures have higher NAG values, while ferrihydrite-pyrite-quartz mixtures have lower values of NAG. Grey lines are drawn by hand and indicates the trend.

Figure 40 demonstrates, similar to Figure 39, that the more ferrihydrite in the mixture, the lower the NAG. This implies that the amount of ferrihydrite in a sample is important, as the results clearly indicate that ferrihydrite counteracts the effect of pyrite and, therefore, the NAG.

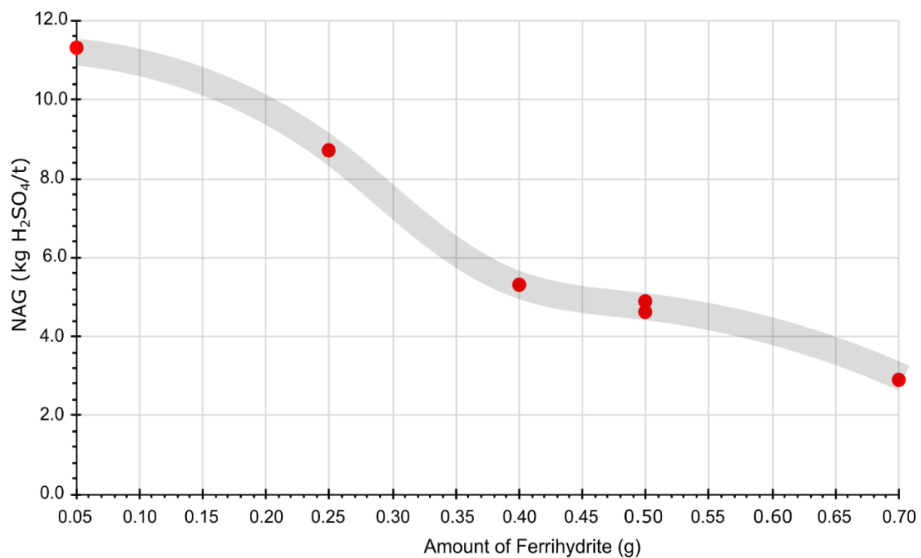


Figure 40: NAG plotted against different amounts of ferrihydrite at the same S wt.% (0.5). The more ferrihydrite, the lower the NAG. Grey lines are drawn by hand to give an indication of the trend.

5.7 Reaction with H₂O₂

Presented in Table 25 are quantitative test results of H₂O₂ reacting with minerals and salts. Zinc chloride (ZnCl₂) and sodium chloride (NaCl) do not react with H₂O₂, while Fe(III)sulphate (also shown in Figure 41), Fe(III)Cl₃, and ferrihydrite react strongly with H₂O₂.

These samples are done by mixing approximately 15% H₂O₂ and an unknown quantity of material. Except LS-tailings which are done by the AMIRA single NAG method. Both Fe(III)sulphate and LS-tailings were done during the lab work for this thesis, while the rest of the samples were done by Gabrielle Dublet-Adli.

Table 25: Quantitative test of different salts and minerals mixed with H₂O₂. Iron(III) reacts strongly with H₂O₂. A strong reaction is visible as the sample boiled over. A small reaction is only detected by the temperature logger.

Sample	Reaction with H ₂ O ₂
Fe(III)sulphate	Strong reaction
Ferrihydrite	Strong reaction
Fe(III)Cl ₃	Strong reaction
NaCl	No reaction
ZnCl ₂	No reaction
LS-tailings	Small reaction

Iron(III)sulphate reacts first slowly after adding H₂O₂ but the reaction becomes stronger over time (Figure 41). When the maximum ΔT is reached, the sample boiled over the beaker.

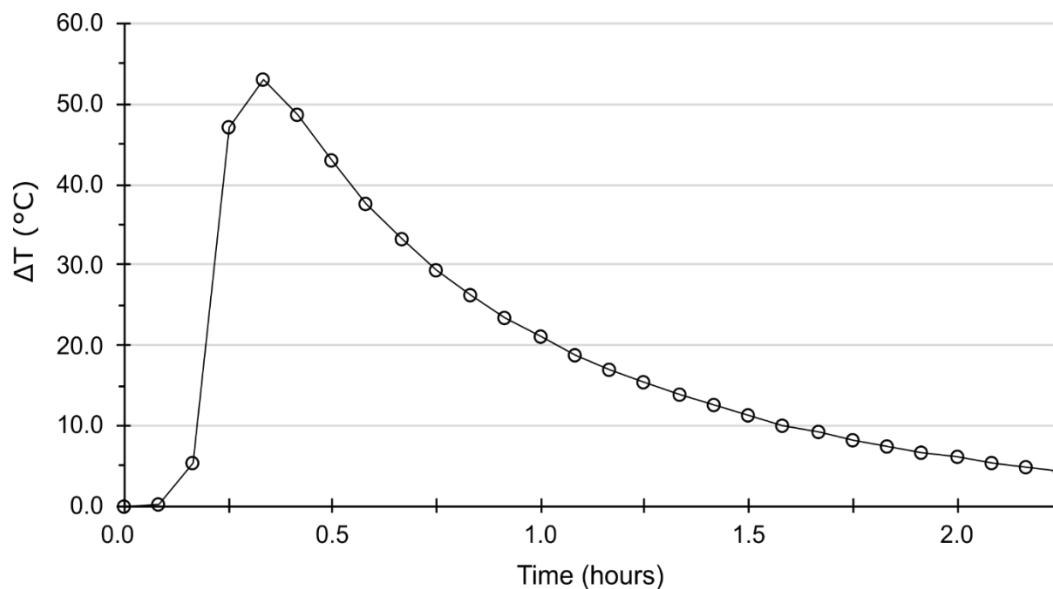


Figure 41: Reaction time and temperature increases for Fe(III)sulphate mixed with H₂O₂.

Pure LS-tailings have a small reaction (Figure 42), and it reacts fast after adding H₂O₂. The LS-tailings - pyrite-quartz mixture reaction with H₂O₂ (Figure 43) shows a greater heat release as the pyrite content increases.

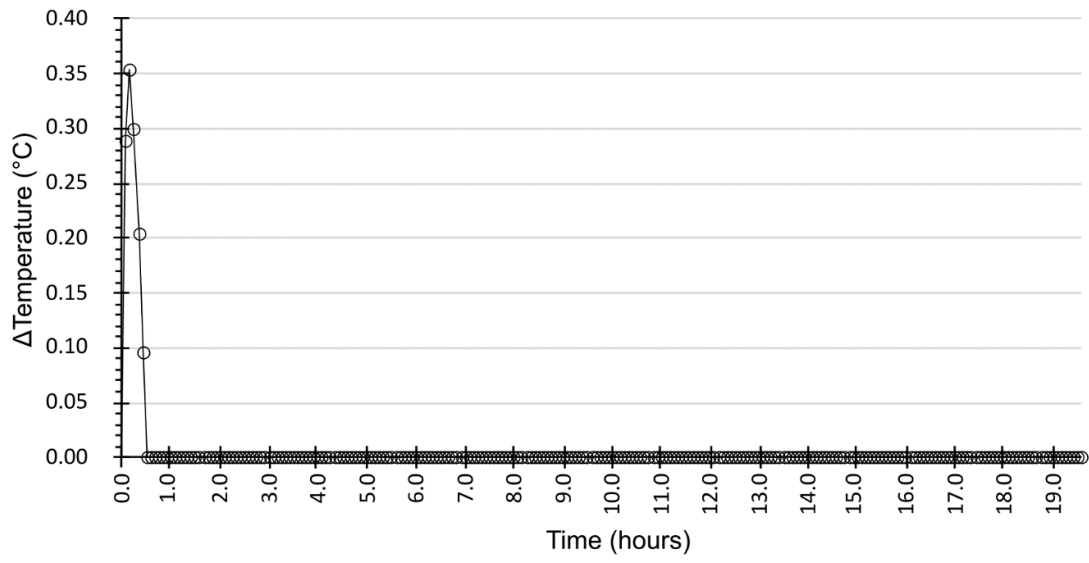


Figure 42: Pure LS-tailings done by the AMIRA single NAG method, including temperature logging. A small reaction is observed.

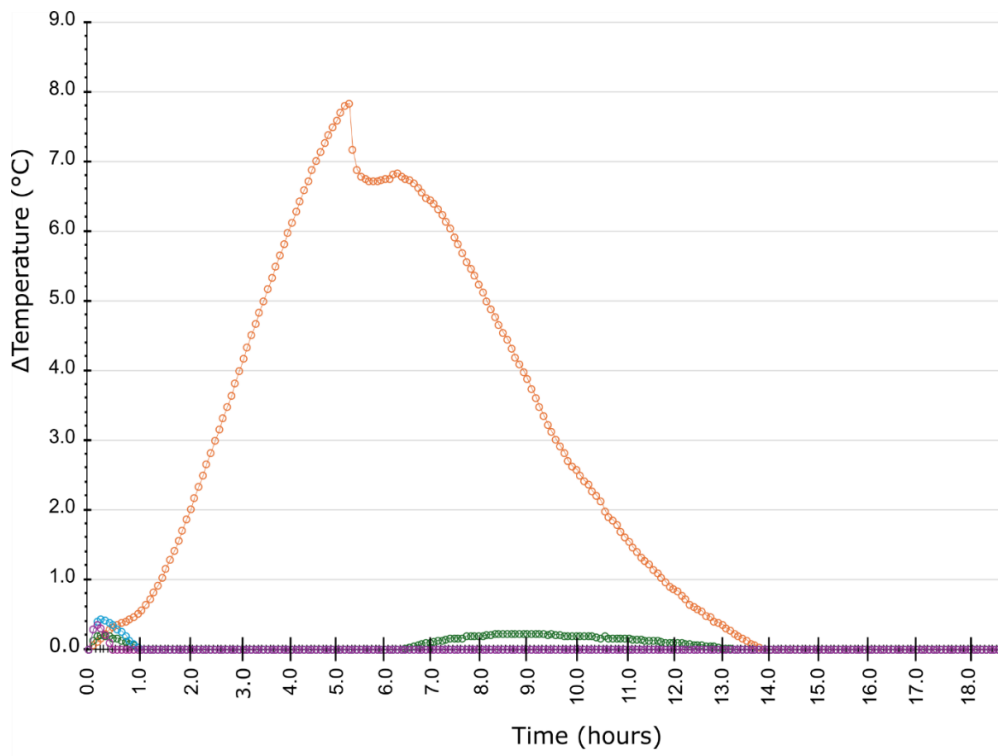


Figure 43: Temperature logging of LS-tailings mixed with pyrite. Orange: LS-tailings with 0.75 wt.% S, green: LS-tailings with 0.5 wt.% S, blue: LS-tailings with 0.25 wt.% S and purple: LS-tailings with 0 wt.% S.

5.8 Water chemistry

Water chemical analysis for H₂O₂ tested solution, oxalate extraction, and solution from H₂O₂ test solution from pre-treated sample material with oxalate extraction are presented in Table 26. Oxalate extraction removes amorphous Fe and Al oxides. Comparing the H₂O₂ tested solution with H₂O₂ tested oxalate extracted pre-treated sample material, there is a reduction of Fe and Al in the samples Birkeland 5 and Tingsaker skole #3. However, this is not shown in the sample Arendal legevakt 4, where the Fe content in the H₂O₂ tested sample solution is below the detection limit, and pre-treated material by oxalate extraction H₂O₂ tested sample solution has a higher value of Fe than only H₂O₂ tested sample. This is not expected as oxalate extraction should remove Fe oxides.

As expected, the highest values of Fe and Al are found in the oxalate extraction solution for the gneiss samples. The oxalate extraction on the sample with ferrihydrite shows an extremely high value of extracted Fe, compared to the gneiss samples and the pyrite sample. This is expected since ferrihydrite is an amorphous Fe oxide and should be removed by oxalate extraction. Less expected is that some Fe was extracted from the pyrite sample.

The extraction of S in the three extraction methods shows, as expected that H₂O₂ tested material extracts S in the highest amount. However, a direct comparison of these three extractions does not necessarily give the full picture as oxalate extraction and H₂O₂ test on oxalate extracted sample material is done on the same sample material. Furthermore, Cu, K, Na, and Zn are removed in lower quantities in the oxalate extraction compared to the H₂O₂ tested materials, both before and after oxalate extraction. However, Mn had the highest amount of extracted element during oxalate extraction.

Table 26: Water chemistry of gneiss, ferrihydrite-pyrite-quartz (ferrihydrite fixed at 0.5 g), and pyrite-quartz mixtures. The gneiss samples are presented as H₂O₂ tested solution, oxalate extraction solution, and solution from H₂O₂ test solution from pre-treated sample material with oxalate extraction. Analysis of the mixtures ferrihydrite-pyrite-quartz (pyrite fixed at 0.025g) and pyrite-quartz is presented from the oxalate extraction. The unit for the elements is mg/L. Note that bdl indicates below detection limit.

Sample	Treatment	Element							
		Fe	Al	S	Cu	K	Na	Mn	Zn
Birkeland 5	H ₂ O ₂ tested	29	17	120	0.85	14	7.3	0.31	3.0
	Oxalate extraction solution	290	47	47	0.20	7	3.2	0.54	0.62
	H ₂ O ₂ test on oxalate extracted material	9.7	8.7	79	0.51	16	7.3	0.20	2.0
Arendal legevakt 4	H ₂ O ₂ tested	bdl	0.007	5.6	bdl	13	7.5	0.089	0.006
	Oxalate extraction solution	0.019	0.032	4.3	bdl	9	6.3	0.054	0.007
	H ₂ O ₂ on oxalate extracted material	0.019	0.032	4.3	bdl	9	6.3	0.054	0.007
Tingsaker skole #3	H ₂ O ₂ tested	5.8	12	66	0.51	21	9.0	0.66	0.31
	Oxalate extraction solution	98	27	5.6	0.035	13	3.0	0.89	0.12
	H ₂ O ₂ on oxalate extracted material	1.2	4.1	49	0.27	14	7.9	0.38	0.23
Ferrihydrite 0.5 g + 0.0025 g pyrite, 0.5 wt.% S	Oxalate extraction solution	1900	2.2	7.2	0.22	bdl	10.4	0.017	0.34
Pyrite 0.038 g, 0.75 wt.% S	Oxalate extraction solution	10	0.48	10	0.34	bdl	2.5	0.022	0.20

5.9 Crystalline and amorphous Fe and S in the gneisses

The crystalline and amorphous Fe and S content were calculated as follows. Total Fe and S are taken from geochemistry results in Table 16, while the amorphous content is calculated from the oxalate extraction of Fe and S (Table 26). Crystalline Fe and S are calculated by total Fe or S minus amorphous content. The calculated percentage of Fe and S relative to the total Fe or S gives an indication of the distribution of amorphous and crystalline content. The results are shown in Tables 27 and 28 and show that the amorphous S content and Fe content in the sample Birkeland 5 are similar to each other in contrast to other samples.

Table 27: Total, amorphous, and crystalline Fe presented in ppm. Percentage of amorphous and crystalline is calculated as a percentage of total Fe.

Sample	Total Fe (ppm)	Amorphous Fe (ppm)	Crystalline Fe (ppm)	Percentage amorphous Fe (%)	Percentage crystalline Fe (%)
Birkeland 5	74800	14500	60300	19.4	80.6
Tingsaker skole #3	43800	4900	38900	11.2	88.8
Arendal legevakt 4	65900	7500	58400	11.4	88.6

Table 28: Total, amorphous, and crystalline S presented in ppm. Percentage of amorphous and crystalline is calculated as a percentage of total S.

Sample	Total S (ppm)	Amorphous S (ppm)	Crystalline S (ppm)	Percentage amorphous S (%)	Percentage crystalline S (%)
Birkeland 5	13000	2350	10650	18.1	81.9
Tingsaker skole #3	5160	280	4880	5.4	94.6
Arendal legevakt 4	559	50	509	8.9	91.1

6 Interpretation and discussion of results

6.1 Oxide/hydroxide bias to temperature change

In the Agder method H_2O_2 causes an exothermic reaction due to the oxidation process of sulphide minerals. However, the degradation of H_2O_2 is exothermic. This degradation can be catalysed by different oxides, oxyhydroxides, and minerals.

6.1.1 Oxides/oxyhydroxide and the effect of H_2O_2

Iron and manganese oxides/hydroxides have the potential to decompose H_2O_2 (Teel Amy *et al.*, 2007; Vafaei Molamahmood *et al.*, 2022). Decomposition of H_2O_2 by Fe and Mn oxides influences the exothermic reaction differently. This section will first address the effect of Mn oxides, and then address the Fe oxides.

Manganese oxides/ oxyhydroxide and the effect on H_2O_2

Manganese oxides have a great capacity to decompose H_2O_2 (Teel Amy *et al.*, 2007; Russo *et al.*, 2013; Vafaei Molamahmood *et al.*, 2022). The decomposition, catalysed by Mn oxides, can be described as follows (Russo *et al.*, 2013):



Teel Amy L. *et al.* (2007) tested two Mn oxides, two Fe oxides and several trace minerals with H_2O_2 . One of the findings from those results was that pyrolusite (MnO_2) was an effective catalyst for the decomposition of H_2O_2 , even better than Fe oxides (Figure 44). Unfortunately, Teel Amy L. *et al.* (2007) did not record the temperature during the decomposition, but an assumption is that pyrolusite emits more heat than goethite. This could lead to false temperature logging in the Agder method if Mn oxides are present in the rocks, which could lead to false characterisation.

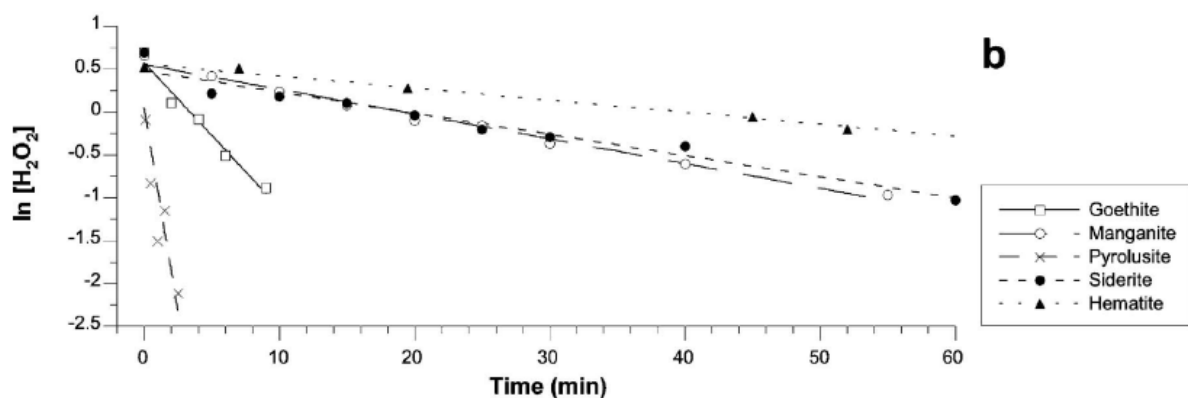
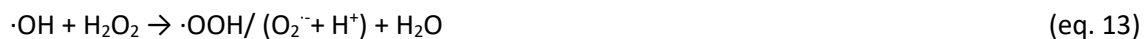
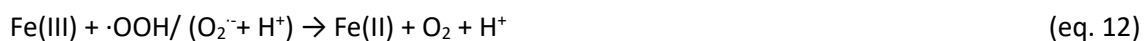


Figure 44: Decomposition of H_2O_2 (2%) in an acidic environment ($\text{pH} = 3$) with time. Figure from Teel Amy *et al.* (2007). Relevant for this section are the Mn-oxides pyrolusite and manganite, and the Fe oxides goethite, hematite.

Iron oxides/ oxyhydroxide and the effect on H₂O₂

Iron oxides could include Fe(II), Fe(III) and Fe(II, III) (Haraldsen and Pedersen, 2023) and occur as a crystalline or amorphous phase. Interestingly, although Fe is an abundant element in rocks and H₂O₂ is widely used for testing rocks, H₂O₂ mixed with Fe oxides is not entirely understood (Vafaei Molamahmood *et al.*, 2022). This has not been taken in consideration when the Agder method was developed.

The decomposition of H₂O₂ by Fe oxides could happen through the Fenton reaction or similar to the Mn oxides (Vafaei Molamahmood *et al.*, 2022). The main difference between the Fenton reaction and Mn oxides decomposition of H₂O₂ is the production of ·OH, which is a product of the Fenton reaction. The decomposition of H₂O₂ through the Fenton reaction could be described as follows (Vafaei Molamahmood *et al.*, 2022):



Both Fe(III) and Fe(II) could initiate this reaction, i.e. eq. 10 and 11, respectively.

In this study, pure mineral phase mixtures of ferrihydrite-pyrite-quartz and pyrite-quartz were tested (Figure 35). The pyrite-quartz mixtures result in higher temperature change when more pyrite is present in the mixture, which is consistent with the NAG pH that is also lower for higher amounts of pyrite (Figure 37). However, already small amounts of pyrite result in an acidic pH due to a lack of buffering minerals. What is observed in the ferrihydrite-pyrite-quartz mixtures is a decreasing trend in temperature with more pyrite in the samples. This contradicts the principle of the Agder test, where the temperature is supposed to increase upon sulphide oxidation. Ferrihydrite alone is very efficient for decomposing H₂O₂ (Vafaei Molamahmood *et al.*, 2022), most likely through the Fenton reaction. Ferrihydrite alone provides a high temperature increase ($\Delta T_{\text{max}} = 40\text{--}50\text{ }^\circ\text{C}$) (Figure 35), which is close to the temperature reaction with pyrite at 1 wt.% S. Therefore, the expected result was that the ferrihydrite-pyrite-quartz mixtures would provide higher temperature increases with more S content in the sample. Unfortunately, no research has been done on how ferrihydrite will act when mixed with other oxides or sulphides, such as pyrite.

The temperature results in Figure 35 show an inhibition of heat release depending on the amount of pyrite present in the ferrihydrite-pyrite-quartz (ferrihydrite fixed at 0.5 g) mixture. This suggests that the reactions in the ferrihydrite-pyrite-quartz-H₂O₂ system involve the endothermic production of an (unknown) thereby lowering the ΔT . By testing mixtures with a fixed amount of pyrite and different amounts of ferrihydrite (Figure 36, ferrihydrite-pyrite-quartz, pyrite fixed at 0.25 g), it appears that the amount of present Fe oxide is influencing the amount of heat released. Mixtures with a fixed amount of ferrihydrite (ferrihydrite-pyrite-quartz, ferrihydrite fixed at 0.5 g) show that the temperature is dependent on the amount of pyrite (Figure 35). This supports that an inhibition of heat released caused by an endothermic reaction is dependent on the ratio between S content and Fe oxides.

Alternatively, the inhibition of temperature increase could also be caused by the complexation of Fe(II) and Fe(III) with the SO₄²⁻, which could lead to the inhibition of the decomposition of H₂O₂ (De Laat *et al.*, 2004). In the system with only ferrihydrite (Figure 35, 0 wt.% S), the reaction (high ΔT_{\max}) could only be a Fenton reaction without ligands present to affect the reaction. However, once the pyrite is added in increasing amounts, the reaction starts to slow down. When H₂O₂ oxidises pyrite, SO₄²⁻ is released, and the more pyrite is present in the sample mixtures, the more SO₄²⁻ is produced that will act as an inhibitor. Unfortunately, this does not explain when Fe(III)sulphate and Fe(III)Cl₃ are tested together with H₂O₂ (Table 25). Here, strong reactions are registered for Fe(III)sulphate (Figure 41). However, it would be expected that the reaction was slower and heat released from Fe(III) sulphate and FeCl₃ was lower, as both SO₄²⁻ and Cl⁻ would act as a ligand (De Laat *et al.*, 2004).

The possibility of products formed in an endothermic reaction is supported by the NAG pH (Figure 37). The NAG pH is slightly higher in the mixtures with ferrihydrite-pyrite-quartz than those with pyrite-quartz. This could support the theory that there are products formed that consume both energy and H⁺ protons. However, it would be more reasonable to expect that SO₄²⁻ produces complexes with Fe(III) (De Laat *et al.*, 2004), and maybe also H⁺ protons. This complex production would inhibit the decomposition of H₂O₂ and could also explain why the NAG pH is slightly higher in the ferrihydrite-pyrite-quartz mixtures, as the pyrite would not be fully oxidised as the H₂O₂ is consumed before it can fully react with pyrite. Table 29 provides an overview of the oxidation of pyrite through H₂O₂ and the use of the oxidation product SO₄²⁻ as ligands in products from the Fenton reaction.

Table 29: Summary table of reaction related to Fe related to H₂O₂. Oxidation of pyrite through H₂O₂ produces SO₄²⁻ which is used as a ligand to the products from the Fenton reaction. Fenton reaction and reactions with SO₄²⁻ as a ligand are modified from De Laat et al. (2004).

Oxidation of pyrite (Knobloch and Lottermoser, 2020)	Fenton reaction (De Laat et al., 2004)	Reaction with SO ₄ ²⁻ to Fenton reaction's products (De Laat et al., 2004)
FeS ₂ + 15/2H ₂ O ₂ → Fe ³⁺ + SO ₄ ²⁻ + H ⁺ + 7H ₂ O	Fe(III) + H ₂ O ₂ → Fe(II) + ·OOH/ (O ₂ ⁻ + H ⁺) + H ⁺ Fe(II) + H ₂ O ₂ → Fe(III) + ·OH + OH ⁻ Fe(III) + ·OOH/ (O ₂ ⁻ + H ⁺) → Fe(II) + O ₂ + H ⁺ ·OH + H ₂ O ₂ → ·OOH/ (O ₂ ⁻ + H ⁺) + H ₂ O	Fe ²⁺ + SO ₄ ²⁻ → FeSO ₄ Fe ³⁺ + SO ₄ ²⁻ → FeSO ₄ ⁺ Fe ³⁺ + 2SO ₄ ²⁻ → Fe(SO ₄) ₂ ⁻ H ⁺ + SO ₄ ²⁻ → HSO ₄ ⁻ H ₂ SO ₄ + ·OH → SO ₄ ⁻ + H ⁺ + H ₂ O HSO ₄ ⁻ + ·OH → SO ₄ ⁻ + H ₂ O SO ₄ ⁻ + H ₂ O → SO ₄ ²⁻ + H ⁺ + ·OH SO ₄ ⁻ + OH ⁻ → SO ₄ ²⁻ + OH ⁻ SO ₄ ⁻ + H ₂ O ₂ → SO ₄ ²⁻ + H ⁺ + ·OOH SO ₄ ⁻ + ·OOH → SO ₄ ²⁻ + H ⁺ + O ₂ SO ₄ ⁻ + Fe ²⁺ → Fe ³⁺ + SO ₄ ²⁻

As already mentioned, Fe oxides can behave differently when mixed with H₂O₂. This is seen in the Fe oxide material LS-tailings, from the temperature logging in Figure 42, which shows that the pure LS-tailings react little. However, there is high uncertainty connected to the results as there is only a small temperature change, which could easily be influenced by other factors, such as fluctuations in the room temperature. The low temperature change was not expected as both decomposition through the Fenton reaction and Mn oxides are heat releasing. It was expected to have a greater reaction with LS-tailings, because LS-tailings are mainly composed of Fe(III) oxides which could be used in the Fenton reaction. The different mixes with LS-tailings and the temperature logging are shown in Figure 43, where the reaction is less than initially thought. Comparison of the results of ΔT_{max} vs. S content for the pyrite-quartz, ferrihydrite-pyrite-quartz, and LS-tailings-pyrite-quartz mixtures (Figure 45) show that the LS-tailings mixture follows the pyrite-quartz mixture rather than ferrihydrite-pyrite-quartz mixture. This leads to the implication that LS-tailings do not react with H₂O₂ as it was expected to follow the ferrihydrite-pyrite-quartz mixture. It looks like only the pyrite in the LS-tailings mixture reacts. This emphasises that different Fe oxides react differently with H₂O₂.

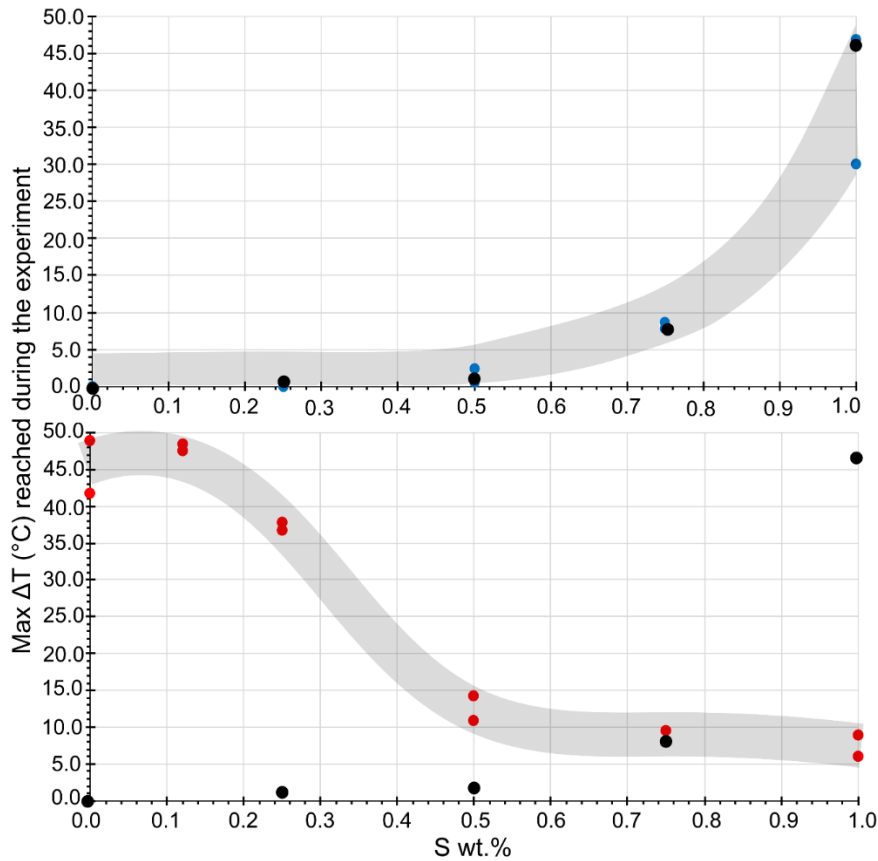


Figure 45: Max ΔT during the experiment for the sample mixes pyrite-quartz (blue points), ferrhydrite-pyrite-quartz, ferrhydrite fixed at 0.5 g (red points), LS-tailings-pyrite-quartz (black points). LS-tailings mixtures follow the reaction of the pyrite mixtures better than the ferrhydrite mixtures. Grey lines are drawn by hand to indicate the reaction trend.

6.1.2 The effect of removal of amorphous Fe oxides in the gneiss samples on temperature
 Acid oxalate extraction removes amorphous inorganic Fe and Al, poorly crystalline Fe and Al oxides, and the organic complexes of Fe and Al (Krogstad et al., 2018). Oxalate extraction on rock powder will remove Fe and Al oxides that could react with H_2O_2 . Removing amorphous Fe oxides in the gneiss samples will reduce the potential decomposition of H_2O_2 through oxides and reduce false temperature increases caused by Fe oxides. To investigate this, the AMIRA single NAG test with temperature logging was conducted on extracted material to indicate the effect Fe oxides could have on temperature increases during the H_2O_2 test.

As expected, oxalate extraction changed the reaction behaviour between H_2O_2 and gneiss samples. Arendal legevakt 4, which is not acid-producing, but has a temperature increase with H_2O_2 that leads to a false characterisation by the Agder method (Table 19). In Figure 29, the temperature logging of Arendal legevakt 4 shows that the sample does not react after oxalate extraction. This sample has magnetite and amorphous material. Magnetite is an effective catalyst for the decomposition of H_2O_2 as it contains Fe(II) and Fe(III) (Vafaei Molamahmood *et al.*, 2022). This leads to the assumption that this might be the case for the false temperature increase in the Agder method. Studies show that acid

oxalate extraction could attack crystalline oxides (Oorschot and Dekkers, 2001; Krogstad et al., 2018), in particular when magnetite is fine grained. The gneiss samples that were oxalate extracted were milled below 75 μm . It is important to note that this is only an assumption as there is not done mineralogy analysis by XRD after oxalate extraction for confirming the removal.

Tingsaker skole #3 has a two-step temperature increase in both untreated and pre-treated oxalate extracted material (Figure 30). The temperature increased in the untreated material after adding H_2O_2 , then temperature change slowed down and increased again. One explanation is that there is most likely not only pyrite that is reacting, confirmed by XRD, but also Fe oxides that react, i.e. the different reactants become available at different times. This is also seen in the oxalate treated material, which shows a different behaviour than the untreated material. After oxalate extraction, Tingsaker skole #3 reacts faster and more than the untreated sample in the beginning before it cools down and reacts less than the untreated sample. The fact that it reacts less in the second reaction and more in the first reaction suggests that there could be Fe oxides that inhibit the reaction with pyrite in the beginning, similar to what is seen in the ferrihydrite-pyrite-quartz mixtures. After some time, more material is available to react with H_2O_2 , which could explain the second phase reaction.

Birkeland 5 is characterised as a well-weathered rock containing pyrite and different Fe oxides such as jarosite and goethite. Figure 31 illustrates the temperature logging of Birkeland 5 for both untreated and the oxalate treated material. The temperature change difference between untreated and treated material is nearly 40 $^{\circ}\text{C}$, where untreated has the highest ΔT_{max} . Supposedly, the oxalate extraction has removed most of the amorphous and poorly crystalline Fe oxides. In that case, it is possible to argue that the reaction in the untreated sample is due to Fe oxides, such as goethite (Teel Amy *et al.*, 2007), which also could accelerate the pyrite oxidation. Looking at the treated sample, where Fe oxides are removed, the reaction is slower and less intense, which could be due to only pyrite reacting.

The oxalate extraction did not only show an effect on the temperature reaction, but also a visible effect on the samples where Fe precipitated during titration under the single NAG test (Figure 46).

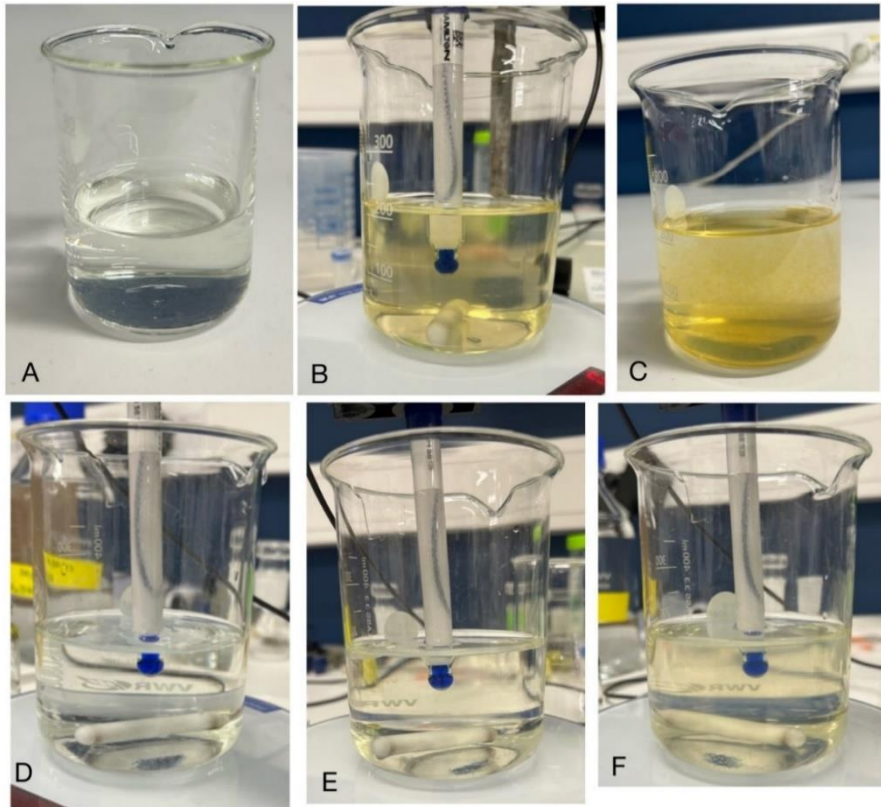


Figure 46: Photos of Birkeland 5 during the titration in the single NAG test. The more yellow, the more precipitation of Fe in the solution. A, B and C are ordinary single NAG test, while D, E and F are modified single NAG test with pre-treated sample with oxalate extraction. A and D = before titration, B and E = pH 4.5, C and F = pH 7. The oxalate extraction had a visual effect on the sample Birkeland 5, F compared to C, where the less coloured picture F showed less precipitation of Fe in solution during titration.

6.1.3 Other oxide minerals affecting H₂O₂ and temperature changes

Minerals that react very clearly with H₂O₂ are pyrite, galena, stibnite, and sphalerite (Knobloch and Lottermoser, 2020). However, it is not only sulphide minerals and Fe oxides that react with H₂O₂ in an exothermic way, but also other types of oxides, including siderite (FeCO₃), ilmenite (FeTiO₃), cuprite (Cu₂O), magnesite (MgCO₃), bauxite (Al(OH)₃), and anatase (TiO₂) (Teel Amy *et al.*, 2007). Teel Amy *et al.* (2007) refer to those minerals as trace minerals. Their contributions to the decomposition of H₂O₂ vary, where siderite, cuprite, willemite and ilmenite contribute most to the decomposition of H₂O₂ in an acidic environment (Teel Amy *et al.*, 2007).

During the experiment in this research, the pH in the H₂O₂ was in the range of 3.2-3.3, which means that it was an acidic environment during the H₂O₂ tests. As the Agder method does not specify the pH in the H₂O₂ solution, it is expected that the pH is in the range of 3-4 as H₂O₂ is often stabilised in acid (Roth, 2023). One could, therefore, expect siderite, manganite, cuprite, and ilmenite to decompose H₂O₂. However, only ilmenite was detected in the gneiss samples Arendal legevakt 4 and Arendal legevakt 5 (Table 17). Ilmenite, which is not considered as acid-producing, could thus contribute to a temperature increase and a false acid-producing characterisation.

6.2 Mineralogy bias on temperature in the gneisses

6.2.1 Mineralogy description of the gneisses in the southern Norway

The gneisses are high-grade metamorphic and without a significant amount of buffering minerals (Tables 17, 18). The lack of buffering minerals makes the rocks less resistant to acid formation.

Abundant minerals in the samples are quartz, biotite, and plagioclase. Considering that 8 out of the 12 rocks are acid-producing, sulphide minerals are expected to be present in the rocks. In general, there is little sign of visible sulphide minerals, such as pyrite. However, some samples have been confirmed to have sulphide minerals (Tables 17, 18), and most samples contain Fe oxides.

Pyrrhotite is claimed to be the primary sulphide mineral in the rock matrix (Hagelia, 2023). This mineral was not detected in any of the 12 gneiss samples (Tables 17, 18), which is surprising as the samples are in bulk material and should represent the whole-rock in the mineralogy. Another reason for this to be surprising is that pyrrhotite was found by Pearce (2018) and Skjønborg (2023) (Appendix E). However, Hagelia (2023) points out that pyrrhotite usually is in small quantities in the rocks, which could explain why it is not detected.

Mineralogical analysis by XRD has limitations as this method is mainly used to determine crystalline minerals and will therefore not detect poorly crystalline minerals and amorphous content. There are also limitations because of the detection limit. This could explain the low detected presence of S containing minerals, and the fact that 8 of the 12 rocks are acid-producing. Complimentary tests for XRD can be Scanning Electron Microscopy (SEM) images and thin sections petrography, which was beyond the scope of this study.

Sulphate oxides as acid-producing phases in the gneisses

During the building of New E18 between Grimstad and Kristiansand in early 2000, there was a belief that the primary sulphide minerals, such as pyrrhotite, were the main cause of acid leaching in the gneisses (Hagelia, 2023). However, Hagelia (2015, 2023) showed that jarosite is the main cause of the acid formation in the gneisses in the Lillesand area. The lack of acceptance of jarosite being the main acid-producing mineral from the developer resulted most likely in the belief that the H₂O₂ test with $\Delta T_{25 \text{ min}}$ measurements in the Agder method would be satisfactory to classify the gneisses (Hagelia, 2023). At a later stage, it became more accepted that jarosite could contribute to acid leaching in the gneisses. Considering that H₂O₂ does not react exothermally with jarosite resulted in a wrong characterisation of the gneisses (Hagelia, 2023).

Dissolution of soluble and less soluble sulphate minerals and salts can contribute to acid drainage, even when present in small amounts (Desborough *et al.*, 2010). Jarosite is a weathering product of primary sulphide minerals and is expected to be present where the rocks are weathered. The dissolution of jarosite is selective, which makes it difficult to determine the contribution to acid leaching (Desborough *et al.*, 2010). Dissolution of jarosite depends on several factors, such as the structure and composition. For example, if the jarosite comprises hydronium, the degree of solubility will be greater than if the jarosite contains K (Gasharova *et al.*, 2005).

Another factor contributing to acid leaching is the mechanic properties of the rocks that host jarosite; if the rocks are more resistant towards external stress the jarosite could decrease the pH down to 3 (Hagelia, 2023). However, if the rocks are weak and crumble easily, the pH could go down as low as 2.2 (Hagelia, 2023). In the 12 gneiss samples from Lillesand only Birkeland 5 has detectable jarosite. During the water chemistry analysis of the metals K, Cu, Mn, Na, and Zn it was expected to find a correlation between the extracted metals (Table 26) and the possibility of linking them to the assumed content of jarosite, as these were selected because of their association with jarosite. It is not possible to see any trends related to the content of jarosite and the content of these metals in the extracts.

Comparison of the gneisses with average upper crust

The geochemical analysis shows the composition of elements in the rocks (Tables 15, 16), those values give an indication of what types of elements exist in the rocks. On the other hand, it does not tell if it is an enrichment or a degradation of the elements. One way of checking for enrichment or degradation is to compare the geochemical data to upper continental crust (UCC) geochemical data.

Comparing the gneisses with the average of the upper continental crust of several elements (Tables 30, 31) shows there is no significant enrichment or depletion. It is observed trace elements with enrichment, such as Cu and Zn, and a greater risk could be associated with the release of those elements depending on which minerals host these elements. Most of the gneiss samples show Fe enrichment, which could indicate Fe enrichment during weathering.

Table 30: Major elements compared with the upper continental crust (UCC). Values are calculated as my values/UCC, where ratio > 1 means enrichment compared with UCC (red numbers), and ratio < 1 is depleted compared to UCC (black numbers). Upper continental crust values are from Table 5 in McLennan (2001). Unit is wt. %.

Major elements	UCC (wt. %)	Eydehavn 1B	Arendal legevakt 2	Arendal legevakt 5	Arendal legevakt 4	RV 420#1	Blakstad 3	Nordbø 1	Tingsaker skole 2	Tingsaker skole 1	Groos 1	Tingsaker skole 3	Birkland 5
Al	8.04	0.99	0.89	0.80	0.90	1.01	0.80	1.18	1.04	1.01	0.93	1.05	0.93
P	0.07	0.80	0.64	0.59	1.42	0.82	0.82	1.16	1.00	0.95	1.13	0.95	1.20
Fe	3.5	2.12	1.32	1.37	1.88	1.01	0.90	1.37	1.33	1.33	1.32	1.25	2.14
K	2.8	0.27	0.32	0.24	0.24	0.64	0.81	0.42	0.64	0.61	0.74	0.60	0.60
Ca	3	2.19	0.29	0.37	1.07	0.58	0.15	1.29	0.70	0.75	0.29	0.78	0.97
Mg	1.33	3.60	0.88	0.93	1.43	0.68	0.97	1.09	0.85	1.01	0.73	0.92	1.41
Mn	0.06	1.90	1.45	1.91	2.63	0.81	0.35	1.14	1.05	1.07	0.50	1.04	1.48
Na	2.89	0.66	1.51	1.30	1.26	0.79	0.18	1.17	0.75	0.79	0.65	0.80	0.50
Si	30.8	0.78	1.04	1.03	0.90	0.99	1.10	0.89	1.02	0.97	0.99	0.99	0.91
Ti	0.41	1.31	0.66	0.68	1.14	0.83	0.91	0.84	1.02	1.05	0.96	1.00	1.72

Table 31: Trace elements contents normalised against the upper continental crust (UCC) values. Values are calculated as my results/UCC, where ratio > 1 means enrichment compared with UCC (red numbers), and ratio < 1 is depleted compared to UCC (black numbers). Upper continental crust values are from Table 5 in McLennan (2001). Unit is ppm.

Trace elements	UCC (ppm)	Eydehavn 1B	Arendal legevakt 2	Arendal legevakt 5	Arendal legevakt 4	RV420#1	Blakstad 3	Nordbø 1	Tingsaker skole 2	Tingsaker skole 1	Groos 1	Tingsaker skole 3	Birkland 5
As	1.50					3.06							
Be	3.00	0.29				0.47	0.30	0.48	0.61	0.51	0.38	0.74	0.39
Cd	0.10	1.53		1.04	1.85				1.29	1.49		1.07	18.67
Co	17.00	2.63	0.43	0.62	1.08	0.38	0.51	0.81	0.79	0.98	0.85	0.91	1.09
Cr	83.00	4.65	0.19	0.14	0.40	0.50	0.66	0.48	0.70	0.55	0.81	0.56	0.84
Cu	25.00	2.51	0.37	0.66	1.39	1.06	2.30	2.05	1.61	1.34	4.12	1.73	2.74
Nb	12.00	0.22				0.35	0.50		0.37	0.35	0.40	0.32	0.27
Ni	44.00	3.20	0.07	0.15	0.38	0.23	0.31	0.29	0.57	0.66	0.74	0.68	0.72
Pb	17.00	0.25	0.35	0.42	0.48	0.86	0.28	0.45	0.63	0.70	0.85	0.65	0.65
Sc	13.60	2.33	1.23	1.18	1.93	0.86	0.83	1.08	1.10	1.04	1.15	0.90	1.88
Sr	350.00	0.51	0.20	0.27	0.47	0.71	0.14	2.06	0.75	0.80	0.28	0.88	0.41
Th	10.70	0.20	0.18	0.23	0.11	0.58	1.21	0.34	0.71	0.69	0.96	0.58	0.38
U	2.80	0.15	0.10	0.12	0.13	0.73	0.90	0.41	0.84	0.79	1.40	0.75	0.95
V	107.00	1.72	0.52	0.74	1.45	0.65	0.57	1.06	0.86	1.14	0.75	0.90	2.17
Y	22.00	1.52	1.03	0.93	1.01	1.27	1.31	0.58	1.18	1.27	1.68	0.98	1.32
Zn	71.00	1.35	1.05	1.38	2.89	1.26	0.56	1.23	1.14	1.36	1.11	1.27	4.10
Zr	190.00	0.60	0.37	0.37	0.34	0.84	1.91	0.52	0.90	0.84	1.09	0.83	0.68

6.2.2 Minerals in the gneisses affecting the H₂O₂ test

The rocks show unexpected mineralogy results considering the acid-forming potential. Some of the samples that are classified as acid-producing, with a pH down to 2.3 (Table 19), have minor to no detectable amounts of sulphide/sulphate minerals (Table 32). The S content from geochemical analysis indicates that S is present, i.e. S-bearing mineral phases can only be present in small amounts below the XRD detection limit.

Table 32: Summary of results connected to S content (wt.%) (from Table 16), S minerals, detected S minerals during petrographic description, and the pH from column experiments from Lindum (2023). Note that Fe oxides minerals could also not contain S, and are therefore just an implication that it can contain S. Red colour means high value (S content: > 0.8 wt.%, ΔT_{25min} : > 1.2 °C), orange is medium (S content: 0.15-0.8 wt.%, ΔT_{25min} : 0.7-1.2 °C), and green is low (S content: < 0.15 wt.%, ΔT_{25min} : < 0.7 °C). Threshold values are from the Agder guideline (Prosjektgruppen for kontroll på svovelholdig avrenning i Agder, 2021). Concentrations below the detection limit are indicated as bdl.

Sample	S (wt.%)	Detected S-minerals by XRD	Detected S- or Fe bearing minerals by petrographic description	pH from column experiment	$\Delta T_{25 min}$ (°C)
Eydehavn 1B	0.1	Amorphous	Fe oxides minerals	7.8 (32w)	3.8
Tingsaker skole #1	0.7	Pyrite	Pyrite/pyrrhotite	3.6 (22w)	0.8
Tingsaker skole #2	0.7	No S-minerals or amorphous	Fe oxides minerals	3.5 (22w)	0.8
Tingsaker skole #3	0.5	Trace of pyrite	Pyrite, Fe oxides minerals	3.2 (22w)	1.1
RV420 #1	0.2	No S-minerals or amorphous	Pyrite, Fe oxides minerals	2.6 (32w)	0.6
Blakstad 3	0.2	No S-minerals or amorphous	Fe oxides minerals	3.2 (22w)	1.0
Birkeland 5	1.3	Pyrite, jarosite	Fe oxides minerals	2.3 (32w)	32.1
Nordbø 1	0.05	Amorphous	Fe oxides minerals	4.3 (32w)	0.45
Gross 1	1.1	Pyrite, amorphous	Pyrite, Fe oxides minerals	2.5 (32w)	1.25
Arendal legevakt 2	bdl	Amorphous	Fe oxides minerals	6.6 (42w)	1.8
Arendal legevakt 4	0.06	Amorphous	Fe oxides minerals	6.7 (42w)	1.7
Arendal legevakt 5	0.1	Amorphous	Fe oxides minerals	6.4 (42w)	2.1

The mineralogy alone does not tell the whole story of the acid-producing potential of the gneisses. The five false negative rocks (Tingsaker skole #1, Tingsaker skole #2, Tingsaker skole #3, Blakstad 3, and Nordbø 1, Table 19) indicate that they are acid-producing but have medium/low S content and low/medium reactivity with H₂O₂. These rocks have small or no amounts of S-bearing minerals (Tables 17, 18). This is unexpected as these five rocks have a pH range of 3.2-4.3 (column experiment), i.e. one would expect to find sulphide minerals in detectable amounts by XRD.

Therefore, one may wonder why acid leaching is formed in the false negative samples classified by the Agder method (Lindum AS, 2023). However, Tingsaker skole #1 and #3 had small amounts of pyrite detected in the XRD analysis. During petrographic description, pyrite/pyrrhotite was observed in Tingsaker skole #1 and #3 (Table 32), which could explain the temperature increase in the H₂O₂ test. Tingsaker skole #2 and Blakstad 3 had no detectable sulphide minerals or amorphous material

but do contain Fe oxides as observed in hand specimen. The observed Fe oxides could explain why it is acid-producing and the medium reactivity with H_2O_2 , as the Fe oxides react differently with H_2O_2 , illustrated by Fe(III)sulphate reacts strongly with H_2O_2 (Table 25), and that jarosite does not react with H_2O_2 (Hagelia, 2023). One could expect that there are other acid-producing Fe oxides that can react with H_2O_2 . Another possibility is that the sulphide/sulphate minerals are present in very small amounts below the detection limit. Nordbø 1 is more concerning, as it has a low S content and a low reactivity with H_2O_2 . Sulphide minerals were not detected but it does contain amorphous material and Fe oxides (Table 32). In Nordbø 1's case an explanation for acid formation could be the presence of amorphous material (including amorphous jarosite).

The four false positive samples are the samples that react with H_2O_2 (Table 32) but are not acid-producing rocks. Common to these samples is that they have low S content and amorphous content, and Fe oxides are observed. The samples Arendal Igeevakt 2, 4, and 5 have magnetite and amorphous material (Table 17), which could react with H_2O_2 . Vafaei Molamahmood *et al.* (2022) confirm that magnetite catalyses the exothermal decomposition of H_2O_2 . However, Eydehavn 1B also reacts with H_2O_2 but does not have magnetite but an amorphous content of 20 wt.%, which is probably the reason for the false positive. This is supported by the high Fe_2O_3 content of 11 wt.% (Table 15); i.e. Fe oxides react with H_2O_2 similar as pure ferrihydrite, and Fe(III)Cl₃ (Table 25, Figure 41).

There are cases of correctly classified rocks through the Agder method. This can be a coincidence and plain luck or indicates an actual correlation between the presence of sulphides, which, in the best-case scenario, is also determined from the mineralogical analyses. The samples Birkeland 5, RV420#1 and Groos 1 are correctly classified. They have in common that they are classified as well-weathered rocks and, therefore, automatically classified as acid-producing rocks (Table 19). Both Birkeland 5 and Groos 1 have a high S content, and S-bearing minerals and Fe oxides (Table 32), which explains the high temperature change at 25 minutes. However, this is not observed in RV420#1, which has a low S content, no S-bearing minerals detected by XRD, no amorphous material and a low temperature change (Table 32). During petrographic description, however, pyrite and Fe oxides were found. The fact that pyrite and Fe oxides were observed during inspection leads to the thought that they should have been detected in XRD. It is likely that these minerals are present in smaller amounts than the detection limit. The observation of pyrite and the low temperature increase is also unexpected. This can be explained by the fact that the pyrite is present in small amounts that it does not react very well with H_2O_2 or, alternatively, the temperature increase is inhibited as was observed in the ferrihydrite-pyrite-quartz mixtures (Figure 35).

The low amounts of S and minor or no amounts of S-bearing minerals (Tables 17, 18) give the impression that these rocks might not be acid-producing to the degree where the pH is below 4 (Table 32). However, the S-bearing minerals could exist in an amorphous form or in smaller amounts below the XRD detection. The low amounts of S-bearing minerals could be more reactive and, therefore, release more acidity. Typically, amorphous material is more reactive than minerals (Paterson et al., 1991). Therefore, it can be argued that the crystallinity of a mineral will play a role in the acid formation potential of a sample. As the gneisses are weathered rocks, it is most likely that both amorphous content and poorly crystalline minerals are present in the rocks. The amorphous and poorly crystalline parts in the rocks could be more reactive, which could explain why gneisses with low amounts of detected S-bearing minerals are acid-producing. To investigate whether the gneiss samples have amorphous content, the gneiss samples were subjected to oxalate extraction (Table 26). To be able to interpret the amorphous content, analysis of the H₂O₂ extract, the oxalate extraction extract, and the pre-treated oxalate extracted material in the H₂O₂ test extraction were performed, making it possible to determine the presence of amorphous and crystalline bounded Fe and S in the gneisses (Tables 27, 28). Most of the Fe and S is bounded in the crystalline phase, but there is amorphous material that contains Fe and S in the selected gneiss samples. Birkeland 5 is the sample with the highest content of amorphous Fe (19.4%) and S (18.1%) (Tables 27, 28), which is expected as this is the sample that is most weathered. The false negative sample, Tingsaker skole #3 has amorphous bounded Fe at 11.4% and S at 8.9% (Tables 27, 28), which could contribute to the explanation that Tingsaker skole #3 is false characterised.

In conclusion, the mineralogy and geochemical data do not explain why most of the rocks are acid-producing. This points out the importance of having other tests to evaluate the sample's acid-producing potential.

6.3 Limitations by the Agder method

6.3.1 Criterion used for quantifying the temperature response

As mentioned in section 1.2.1, the H₂O₂ test used in the Agder method uses temperature increases after 25 minutes to determine the acid-producing potential of a sample. The guideline specifies limit values for $\Delta T_{25\text{min}}$. If $0.7\text{ }^{\circ}\text{C} < \Delta T_{25\text{min}} < 1.2\text{ }^{\circ}\text{C}$ (medium category), the rock could potentially be classified as acid-producing depending on the S content (Prosjektgruppen for kontroll på svovelholdig avrenning i Agder, 2021). The Agder guideline does not give any justification for the choice of the temperature limit values and why temperature should be measured at 25 minutes. The results presented in this study demonstrate that the samples may behave very differently, i.e. the prescribed values are meaningless as will be explained below.

Time used for measurements

Measuring temperature at a given time, in this case 25 minutes, is practical as it is a fast test that is measured at the same time every time. In contrast, a maximum temperature measurement would require more time and equipment. As samples react very differently, it is challenging to set a specific time to measure the temperature increase. The sample's reaction with H_2O_2 is dependent on the mineralogy, such as the sulphide minerals, the availability of the minerals in the sample, the presence of other minerals and oxides, and the reaction pattern when mixed with H_2O_2 . Measuring temperature at 25 minutes could therefore be either too late or too early. For example, in the case of the sample Birkeland 5, which has a high and fast reaction and reaches the maximum temperature after 10 minutes (Figure 25) by the Agder method. This results in cooling down of the samples, resulting in an obvious incorrect $\Delta T_{25 \text{ min}}$. Other samples (Figures 26, 27) show similar issues.

Considering that reaction time and heat generation can occur at different times, the characterisation of the rocks could obviously be affected by changing the $\Delta T_{25 \text{ min}}$ to ΔT_{max} . Lindum (2023) supports this by showing that several samples are upgraded to acid-producing when using ΔT_{max} (Table 33), which is not time dependent. Changing the $\Delta T_{25 \text{ min}}$ to ΔT_{max} would potentially limit the false classification, especially for samples that are acid-producing but uses longer time to react than the respectively 25 minutes. The test would benefit from using the ΔT_{max} as there is lesser risk of cooling. The samples would benefit from having more reaction time as sulphides could be unavailable for H_2O_2 , as the sulphides could be covered by Fe oxides that need to be removed before being available for H_2O_2 . There might be a lesser risk of having different classifications on the same sample if it is allowed to react fully with the H_2O_2 , i.e. it would increase reproducibility. Changing the $\Delta T_{25 \text{ min}}$ to ΔT_{max} would not limit the wrong classification of rocks that contain minerals that are not acid-producing but are reactive with H_2O_2 . Examples of this case are Arendal legevakt 2, 4 and 5, and Eydehavn 1B, which are all samples that shows a significant $\Delta T_{25 \text{ min}}$ but are not acid-producing as confirmed by column experiments (Table 33).

Table 33: The gneiss samples presented as ΔT_{25min} and ΔT_{max} with associated reaction time by the Agder method. Table is modified from Lindum (2023). For temperature columns: red colour means high value (ΔT_{25min} : > 1.2 °C), orange is medium (ΔT_{25min} : 0.7-1.2 °C), and green is low (ΔT_{25min} : < 0.7 °C). Threshold values are from the Agder guideline (Prosjektgruppen for kontroll på svovelholdig avrenning i Agder, 2021). In characterisation: green is not acid-producing, red is acid-producing.

Sample	ΔT_{25min} (°C)	ΔT_{max} (°C)	Reaction time ΔT_{max}	Characterisation ΔT_{25min}	Characterisation ΔT_{max}	pH from column experiment
Eydehavn 1B	3.8	5.0	1.5 hours	Acid-producing	Acid-producing	7.8 (32w)
Tingsaker skole #1	0.8	10.6	3.5 hours	Not acid-producing	Acid-producing	3.6 (22w)
Tingsaker skole #2	0.8	5.7	3.75 hours	Not acid-producing	Acid-producing	3.5 (22w)
Tingsaker skole #3	1.1	11.1	3 hours	Not acid-producing	Acid-producing	3.2 (22w)
RV420#1	0.6	7.3	4 hours	Acid-producing	Acid-producing	2.6 (32w)
Blakstad 3	1.0	4.6	5.5 hours	Not acid-producing	Acid-producing	3.2 (22w)
Birkland 5	32.1	32.1	25 minutes	Acid-producing	Acid-producing	2.3 (32w)
Nordbø 1	0.45	0.85	2.5 hours	Not acid-producing	Not acid-producing	4.3 (32w)
Groos 1	1.25	19.5	1.75 hours	Acid-producing	Acid-producing	2.5 (32w)
Arendal legevakt 2	1.8	3.2	3.25 hours	Acid-producing	Acid-producing	6.6 (42w)
Arendal legevakt 4	1.7	4.7	3 hours	Acid-producing	Acid-producing	6.7 (42w)
Arendal legevakt 5	2.1	5.4	2 hours	Acid-producing	Acid-producing	6.4 (42w)

6.3.2 Environmental conditions bias to temperature change

Changing ΔT_{25min} to ΔT_{max} will not completely solve the problem of false results as the temperature limits significantly contribute when characterising the gneiss. The temperature limits are the deciding factor during the H_2O_2 test, and a temperature limit of 0.7 °C could lead to classification as acid-producing rocks if the S content in the sample is in the high category ($S > 0.8$ wt.%). Such a low temperature change is, therefore, sensitive to environmental conditions during the experiment.

Experimental set up

The temperature measurements could be contaminated by other temperature changes in the laboratory and the experimental set-up. If the samples are done together in a box, such as the set-up for AMIRA single NAG (Figure 9), a very reactive sample would contaminate the low reactive sample. The container type used during the test will influence the results, and the Agder guideline does not specify what type of container should be used, making the use of container type open to interpretation. The type of container would influence the outcome of the results, for example, the use of a beaker vs thermos, where the beaker is more prone to heat loss than the thermos. As a thermos maintains heat, it will give a whole different temperature result. It is most likely used a

beaker during the experiment as this is standard laboratory equipment. The shape and size of the beaker will influence the temperature as it is different properties connected to the area of contact of liquid and air would influence the heat loss, i.e. a bigger beaker would be more prone to heat loss than a smaller beaker, as the areal in contact with air is bigger.

The freshness of the H_2O_2 also influences the reaction between the H_2O_2 and the gneiss sample. The age of the H_2O_2 is important for the freshness; it starts to decompose after being opened. Since H_2O_2 is an unstable chemical, the way of storing the chemical is essential. When exposed to light and heat, H_2O_2 starts to decompose (Roth, 2023). Therefore, the room temperature and the storage container matters. Roth (2023) recommends a storing temperature between 15-25 °C, and even then, there is still a risk of decomposition.

H_2O_2 decomposes faster when exposed to light. During the lab experiments, the Agder method H_2O_2 test was conducted twice on the sample Arendal legevakt 4, once with the light on and once with the light off, resulting in different outcomes. Table 20 presents the results from the Agder test, and it is noteworthy that Arendal legevakt 4 tested in a dark atmosphere did not have a significant temperature change ($\Delta T_{25\text{min}}$ at 0.22 °C), in contrast to when the sample was done in light which resulted in $\Delta T_{25\text{min}}$ of 1 °C.

6.4 Evaluation of the AMIRA method

As mentioned in section 1.2.2, the AMIRA handbook comprises several test methods for predicting the acid drainage potential in a sample. As this handbook mentions all these tests, it makes it possible to choose between several tests, making this handbook more robust to give the best assessment for predicting the acid potential in a sample.

6.4.1 Evaluation of H_2O_2 used in the single NAG test

Before starting with the H_2O_2 experiments on the gneiss samples, paste pH was performed. This will provide a first impression of the acid-producing potential of a sample and is a quick and easy test as it uses 12 hours or overnight (Smart *et al.*, 2002). Paste pH provides information on the easily available acidity in a sample, such as minerals that easily dissolve in water, like jarosite and other acid-producing secondary minerals (Smart *et al.*, 2002). A sample with a low paste pH (less than 5.5) usually turns out acid-producing during further testing with, for example, H_2O_2 during the single NAG test (Olds *et al.*, 2016). Furthermore, the single NAG test with H_2O_2 will provide information on both easily available acidity and acidity through oxidation.

The sample Tingsaker skole #3 had a paste pH of 7.3 (Table 21), which was surprising as the pH from the column test at Lindum is approximately 3 (Figure 28). The past pH indicates that the acidity in this

sample is not easily available. However, the column test and single NAG test (Table 21) show that the oxidation processes will result in acidic runoff from Tingsaker skole #3. This emphasises the importance of using other tests to gain a better understanding of the sample. The sample Birkeland 5, was expected to have a low paste pH as it is a well-weathered rock. This was indeed the case as the paste pH was 4.2. The low paste pH indicates that there is easily available acidity in Birkeland 5. Furthermore, the column pH of around 3 confirms that this is an acid-producing rock. The NAG pH is around 2.8 for Birkeland 5, which is lower than the column pH. This could suggest that more pyrite is oxidised by the H₂O₂ compared to the column tests. Arendal legevakt 4 has a paste pH of 7.8, a column pH of approximately 7.8, and a NAG pH of 6.8. This sample is not acid-producing, but it can be argued that there might be tracers of acid-producing minerals as the NAG pH is lower than the column pH.

Characterisation through the AMIRA single NAG method uses NAG pH and NAG calculations to predict the net acid generation of a sample. The sample Birkeland 5 had the lowest NAG pH and the highest NAG, which led to the classification of the sample as acid-producing (Table 21). This was expected as the theory behind the paste pH is that pH below 5.5 is often acid-producing rocks (Olds *et al.*, 2016). Tingsaker skole #3 had a low NAG pH and a high NAG, which led to the classification as acid-producing rocks, whereas Arendal legevakt 4 had a high NAG pH at 6.8, and a low NAG resulted in the sample being classified as non-acid-producing (Table 21). In conclusion, the results from the single NAG test and column experiments correspond well, as the acid-producing samples are acid-producing in both the column test and the single NAG test.

The gneiss samples that were pre-treated with oxalate extraction of Fe and Al oxides before the single NAG test show that the single NAG test and the classification are not affected by the extraction of the oxides (Table 23). This is very interesting as it shows that the AMIRA single NAG method is more reliable as the final classification was not affected when it is based on NAG pH and NAG, while temperature measurements were clearly affected by removing Fe oxides (Figures 29, 30, 31). This emphasises that temperature measurements are more sensitive to other non-acid generating minerals.

Compared to the Agder method, which uses temperature measurements, the AMIRA single NAG method has proven to be more stable and reliable. This is also shown by the fact that the samples Birkeland 5, Arendal legevakt 4 and Tingsaker skole #3 are done in two separate experiments by the single NAG method, which gave the same classification for the same sample. What is seen in the AMIRA single NAG method is that the NAG pH is stable, but the titration with NaOH varies more, and this is carried forward into the NAG calculations (Table 21). However, the small variations do not

affect the final classification, which is the same for the same type of sample. In contrast, the Agder method showed that samples Birkeland 5 and Tingsaker skole #3 are classified as acid-producing rocks (combined with the S content, Table 20). Arendal legevakt 4 was classified as a non-acid-producing rock (combined with the S content, Table 20). These classifications are in agreement with the column experiments (Table 33). However, the classification done by Lindum (2023) on the same sample material shows different results for Tingsaker skole #3 and Arendal legevakt 4 (Table 33). Tingsaker skole #3 is characterised as non-acid-producing, and Arendal legevakt is characterised as acid-producing by using $\Delta T_{25 \text{ min}}$ by Lindum (2023). This emphasises that classification through the Agder method $\Delta T_{25 \text{ min}}$ could vary for the same sample, which is concerning. This supports the claim that the AMIRA single NAG method is a more stable method than the Agder method.

6.4.2 Considerations during the AMIRA single NAG procedure

During the AMIRA single NAG procedure, the pH in the H_2O_2 solution used in the experiments in this report was not adjusted with NaOH to $\text{pH} > 4.5$, as the method description in Smart et al. (2002) says. It is recommended to adjust the pH because the stabilising agents in the H_2O_2 can influence the tests. Phosphoric acid is one of the stabilising agents in the H_2O_2 used during the experiments, which means that the results could be affected by the stabilising agents. As temperature changes were logged during the experiment, a decision was made to not adjust the pH. One of the reasons for not adjusting the pH was to ensure that the H_2O_2 was less exposed to light, which could influence the temperature logging results. Adjusting the H_2O_2 would take a long time and therefore increase the chance that light affected the H_2O_2 .

6.4.3 Advantages and disadvantages of the AMIRA

There are advantages and disadvantages with the AMIRA method. Firstly, it is beneficial that the AMIRA handbook addresses several assessment methods of acid-forming material. This makes it possible to assess the material in several different ways. However, the single NAG test is widely used in several countries and tested thoroughly. In Sweden, the single NAG test is widely (Frogner-Kockum et al., 2015; Miškovský *et al.*, 2022). The single NAG test is standardised and available at approved labs in contrast to the Agder method.

It is also advantages that after the reaction with H_2O_2 the sample is heated up to deplete leftover H_2O_2 and release potential buffering capacity (Stewart et al., 2006). There are also advantages during the execution of the method that the H_2O_2 concentration used in the experiments is 15%, which is easy to mix as the ratio is 1:1 between 30% H_2O_2 and milli-Q water, compared to the Agder method where the H_2O_2 has a concentration at 7%. This would limit the potential errors related to the concentration of the H_2O_2 . Another advantage is that the single NAG test appears to be more stable

than the Agder method. For example, pre-treated gneiss material with oxalate extraction (Table 22) is characterised at the same acid potential as the ordinary test (Table 21), which indicates that the single NAG test is more stable and less susceptible to the effects of, for example, Fe oxides.

The disadvantages of the AMIRA single NAG method are that it requires more equipment and chemicals than the Agder method, as the single NAG test requires a hotplate, H₂O₂, and NaOH. The adjustment with NaOH of H₂O₂ takes longer time than just adding H₂O₂ to the sample material, it will also expose the H₂O₂ to light. Another consideration is that the single NAG method without kinetic test (temperature logging) does not provide any information on the temperature increase, which could indicate the oxidation of sulphide minerals and the presence of reactive Fe oxides. During the experiment it is important to fully decompose the H₂O₂, due to an acidic pH (around 3) in the H₂O₂ as leftover could influence NAG pH and the classification of the rocks. The heating process has an effect, confirmed by doing unofficial measurements of the pH on the sample Arendal legevakt 4 (NAG pH around 6.8), where the pH becomes higher the more depleted the H₂O₂ becomes.

However, there is a possibility that the single NAG method may overestimate the acid potential in a sample as it is done at particles below 75 µm, and H₂O₂ would theoretically oxidise all available sulphide minerals, which may not be available in a natural sample in field conditions.

6.5 Representative sampling

6.5.1 Sampling

Representative sampling is essential as this can influence the results. Since the yellow crust material in the gneisses is regarded as the acid-producing factor, it might be more beneficial to test in this material. This is one of the challenges when using drilling dust as test material, as this often represents bulk materials and could dilute the sample with non-acid-forming minerals. The dilution of the yellow crust would particularly apply in cases where mineralogy and geochemical analysis are performed. However, bulk materials could provide information on how the assumed acid-forming material (yellow crust) will behave in conjunction with the rest of the gneiss mass, considering the presence of acid consuming minerals such as calcite, dolomite, and to a lesser extent, plagioclase.

6.5.2 Biological matter and reaction with H₂O₂

Well-known in soil science, H₂O₂ is used to remove of biological matter. Using H₂O₂ is an efficient way of removing biological matter (Leifeld and Kögel-Knabner, 2001). As this process is based on the oxidation of the biological matter, this will also generate heat. Therefore, when using drilling dust during the Agder test, it is essential to remember that polluted samples with biological matter could lead to false temperature increases.

7 Conclusion

The current method to characterise acid-producing gneisses, the so-called Agder method, in which H_2O_2 temperature tests are used, leads to an incorrect classification. There are uncertainties associated by using temperature increases as classification requirements. The H_2O_2 test is biased, and there are other tests available that are better suited for assessing acid-producing gneiss. With reference to the aims defined for this study, the following conclusions can be drawn:

- **Investigate if secondary minerals may affect temperature changes during the H_2O_2 test and cause false negative or false positive results.**
 - The results show that secondary minerals influence the temperature logging during the AMIRA single NAG method, which can be transferred to the Agder method. Several secondary minerals that do not contain S react exothermally with H_2O_2 , which causes temperature increases leading to a false characterisation of the gneisses.
 - Iron oxides in the presence of H_2O_2 will react differently. Ferrihydrite, Fe(III)sulphate, and Fe(III) Cl_3 react strongly with H_2O_2 , while LS-tailings hardly react with H_2O_2 . This implies that the exothermic reaction is dependent on the type of Fe oxide.
 - Ferrihydrite in the presence of pyrite causes an endothermic reaction, and the more pyrite present, the lower the heat release, as seen in the ferrihydrite-pyrite-quartz (ferrihydrite fixed at 0.5 g) mixtures. However, it appears that the amount of ferrihydrite will affect the exothermic reaction, seen in ferrihydrite-pyrite-quartz (fixed amount of pyrite), where ferrihydrite in increasing amounts results in higher temperature increases.
 - By removing the Fe oxides through oxalate extraction, the gneiss samples reacted less than the original material containing Fe oxides. This supports the conclusion that secondary minerals influence the temperature increase during the AMIRA single NAG test and, therefore, also the Agder method.
 - The Agder method results in false characterisation of gneisses because of temperature measurements, in general there are small amounts of S-bearing minerals detected in the gneiss samples. However, most of them have Fe oxides and amorphous material. There is no clear correlation between acid-forming minerals and heat generation, as non-acid-forming samples react with H_2O_2 .
- **Evaluate the AMIRA single NAG test, with NAG pH and temperature logging.**
 - Evaluation of the AMIRA method single NAG test shows that it is an overall more stable and reliable test compared to the Agder method.
 - Compared to the Agder method, which uses temperature increases after 25 minutes, AMIRA uses NAG pH and NAG calculation after H_2O_2 has been decomposed when assessing

the acid-producing gneisses. By not using temperature increases as an assessment factor will limit the errors of false temperature increases.

As there is no clear correlation between acid-forming minerals and heat generation through H₂O₂, the Agder method H₂O₂ test is clearly biased by secondary minerals and minerals that can generate heat but are not acid-producing. This shows that there is a need for changing the Agder method as it is biased by secondary minerals, environmental conditions, i.e. containers, H₂O₂ freshness, light conditions, sample representative, and causes wrong classification of acid-producing gneisses.

I recommend changing the Agder guideline, with a special need to replace the H₂O₂ test that uses temperature increases as a characterisation requirement. The AMIRA single NAG test and paste pH are recommended to implement as a quick test instead of the H₂O₂ test in the Agder method. The single NAG test does not rely on temperature changes but rather on the oxidation and dissolution of acid-producing minerals, which is more reliable.

8 Future work for improvement in assessment of acid-producing rocks

Assessing acid-producing rocks is challenging, and the industry is asking for clearer guidelines on how to assess acid-producing rocks. As mentioned in section 1.1, there is a national guideline called *“Identifisering og karakterisering av syredannende bergarter”* written by the Norwegian Geotechnical Institute for the Norwegian Environment Agency, unfortunately, this guideline does not assess the acid-producing gneiss. However, *“Retningslinjer for tiltak i områder med syredannende gneis»* written by the Prosjektgruppen for kontroll av svovelholdig avrenning i Agder (Project Group for Control of sulphurs runoff in Agder) assess the acid-producing gneiss. There is a need for updating the guidelines, which includes both gneisses, alum shale and other potential acid-producing rocks, i.e. collect the guidelines in one place and update them.

Improvement of the Agder guideline should be prioritised, as it is leading to false classifications and environmental problems. It is difficult to classify a rocks acid potential through the S content and the degree of weathering. A sample with low S content could be acid-producing, and during this report it is not observed any good correlations between the S content and the acid-producing potential in a sample. Assessment of the degree of weathering today is organised in a way that if the rocks are highly or well weathered, the rocks are automatically classified as acid-producing. However, the assessment of the weathering degree is based on a judgment call by a geologist without a standard method. A recommendation to describe a standardised method should be prioritised. An assessment of the weathering degree could involve the colour of the rock, grain size, foliation, mechanical resistance, and mineralogy, such as feldspar can crumble along grain boundaries and biotite could change colour to more brown or yellow (Anke Degelmann, e-mail correspondence April 2024). The colour of the rocks is a very important factor as weathered sulphide minerals normally turn to the Fe oxides goethite (dark brown-red), hematite (dark purple), and other Fe oxides with normal rust in the colour orange-red (Anke Degelmann, e-mail correspondence April 2024), and jarosite in a brown colour (Hagelia, 2023). The H₂O₂ test must be replaced, and preferably with a standard test such as the AMIRA single NAG test and paste pH. This will provide the opportunity to send the samples to approved laboratories.

9 References list

Akcil, A. and Koldas, S. (2006) 'Acid mine drainage (AMD): causes, treatment and case studies', *Journal of Cleaner Production*, 14(12–13), pp. 1139–1145. Available at: <https://doi.org/10.1016/j.jclepro.2004.09.006>.

De Laat, J., Truong Le, G. and Legube, B. (2004) 'A comparative study of the effects of chloride, sulfate and nitrate ions on the rates of decomposition of H₂O₂ and organic compounds by Fe(II)/H₂O₂ and Fe(III)/H₂O₂', *Chemosphere*, 55(5), pp. 715–723. Available at: <https://doi.org/10.1016/j.chemosphere.2003.11.021>.

Desborough, G.A., Smith, K.S., Lowers, H.A., Swayze, G.A., Hammarstrom, J.M., Diehl, S.F., Leinz, R.W. and Driscoll, R.L. (2010) 'Mineralogical and chemical characteristics of some natural jarosites', *Geochimica et Cosmochimica Acta*, 74(3), pp. 1041–1056. Available at: <https://doi.org/10.1016/j.gca.2009.11.006>.

Dold, B. (2017) 'Acid rock drainage prediction: A critical review', *Journal of Geochemical Exploration*, 172, pp. 120–132. Available at: <https://doi.org/10.1016/j.gexplo.2016.09.014>.

Dublet, G., Lezama Pacheco, J., Bargar, J.R., Fendorf, S., Kumar, N., Lowry, G.V. and Brown, G.E. (2017) 'Partitioning of uranyl between ferrihydrite and humic substances at acidic and circum-neutral pH', *Geochimica et Cosmochimica Acta*, 215, pp. 122–140. Available at: <https://doi.org/10.1016/j.gca.2017.07.013>.

Eurofins (2023) 'Analyser för sulfid innehållande jord, lera och berg'. Available at: <https://www.eurofins.se/tjaenster/miljoe-och-vatten/nyheter-miljo/analyser-foer-sulfidinnehaallande-jord-lera-och-berg/> (Accessed: 18 April 2024).

Frogner-Kockum, P., Loorents, K.-J. and Lindgren, Å. (2015) 'Handbok för hantering av sulfidförande bergarter'. 1. *Trafikverket*. pp. 1-51 Available at: <https://trafikverket.diva-portal.org/smash/record.jsf?pid=diva2%3A1364275&dswid=-709>.

Gasharova, B., Göttlicher, J. and Becker, U. (2005) 'Dissolution at the surface of jarosite: an in situ AFM study', *Geochemistry of Sulfate Minerals: A tribute to Robert O. Rye*, 215(1–4), pp. 499–516. Available at: <https://doi.org/10.1016/j.chemgeo.2004.06.054>.

Hagelia, P. (2015) 'Impact of iron sulfides and secondary sulfate minerals on the potential for acid rock drainage (ARD)', in: *12th Urban environment symposium urban future for a sustainable world*, Oslo. Available at: <http://dx.doi.org/10.13140/RG.2.2.17208.65287>.

Hagelia, P. (2023) 'Sur avrenning frå rusta svovelförande gneis'. Statens vegvesens report 922. *Statens vegvesen*. pp.1-153 Available at: <https://hdl.handle.net/11250/3083450>.

Hammarstrom, J.M., Seal, R.R., Meier, A.L. and Kornfeld, J.M. (2005) 'Secondary sulfate minerals associated with acid drainage in the eastern US: recycling of metals and acidity in surficial environments', *Chemical Geology*, 215(1–4), pp. 407–431. Available at: <https://doi.org/10.1016/j.chemgeo.2004.06.053>.

Haraldsen, H. and Pedersen, B. (2023) 'Jernoksider', *Store norske leksikon*. Available at: <https://snl.no/jernoksider> (Accessed: 7 March 2024).

Hindar, A. (2012) 'E18 Grimstad-Kristiansand gjennom sulfidholdige bergarter - syreproduksjon og effekter på avrenningsvann', in: *Norsk vannforening*. Available at: <https://vannforeningen.no/dokumentarkiv/e18-grimstad-kristiansand-gjennom-sulfidholdige-bergarter-syreproduksjon-og-effekter-pa-avrenningsvann/>.

Kampestuen, K.Å. (2020) 'Tonnevis med gift renner hvert år i elva fra nedlagt gruve – staten som eier har ingen løsning', *nrk.no*. Available at: <https://www.nrk.no/innlandet/talmodigheten-slutt--staten-ma-ordne-opp-i-gruveforurensning-i-folldal-1.14909479> (Accessed: 20 February 2024).

Knobloch, M. and Lottermoser, B.G. (2020) 'Infrared thermography: A method to visualise and analyse sulphide oxidation', *Minerals*, 10(11), pp. 933. Available at: <http://dx.doi.org/10.3390/min10110933>.

Krogstad, T., Børresen, T. and Almås, Å. (2018) 'Field and laboratory methods for the analysis of soil'. *NMBU: Faculty of environmental science and natural resources management*, pp. 35.

Leifeld, J. and Kögel-Knabner, I. (2001) 'Organic carbon and nitrogen in fine soil fractions after treatment with hydrogen peroxide', *Soil Biology and Biochemistry*, 33(15), pp. 2155–2158. Available at: [https://doi.org/10.1016/S0038-0717\(01\)00127-4](https://doi.org/10.1016/S0038-0717(01)00127-4).

Lindum AS (2023) 'Sluttrapport: Karakterisering av syredannende gneis - kunnskapsgrunnlag for utforming av retningslinjer'. Unpublished report.

McLennan, S.M. (2001) 'Relationships between the trace element composition of sedimentary rocks and upper continental crust', *Geochemistry, Geophysics, Geosystems*, 2(4). Available at: <https://doi.org/10.1029/2000GC000109>.

Miškovský, K., Bida, J., Arvidsson, H., Göransson, M., Andersson, J., Lövgren, L. and Johansson, E. (2022) 'Sluttrapport: Utveckling av effektiva och relevanta metoder för bedömning av bergmaterial innehållande metallförande sulfidmineral'. *Umeå: ENVIX*. pp. 1-96 Available at: <https://vti.diva-portal.org/smash/record.jsf?pid=diva2%3A1795551&dswid=-2456>.

Nijland, T.G., Harlov, D.E. and Andersen, T. (2014) 'The Bamble sector, South Norway: A review', *Geoscience Frontiers*, 5(5), pp. 635–658. Available at: <https://doi.org/10.1016/j.gsf.2014.04.008>.

Nordstrom, D. and Alpers, C. (1999) 'Geochemistry of acid mine waters', in *The Environmental Geochemistry of Mineral Deposits. Part A. Processes, Methods, and Health Issues*, pp. 133–160. Available at: https://www.researchgate.net/publication/236246844_Geochemistry_of_acid_mine_waters.

Olds, W., Bird, B., Pearce, J., Sinclair, E., Orr, M. and Weber, P. (2016) 'Geochemical classification of waste rock using process flow diagrams', in *AusIMM New Zealand Branch Annual Conference 2015*, New Zealand, pp. 307–218. Available at: <http://dx.doi.org/10.13140/RG.2.1.4404.0564>.

Oorschot, I. and Dekkers, M. (2001) 'Selective dissolution of magnetic iron oxides in the acid–ammonium oxalate/ferrous iron extraction method—I. Synthetic samples', *Geophysical Journal International*, 145(3), pp. 740–748. Available at: <https://doi.org/10.1046/j.0956-540x.2001.01420.x>.

Paterson, E., Goodman, B.A., and Farmer, V.C. (1991) 'The chemistry of aluminium, iron and manganese oxides in acid soils', in B. Ulrich and M.E. Sumner (eds) *Soil Acidity*. Berlin, Heidelberg: Springer Berlin Heidelberg, pp. 97–124. Available at: https://doi.org/10.1007/978-3-642-74442-6_5.

Pearce, A. (2018) 'A mineralogical and geochemical description of potentially acid-producing gneisses from the Lillesand Area - Implications for leaching behaviour'. Master thesis. *UiO - University in Oslo*. pp. 1 -147. Available at: <http://urn.nb.no/URN:NBN:no-66959>.

Prosjektgruppen for kontroll på svovelholdig avrenning i Agder (2021) 'Retningslinjer for tiltak i områder med syredannende gneis: Felles saksbehandlingsrutiner, krav til prøvetakning, klassifisering av steinmasser og miljøoppfølging. Versjon 2,4' pp. 1-65.

Raade, G. (2023) 'Sekundærmineral', *Store norske leksikon*. Available at: <https://snl.no/sekund%C3%A6rmineral> (Accessed: 11 november 2023).

Roth (2023) 'Sikkerhetsdatablad Hydrogenperoksyd 30%'. Available at: <https://www.carlroth.com/medias/SDB-9681-NO-NO.pdf?context=bWFzdGVyfHNIY3VyaXR5RGF0YXNoZWV0c3wzNDQ0ODF8YXBwbGljYXRpb24vcGRmfHNIY3VyaXR5RGF0YXNoZWV0cy9oNGIvaGY3LzlxMDM0ODI3MTYxOTAucGRmfGZjYTBiYWNmMjczZDY0ODExOGVINjJMDA4NzNkYjRiYzAyODMzMzMGVjNzEyNWJjNjdiY2QzMzYjBjZjdmNGQ>.

Russo, V., Protasova, L., Turco, R., de Croon, M.H.J.M., Hessel, V. and Santacesaria, E. (2013) 'Hydrogen peroxide decomposition on manganese oxide supported catalyst: From batch reactor to continuous microreactor', *Industrial & Engineering Chemistry Research*, 52(23), pp. 7668–7676. Available at: <https://doi.org/10.1021/ie303543x>.

Skjønborg, I. (2023) 'An evaluation of methods for acid rock drainage prediction'. Master thesis. *UiO - University in Oslo*. pp. 1- 213. Available at: <https://www.duo.uio.no/bitstream/handle/10852/105981/Skjonborg---An-evaluation-of-methods-for-ARD-prediction.pdf?sequence=1&isAllowed=y>.

Smart, R., Skinner, B., Levay, G., Gerson, A., Thomas, J., Sobieraj, H., Schumann, R., Weisener, C. and Weber, P. (2002) 'ARD test handbook: Prediction and kinetic control of acid mine drainage'. *Ian Wark Research Institute*.

Smith, A.M.L., Hudson-Edwards, K.A., Dubbin, W.E. and Wright, K. (2006) 'Dissolution of jarosite [KFe₃(SO₄)₂(OH)₆] at pH 2 and 8: Insights from batch experiments and computational modelling', *Geochimica et Cosmochimica Acta*, 70(3), pp. 608–621. Available at: <https://doi.org/10.1016/j.gca.2005.09.024>.

Stewart, W.A., Miller, S.D. and Smart, R. (2006) 'Advances in acid rock drainage (ARD) characterisation of mine wastes', in: *International Conference on Acid Rock Drainage (ICARD)*, St. Louis MO.: American Society of Mining and Reclamation (ASMR), pp. 2098–2119. Available at: <http://dx.doi.org/10.21000/JASMR06022098>.

Teel Amy, L., Finn Dennis D., Schmidt Jeremy T., Cutler Lynn M., and Watts Richard J. (2007) 'Rates of trace mineral - Catalyzed decomposition of hydrogen peroxide', *Journal of Environmental Engineering*, 133(8), pp. 853–858. Available at: [https://doi.org/10.1061/\(ASCE\)0733-9372\(2007\)133:8\(853\)](https://doi.org/10.1061/(ASCE)0733-9372(2007)133:8(853)).

Teien, H.-C., Pettersen, M.N., Kassaye, Y.A., Hindar, A., Lind, O.C. and Håvardstun, J. (2017) 'Aluminium og spormetaller i Kaldvellfjorden- tilstandsformer og opptak i fisk'. Fagrapport 47. Ås: *NMBU*. pp. 1- 61. Available at: <https://hdl.handle.net/11250/2648382>.

Vafaei Molamahmood, H., Geng, W., Wei, Y., Miao, J., Yu, S., Shahi, A., Chen, C. and Long, M. (2022) 'Catalyzed H₂O₂ decomposition over iron oxides and oxyhydroxides: Insights from oxygen production and organic degradation', *Chemosphere*, 291(1), pp. 133037. Available at: <https://doi.org/10.1016/j.chemosphere.2021.133037>.

Warren, L.A. (2011) 'Acid rock drainage', in J. Reitner and V. Thiel (eds) *Encyclopedia of Geobiology*. Dordrecht: Springer Netherlands, pp. 5–8. Available at: https://doi.org/10.1007/978-1-4020-9212-1_3.

Welch, S.A., Kirste, D., Christy, A.G., Beavis, F.R. and Beavis, S.G. (2008) 'Jarosite dissolution II— Reaction kinetics, stoichiometry and acid flux', *Chemical Geology*, 254(1–2), pp. 73–86. Available at: <https://doi.org/10.1016/j.chemgeo.2008.06.010>.

Xu, G., Chen, C., Shen, C., Zhou, H., Wang, X., Cheng, T. and Shang, J. (2022) 'Hydrogen peroxide and high-temperature heating differently alter the stability and aggregation of black soil colloids', *Chemosphere*, 287(1), pp. 132018. Available at: <https://doi.org/10.1016/j.chemosphere.2021.132018>.

Zarroca, M., Roqué, C., Linares, R., Salminci, J.G. and Gutiérrez, F. (2021) 'Natural acid rock drainage in alpine catchments: A side effect of climate warming', *Science of The Total Environment*, 778, pp. 146070. Available at: <https://doi.org/10.1016/j.scitotenv.2021.146070>.

Appendix

Appendix A: Paste pH and EC of gneiss samples, quartz and ferrihydrite

Raw data from paste pH and EC of gneiss samples.

Sample	Sample number	Weight rock (g)	milli-Q water (mL)	pH	Mean pH	EC ($\mu\text{S/cm}$)	Mean EC ($\mu\text{S/cm}$)	SD EC ($\mu\text{S/cm}$)	Temperature ($^{\circ}\text{C}$)
Tingsaker skole #3	1.1	5	10	7.2		276			17.9
	1.2	5	10	7.4	7.3	374	276.07	97.90	17.9
	1.3	5	10	7.4		178.2			17.9
Arendal legevakt 4	2.1	5	10	8.0		44.5			17.9
	2.2	5	10	7.5	7.8	126.6	105.37	53.51	17.9
	2.3	5	10	8.0		145			17.9
Birkeland 5	3.1	5	10	4.2		1350			17.9
	3.2	5	10	4.2	4.2	1844	1136.33	835.25	17.9
	3.3	5	10	4.2		215			17.9

Raw data from paste pH and EC of quartz and ferrihydrite

Sample	Weight of sample (g)	milli-Q (mL)	pH	EC ($\mu\text{S/cm}$)
Quartz	2.5	250	8.1	13.3
Ferrihydrite	2.5	250	3.6	234

Appendix B: Geochemical raw data

Raw data from geochemical analysis at ALS.

ELEMENT	[unit]	Eydehavn 1B	Arendal legevakt 2	Arendal legevakt 5	Arendal legevakt 4	RV420#1
Aluminium (Al ₂ O ₃)	% dry weight	15	13.5	12.2	13.6	15.4
Phosphorus (P ₂ O ₅)	% dry weight	0.129	0.102	0.0949	0.228	0.132
Jern (Fe ₂ O ₃)	% dry weight	10.6	6.61	6.84	9.42	5.04
Kalium (K ₂ O)	% dry weight	0.901	1.09	0.809	0.818	2.16
Calcium (CaO)	% dry weight	9.19	1.2	1.56	4.51	2.44
Magnesium (MgO)	% dry weight	7.93	1.94	2.05	3.15	1.5
Mangan (MnO)	% dry weight	0.147	0.112	0.148	0.204	0.0627
Natrium (Na ₂ O)	% dry weight	2.56	5.88	5.05	4.92	3.06
SiO ₂	% dry weight	51.6	68.7	67.7	59.2	65.1
Titan (TiO ₂)	% dry weight	0.896	0.449	0.463	0.777	0.571
As (Arsen)	mg/kg TS	<3	<3	<3	<3	4.59
Ba (Barium)	mg/kg TS	283	211	195	135	353
Be (Beryllium)	mg/kg TS	0.865	<0.5	<0.5	<0.5	1.42
Cd (Cadmium)	mg/kg TS	0.15	<0.1	0.102	0.181	<0.1
Co (Cobalt)	mg/kg TS	44.7	7.33	10.5	18.3	6.52
Cr (Krom)	mg/kg TS	386	15.9	11.8	33	41.4
Cu (Kopper)	mg/kg TS	62.8	9.13	16.5	34.7	26.5
Fe (Jern)	mg/kg TS	74500	46300	47900	65900	35300
Hg (Mercury)	mg/kg TS	<0.010	<0.010	<0.010	<0.010	<0.010
Mo (Molybdenum)	mg/kg TS	<5	<5	<5	<5	<5
Nb (Niobium)	mg/kg TS	5.84	<5	<5	<5	9.01
Ni (Nickel)	mg/kg TS	141	3.1	6.46	16.7	10.1
Pb (Lead)	mg/kg TS	4.24	5.9	7.07	8.15	14.6
S (Sulphur)	mg/kg TS	1110	<100	125	559	2190
Sc (Scandium)	mg/kg TS	31.7	16.7	16.1	26.3	11.7
Sn (Tin)	mg/kg TS	<20	<20	<20	<20	<20

Continue of table.

ELEMENT	[unit]	Eydehavn 1B	Arendal legevakt 2	Arendal legevakt 5	Arendal legevakt 4	RV420#1
Sr (Strontium)	mg/kg TS	177	70.9	94.8	165	249
Th (Thorium)	mg/kg TS	2.13	1.91	2.51	1.15	6.25
U (Uranium)	mg/kg TS	0.42	0.293	0.347	0.365	2.03
V (Vanadium)	mg/kg TS	184	55.5	79.6	155	69.7
W (Wolfram)	mg/kg TS	<50	<50	<50	<50	<50
Y (Yttrium)	mg/kg TS	33.4	22.6	20.5	22.2	27.9
Zn (Sink)	mg/kg TS	95.7	74.6	97.8	205	89.2
Zr (Zirconium)	mg/kg TS	114	70.4	70.8	64.9	160
LOI 1000°C	% dry weight	0.486	0.0436	0.104	0.344	0.981
Dry weight 105 °C	%	99.6	99.8	99.6	99.7	99.8
Dry weight 105 °C	%	99.5	99.8	99.6	99.7	99.8
S-SUM-OXID	% dry weight	99	99.6	96.9	96.8	95.5
C-total Karbon-total	% dry weight	0.074	0.056	0.054	0.046	0.035
TIC Total inorganic carbon	% dry weight	0.088	<0.010	<0.010	0.056	<0.010
Total organic carbon (TOC)	% dry weight	<0.10	<0.10	<0.10	<0.10	<0.10

ELEMENT	[unit]	Blakstad 3	Nordbø 1	Tingsaker skole #2	Tingsaker skole #1	Groos #1	Tingsaker skole #3	Birkeland 5
Aluminium (Al ₂ O ₃)	% dry weight	12.2	17.9	15.8	15.4	14.1	16	14.1
Phosphorus (P ₂ O ₅)	% dry weight	0.131	0.186	0.161	0.152	0.181	0.152	0.192
Jern (Fe ₂ O ₃)	% dry weight	4.49	6.85	6.66	6.64	6.59	6.27	10.7
Kalium (K ₂ O)	% dry weight	2.75	1.41	2.17	2.06	2.51	2.04	2.02
Calcium (CaO)	% dry weight	0.622	5.4	2.96	3.14	1.22	3.26	4.09
Magnesium (MgO)	% dry weight	2.14	2.4	1.88	2.22	1.6	2.04	3.11
Mangan (MnO)	% dry weight	0.0268	0.0882	0.0816	0.083	0.0386	0.0804	0.115
Natrium (Na ₂ O)	% dry weight	0.713	4.55	2.92	3.06	2.55	3.13	1.93
SiO ₂	% dry weight	72.7	58.4	67.1	63.8	65.4	65.4	60
Titan (TiO ₂)	% dry weight	0.62	0.577	0.697	0.715	0.656	0.683	1.18
As (Arsen)	mg/kg TS	<3	<3	<3	<3	<3	<3	<3
Ba (Barium)	mg/kg TS	484	313	379	349	447	332	576
Be (Beryllium)	mg/kg TS	0.906	1.45	1.84	1.54	1.15	2.23	1.17
Cd (Cadmium)	mg/kg TS	<0.1	<0.1	0.126	0.146	<0.1	0.105	1.83
Co (Cobalt)	mg/kg TS	8.69	13.8	13.5	16.7	14.5	15.4	18.6
Cr (Krom)	mg/kg TS	54.9	39.7	58.5	45.8	67.1	46.4	69.8
Cu (Kopper)	mg/kg TS	57.5	51.2	40.2	33.4	103	43.2	68.5
Fe (Jern)	mg/kg TS	31400	47900	46600	46500	46100	43800	74800
Hg (Mercury)	mg/kg TS	<0.010	<0.010	<0.010	<0.010	<0.01	<0.01	<0.010
Mo (Molybdenum)	mg/kg TS	<5	<5	<5	<5	<5	<5	<5
Nb (Niobium)	mg/kg TS	12.9	<5	9.67	9.2	10.3	8.41	7.01
Ni (Nickel)	mg/kg TS	13.5	12.9	25	29	32.7	29.8	31.8
Pb (Lead)	mg/kg TS	4.72	7.71	10.7	11.9	14.5	11.1	11
S (Sulphur)	mg/kg TS	1980	531	7120	7330	11400	5160	13000
Sc (Scandium)	mg/kg TS	11.3	14.7	15	14.2	15.6	12.3	25.5
Sn (Tin)	mg/kg TS	<20	<20	<20	<20	<20	<20	<20
Sr (Strontium)	mg/kg TS	48.7	720	263	280	99.6	307	145
Th (Thorium)	mg/kg TS	12.9	3.59	7.62	7.42	10.3	6.2	4.02
U (Uranium)	mg/kg TS	2.53	1.14	2.35	2.2	3.93	2.11	2.67

Continue of table.

ELEMENT	[unit]	Blakstad 3	Nordbø 1	Tingsaker skole #2	Tingsaker skole #1	Groos #1	Tingsaker skole #3	Birkeland 5
V (Vanadium)	mg/kg TS	60.5	113	92.4	122	80.4	96.6	232
W (Wolfram)	mg/kg TS	<50	<50	<50	<50	<50	<50	<50
Y (Yttrium)	mg/kg TS	28.8	12.7	25.9	27.9	36.9	21.5	29
Zn (Sink)	mg/kg TS	40.1	87.6	80.6	96.7	78.9	89.9	291
Zr (Zirconium)	mg/kg TS	363	97.9	171	160	207	157	130
LOI 1000°C	% dry weight	1.86	0.798	0.951	1.13	2.64	0.914	3.13
Dry weight 105 °C	%	99.8	99.7	99.9	99.9	99.8	99.8	99.3
Dry weight 105 °C	%	99.8	99.7	99.7	88.1	99.8	99.8	99.2
S-SUM-OXID	% dry weight	96.4	97.8	100	97.3	94.8	99.1	97.4
C-total Karbon-total	% dry weight	0.109	0.258	0.13	0.084	0.433	0.071	0.229
TIC Total inorganic carbon	% dry weight	<0.010	<0.010	<0.010	<0.010	<0.010	<0.010	<0.010
Total organic carbon (TOC)	% dry weight	0.11	0.26	0.13	<0.10	0.43	<0.10	0.23

Appendix C: Raw data from single NAG test by AMIRA

Single NAG test experiment done by AMIRA method.

Dato	Sample	H2O2 pH	15% H2O2 (ml)	NaOH to H2O2	Exposure to light (min)	Paste pH	NAG pH	NAG pH - H2O2 pH	EC (µS/cm)	Temperature for pH (°C)	Solution to titration (mL)	Titration to pH 4,5 (mL)	Titration pH 4,5 to pH 7 (mL)	Total NaOH (mL)	NAG ((49*M*V)/W)
	Tingsaker skole #1	3.4	250	0	Transmission only	2.7			1162.0	18.2	200	8.35	1.71	10.06	19.7
	Tingsaker skole #1	4.5	250	0.55	15	2.7			1261.0	18.2				0	0.0
31.10.2023	Tingsaker skole #3	3.3	250	0	minimal	7.3	2.9	-0.4	810	21.6	200	3.225	2	5.225	10.2
31.10.2023	LS tailings	3.3	250	0	minimal	4.6	3.4	0.1	349	22.3	200	1	0.08	1.08	2.1
02.11.2023	Birkeland 5	3.3	250	0	minimal	4.2	2.7	-0.6	1425	21.6	200	8.54	2.91	11.45	22.4
02.11.2023	Arendal legevakt 4	3.3	250	0	minimal		6.8	3.5	113.6	20	200	0	0.12	0.12	0.2
06.11.2023	Mix 1	3.4	250	0	minimal		2.6	-0.8	1576	19.8	200	9.215	1.2	10.415	20.4
06.11.2023	LS Mix 2	3.4	250	0	minimal		2.7	-0.7	1571	17.3	200	9.33	1.21	10.54	20.7
08.11.2023	LS mix 3	3.3	250	0	minimal		2.7	-0.6	1036	19.5	200	4.81	0.77	5.58	10.9
08.11.2023	LS mix 4	3.3	250	0	minimal		3.0	-0.3	686	20.6	200	2.86	0.905	3.765	7.4
13.11.2023	Quartz	3.2	250	0	minimal	8.1	3.8	0.5	123.4	21.3	200	0.4	0.55	0.95	1.9
16.11.2023	Pyrite mix 2 (0.75 wt.% S)	3.3	250	0	minimal		2.6	-0.7	1432	19.6	200	7.34	0.85	8.19	16.1
16.11.2023	Pyrite mix 4 (0.25wt.%S)	3.3	250	0	minimal		2.9	-0.3	534	22.6	200	2	0.6	2.6	5.1
17.11.2023	Arendal legevakt 4	3.3	250	0	minimal		6.9	3.6	109.3	22.1	200	0	0.09	0.09	0.2
17.11.2023	Pyrite mix 3 (0.5wt.%S)	3.3	250	0	minimal		2.6	-0.7	1046	22.6	200	6.54	0.78	7.32	14.3
20.11.2023	LS mix 3 (0.5wt.%S)	3.2	250	0	minimal		2.6	-0.6	1049	22.4	200	5.32	1.15	6.47	12.7
20.11.2023	Ferrihydrite mix 3 (0.5wt.%S) (0.5g ferrihydrite)	3.2	250	0	minimal		3.0	-0.2	473	19.7	200	1.93	0.42	2.35	4.6
21.11.2023	Birkland 5	3.2	250	0	minimal		2.4	-0.8	1911	22.2	200	9.71	4.2	13.91	27.3
21.11.2023	Pyrite mix 1 (1wt.%S)	3.2	250	0	minimal		2.3	-0.9	1781	21.3	200	10.2	2.4	12.6	24.7

Continue of table.

Dato	Sample	H2O2 pH	15% H2O2 (ml)	NaOH to H2O2	Exposure to light (min)	Paste pH	NAG pH	NAG pH - H2O2 pH	EC (µS/cm)	Temperature for pH (°C)	Solution to titration (mL)	Titration to pH 4,5 (mL)	Titration pH 4,5 to pH 7 (mL)	Total NaOH (mL)	NAG ((49*M*V)/W)
22.11.2023	Ferrihydrite mix 2 (0.75 wt.% S)(0.5g ferrihydrite)	3.2	250	0	minimal	2.8	-0.4	864	21	200	4.02	0.81	4.83	9.5	
22.11.2023	Ferrihydrite mix 4 (0.25 wt.% S)(0.5g ferrihydrite)	3.2	250	0	minimal	3.7	0.5	161	21.5	200	0.4	1.1	1.5	2.9	
23.11.2023	LS mix 3 (0.5wt.%S)	3.2	250	0	minimal	3.0	-0.2	726	19.8	200	2.6	1.96	4.56	8.9	
23.11.2023	LS mix 2 (0.75wt.%S)	3.2	250	0	minimal	2.8	-0.4	977	23.8	200	3.73	1.78	5.51	10.8	
24.11.2023	Ferrihydrite mix 3, 0,25g ferrihydrite (0.5wt.%S)	3.3	250	0	minimal	2.8	-0.5	716	21.9	200	3.42	1	4.42	8.7	
24.11.2023	Ferrihydrite mix 3, 0,05g ferrihydrite (0.5wt.%S)	3.3	250	0	minimal	2.6	-0.6	947	25.3	200	4.5	1.25	5.75	11.3	
27.11.2023	Pyrite mix 1 (1wt.%S)	3.3	250	0	minimal	2.3	-1.0	1745	22.8	200	9.48	3.75	13.23	25.9	
27.11.2023	Ferrihydrite 5 (0.12wt.%S)(0.5g ferrihydrite)	3.3	250	0	minimal	4.1	0.8	106.8	24.3	200	0.16	0.29	0.45	0.9	
28.11.2023	Pyrite 3 (0.5wt.%S)	3.2	250	0	minimal	2.6	-0.6	976	24.6	200	5.11	0.23	5.34	10.5	
28.11.2023	Ferrihydrite1 (1wt.%S)(0.5g ferrihydrite)	3.2	250	0	minimal	2.6	-0.6	1120	22.4	200	5.38	0.5	5.88	11.5	
29.11.2023	Pyrite 4 (0.25wt.%S)	3.2	250	0	minimal	2.9	-0.3	613	18.2	200	3	0.2	3.2	6.3	
29.11.2023	Ferrihydrite 2 (0.75wt.%S)(0.5g ferrihydrite)	3.2	250	0	minimal	2.7	-0.5	915	21.8	200	4.12	0.69	4.81	9.4	
30.11.2023	Pyrite 2 (0.75wt.%S)	3.2	250	0	minimal	2.5	-0.8	1512	18.9	200	8.5	1.25	9.75	19.1	
30.11.2023	Ferrihydrite 3 (0.5wt.%S)(0.5g ferrihydrite)	3.2	250	0	minimal	3.0	-0.2	507	16	200	2	0.49	2.49	4.9	

Continue of table.

Dato	Sample	H2O2 pH	15% H2O2 (ml)	NaOH to H2O2	Exposure to light (min)	Paste pH	NAG pH	NAG pH - H2O2 pH	EC (μ S/cm)	Temperature for pH ($^{\circ}$ C)	Solution to titration (mL)	Titration to pH 4,5 (mL)	Titration pH 4,5 to pH 7 (mL)	Total NaOH (mL)	NAG ((49*M*V)/W)
01.12.2023	Tingsaker skole 3 Ferrihydrite 1 (1wt.%S)(0.5g	3.2	250	0	minimal	3.0	-0.2	744	23.6	200	2.9	2.6	5.5	10.8	
01.12.2023	ferrihydrite) Ferrihydrite 4 (0.25wt.%S)(0.5g	3.2	250	0	minimal	2.7	-0.5	1259	18.4	200	6.6	0.89	7.49	14.7	
04.12.2023	ferrihydrite) Ferrihydrite 3, 0,7g	3.2	250	0	minimal	3.8	0.6	143.1	19.3	200	0.335	0.29	0.625	1.2	
04.12.2023	ferrihydrite (0.5wt.%S) Pure Ferrihydrite, 0.5g	3.2	250	0	minimal	3.4	0.2	303	20	200	1.08	0.4	1.48	2.9	
05.12.2023	ferrihydrite ferrihydrite 5 (0.12wt.%S)(0.5g	3.2	250	0	minimal	3.6	4.7	1.5	78.2	19.3	200	0	0.102	0.102	0.2
06.12.2023	ferrihydrite) Ferrihydrite 3, 0,4g (0.5wt.%S)	3.2	250	0	minimal	4.2	1.0	109.5	21.5	200	0.1	0.2	0.3	0.6	
06.12.2023		3.2	250	0	minimal	3.0	-0.2	566	17	200	2.45	0.265	2.715	5.3	
08.12.2023	Arendal legevakt 4	3.3	250	0	minimal	6.8	3.6	108.4	22.6	200	0	0.105	0.105	0.2	
08.12.2023	Tingsaker skole 3	3.3	250	0	minimal	2.9	-0.4	1009	19.6	200	4.04	2.8	6.84	13.4	
11.12.2023	Birkeland 5 Pure Ferrihydrite, 0.5g	3.2	250	0	minimal	2.5	-0.7	1714	23.1	200	9.87	3.6	13.47	26.4	
11.12.2023	ferrihydrite	3.2	250	0	minimal	3.6	4.4	1.2	91.3	23.1	200	0.045	0.2	0.245	0.5

Appendix D: Raw data from oxalate extraction

Oxalate extraction overview.

Dato	Sample	Comments	Start weight (g)	Weight after washing (g)	Loss of sample (g)	EC start	EC 1	EC 2	EC 3	EC 4
29.01.24	Birkeland 5 (1)	Dropped out of end over end shaker	2.5	2.11	0.39	13300	782	123.7	62.7	25.4
29.01.24	Birkeland 5 (2)	Dropped out of end over end shaker	2.5	1.97	0.53	14220	287	96.4	49.4	17.4
29.01.24	Tingsaker skole #3 (1)	Dropped out of end over end shaker	2.5	2.24	0.26	10690	399	62.1	22	15.3
29.01.24	Arendal legevakt 4 (1)	Dropped out of end over end shaker	2.5	2.22	0.28	12840	426	48	22.8	17.6
30.01.24	Arendal legevakt 4 (2)		2.5	2.37	0.13	17880	248	50.6	23.8	19.3
30.01.24	Ferrihydrite 0.5g, 0.5wt% S	Broke in the centrifuge, tried to save what I can. Did not do H2O2 due to too much broken glass in the sample	2.5			11850	1647	133.8	13.7	
01.02.24	Pyrite, 0.75wt% S		2.5	2.45	0.05		970	180.5	31	6.6
01.02.24	Tingsaker skole 3 (2)		2.5	2.38	0.12		1106	226	51.3	23.3

Appendix E: Overview of existing data on gneiss samples

Project	Sample	Placement of material	Column test	pH, column test	Mineralogy					Chemistry		Agder method H ₂ O ₂ [°C]	AMIRA NAG pH
					XRD	XRD (Fe(II))	XRD (Fe(III))	Amorphous content	Thin section	XRF (Fe ₂ O ₃) [wt. %]	XRF		
Skattefunn, Lindum	Tingsaker skole #1	Lindum	Yes	3.6	Yes			Yes	No	Yes	6.64	<0.7	
	Tingsaker skole #2	Lindum	Yes	3.4	Yes				No	Yes	6.66	< 0.7	
	Tingsaker skole #3	Lindum	Yes	3.2	Yes	Trace: pyrite			No	Yes	6.27	<0.7	2.9
	RV420#1	Lindum	Yes	2.6	Yes				No	Yes	5.04	>1.2	
	Birkeland 5	Lindum	Yes	2.3	Yes	pyrite	Jarosite, goethite		No	Yes	10.7	>1.2	2.5
	Eydehavn 1B	Lindum	Yes	7.9	Yes			Yes	No	Yes	10.6	>1.2	
	Arendal legevakt 2	Lindum	Yes	6.6	Yes	Magnetite	Magnetite	Yes	No	Yes	6.61	>1.2	
	Arendal legevakt 5	Lindum	Yes	6.4	Yes	Magnetite	Magnetite	Yes	No	Yes	6.84	>1.2	
	Arendal legevakt 4	Lindum	Yes	7	Yes	Magnetite	Magnetite	Yes	No	Yes	9.42	>1.2	6.9
	Blakstad 3	Lindum	Yes	3.2	Yes				No	Yes	4.49	<0.7	
Nordbø 1	Lindum	Yes	4.3	Yes			Yes	No	Yes	6.85	<0.7		
Groos 1	Lindum	Yes	2.5	Yes	pyrite		Yes	No	Yes	6.59	>1.2		
Ingrid Skjønborg	Birkeland 5	UiO	Yes	4	Yes	pyrrhotite, arsenopyrite, chalcopyrite			Pyrite, pyrrhotite	Yes	3.28	>1.2	2.8
	PRF 1	UiO	Yes	5	Yes	pyrite, pyrrhotite, arsenopyrite			pyrrhotite	Yes	8.19	>1.2	2.3
	H11-12M	UiO	Yes	8.5	Yes	arsenopyrite				Yes	5.14	>1.2	7.7
	Blåbæråsen	UiO	Yes	5.5	Yes	arsenopyrite, pyrrhotite, pyrite, pyrrhotite			Pyrrhotite, Fe oxides	Yes	6.06	>1.2	2.6
	Tingsaker	UiO	Yes	6	Yes	pyrite, pyrrhotite			Fe oxides	Yes	1.83	<0.7	5.7

Continue of table.

Project	Sample	Placement of material	Column test	pH, column test	XRD	XRD (Fe(II))	XRD (Fe(III))	Amorphous content	Thin section	XRF	XRF (Fe ₂ O ₃)	Agder method H ₂ O ₂ [°C]	AMIRA NAG pH
Adam	5 (Birkeland)		Yes	< 3	Yes	Pyrite/pyrrhotite			Yes	Yes	5.68		
	12 (Kryss ved Glamslandveien og Sangreid)		Yes	< 3	Yes	Pyrite/pyrrhotite			Yes	Yes	5.89		
	7 (Sangreid)		Yes	8.4	Yes	Pyrite/pyrrhotite			Yes	Yes	5.12		
	E (Urevann)		Yes	< 3	Yes	Pyrite/pyrrhotite			Yes	Yes	4.74		
	5w (Birkeland)		Yes	<3	Yes	Pyrite/pyrrhotite	Jarosite, goethite		Yes	Yes	11.02		

Appendix F: Blank samples for water chemistry analysis

The blank samples for the H₂O₂ solution and the oxalate extraction acid.

Blank samples for water chemistry. Milli-Q is for samples with H₂O₂, and oxalate extraction is blank sample for oxalate extraction solution. Unit for elements is mg/L.

Sample	Element							
	Fe	Al	S	Cu	K	Na	Mn	Zn
Milli-Q	bdl	bdl	bdl	bdl	bdl	bdl	bdl	0.001
Milli-Q	bdl	bdl	bdl	bdl	bdl	<0.003	bdl	<0.001
Milli-Q	bdl	bdl	bdl	bdl	bdl	bdl	bdl	<0.001
Oxalate extraction acid	0.037	0.009	0.41	0.001	bdl	0.019	0.004	0.008
Oxalate extraction acid	0.035	0.010	0.45	0.002	bdl	0.019	0.004	0.008
Oxalate extraction acid	0.032	0.009	0.42	0.001	bdl	0.018	0.004	0.008

Appendix G: Raw data from XRD analysis

Due to a large Excel spreadsheet, raw data from XRD can be sent on request.

Contact information: adamariekarsen@gmail.com



Norges miljø- og biovitenskapelige universitet
Noregs miljø- og biovitenskapelige universitet
Norwegian University of Life Sciences

Postboks 5003
NO-1432 Ås
Norway